

1979/33

074816

BMR PUBLICATIONS COMPACTUS
(NON-LENDING SECTION)



BUREAU OF MINERAL RESOURCES, GEOLOGY AND GEOPHYSICS

RECORD
Record No. 1979/33

CHRISTMAS ISLAND (INDIAN OCEAN) GEOPHYSICAL
SURVEY FOR GROUNDWATER, 1976

by

BMR
Record
1979/33
c.2

G.R. Pettifer & E.J. Polak

on contained in this report has been obtained by the Bureau of Mineral Resources, Geology and Geophysics as policy of the Australian Government to assist in the exploration and development of mineral resources. It may not be in any form or used in a company prospectus or statement without the permission in writing of the Director.

Record No. 1979/33

CHRISTMAS ISLAND (INDIAN OCEAN) GEOPHYSICAL
SURVEY FOR GROUNDWATER, 1976

by

G.R. Pettifer & E.J. Polak

CONTENTS

	<u>Page</u>
ABSTRACT	
1. INTRODUCTION	1
2. GEOLOGY	1
2.1 Literature review	1
2.2 General geology	2
2.3 Volcanics	2
2.4 Limestone	4
2.5 Phosphate overburden	4
3. HYDROLOGY	5
3.1 Literature review	5
3.2 Hydrogeology of volcanic terrains	5
3.2.1 Rock type	5
3.2.2 Structure	5
3.2.3 Effect of the limestone mantle	8
3.3 Hydrogeology of Christmas Island	9
3.3.1 Rainfall, spring discharge, and karst flow data	9
3.3.2 Water-table and the volcanics-limestone boundary	10
3.3.3 Limestone distribution	11
3.3.4 Phosphate distribution-central area	11
3.3.5 Chemical and conductivity analysis of water	12
4. METHODS AND EQUIPMENT	12
4.1 Resistivity method	12
4.1.1 Resistivity depth probing	12
4.1.2 Gradient array	13
4.1.3 Equipment	14
4.1.4 Interpretation methods	14
4.1.5 Errors in interpretation	15
4.1.6 Transverse resistance of the limestone	16
4.2 Gravity method	17
4.2.1 Field procedures, data reduction, and map compilation	17
4.2.2 Sources of error in the gravity map	18
4.2.3 Interpretation procedures	19
4.3 Magnetic method	20
4.3.1 Field procedures, data reduction, and presentation	20
4.3.2 Interpretation methods	20

	<u>Page</u>
5. INTERPRETATION OF THE GEOPHYSICAL RESULTS	20
5.1 General	20
5.2 Gravity and Bathymetry	21
5.2.1 Bathymetry	21
5.2.2 Gravity evidence for the bulk density of Christmas Island	21
5.2.3 Gravity and geological structure	22
5.3 Limestone mantle and the limestone-volcanics contact	23
5.3.1 Thickness of the limestone mantle	23
5.3.2 Topography of the top of the volcanics	23
5.3.3 Relation of the water-table to the top of the volcanics	24
5.3.4 Transverse resistance map	25
5.4 Vertical structure of the volcanics	26
5.4.1 Interpretation of the magnetic data	26
5.4.2 Detailed gravity profiles	28
5.4.2.1 Gravity anomalies associated with Hanitch Hill ridge	28
5.4.2.2 Gravity expression of Grants Well dyke system	28
5.4.2.3 Gravity high on the southeastern margin of the postulated caldera	29
5.4.3 Resistivity gradient array results	29
5.5 Interpretation of resistivity depth probes	30
5.5.1 Central area	30
5.5.2 Resistivity evidence for basal groundwater	32
5.5.2.1 General	32
5.5.2.2 Relation of resistivity of volcanics to permeability and groundwater salinity	32
5.5.2.3 Possible evidence for saline intrusion - central area	32
5.5.2.4 Areas of low permeability	33
5.5.2.5 Areas of possible basal groundwater in the central area	33
5.5.3 Resistivity depth probes outside the central area	34
5.6 Ross Hill Gardens - geophysical results	34
5.6.1 Resistivity measurements	36
5.6.2 Magnetic measurements	36
6. CONCLUSIONS	37
6.1 Structure of Christmas Island	37
6.2 Limestone mantle	38
6.3 High-level groundwater in volcanics	38
6.4 Ross Hill Garden springs	39
6.5 Basal groundwater	39

	<u>Page</u>
7. RECOMMENDATIONS	40
7.1 Limestone - further investigations	40
7.2 Volcanics - further investigations	41
8. ACKNOWLEDGEMENTS	42
9. REFERENCES	

APPENDIX 1: Gravity survey statistics

TABLES:

1. Volcanic series - Christmas Island
2. Sources of water on Christmas Island
3. Ross Hill Gardens Springs - flow data

PLATES:

1. Geological map
2. Schematic groundwater models of volcanic islands
3. Distribution of phosphate (Central area)
4. Preliminary simple Bouguer anomalies
5. Topography and bathymetry map - Christmas Island
6. Detailed gravity profiles
7. Vertical magnetic intensity contours and interpretation
8. Magnetic intensity profiles (along east-west grid lines)
9. Magnetic intensity profiles (along north-south grid lines)
10. Total intensity magnetic profile - NS-baseline to Toms Ridge
11. Interpretation of resistivity depth probes - central area
12. Resistivity depth probe interpretation - Grants Well to powerline traverse
13. Minimum transverse resistance map of limestone (and dry volcanics) - central area
14. Top of volcanics - central area
15. Gradient array results
16. Ross Hill Gardens - total magnetic intensity profiles and resistivity results
17. Ross Hill Gardens sections
18. Interpretation map

FIGURES:

1. Christmas Island - existing water sources and deep water-bores
2. Electrode arrangements used on Christmas Island

ABSTRACT

A BMR geophysical survey on Christmas Island in 1976 - following up a similar BMR survey that investigated groundwater in Tertiary to Recent limestone - was designed to investigate the possibility of additional groundwater supplies in the volcanic core of the island.

Detailed gravity traverses over the postulated caldera in the central plateau area of the island indicate small gravity anomalies associated with previously interpreted magnetic features. Gravity, together with magnetics (total and vertical field) and resistivity data, have indicated the importance to groundwater distribution of vertical structure within the volcanics. A major structural northeasterly trend of possible hydrological significance is inferred from the bathymetry and geophysical data. Resistivity depth probes have delineated the generalised topography of the volcanics beneath the limestone mantle, and indicated the possibility of an undetected major karst flow towards the southeast, northeast of Grants Well.

Two low-resistivity zones within the volcanics are designated for drilling to test for the potential of high-level water supplies in the volcanics: one along the dyke system which controls the major Grants Well/Jedda Cave karst flow; the other on the postulated southwest margin of the central caldera.

Resistivity evidence suggests that the volcanics are of sufficient permeability to sustain a basal groundwater body over most of the central part of the island, though the geometry of such a body is undefined.

1. INTRODUCTION

Christmas Island, which is in the southeast Indian Ocean (Plate 1 inset), is a raised atoll comprising a volcanic core covered by a sequence of Tertiary to Recent limestones overlain by a superficial layer of phosphate.

The Christmas Island Phosphate Commission (CIPC) works the phosphate deposits on behalf of the British Phosphate Commissioners (BPC).

The Bureau of Mineral Resources, Geology and Geophysics (BMR) has been investigating the geology of the island intermittently since 1964; Barrie (1967); and Rivereau, (1965) have reported on the results of geological and geomorphological mapping, and Polak (1976) has reported on the search for water between 1967 and 1973.

Up to and including 1973 when the Engineering Geophysics Group of BMR made a detailed survey for groundwater, investigations of water supplies were confined to the limestone cover, because most of the rainwater was assumed to reach the ocean via cavities in the limestone, and along the boundary between the limestone and basalt. One of the conclusions of the 1973 survey was that the investigation should be extended to find where rainwater passes from the limestone into the volcanics before entering the ocean. The object of the 1976 survey was to investigate for water in the volcanics.

The survey took place between August 8th 1979 and October 6th 1976. The geophysical party consisted of E.J. Polak, G.R. Pettifer, W. Burhop and M. Preston-Stanley. Electrical, magnetic and gravity methods were used. BPC provided the field hands and topographical surveyors, transport to the island, and accommodation and food for the BMR personnel.

2. GEOLOGY

2.1. Literature Review

Barrie (1967) described the detailed geology of the Christmas Island phosphate deposits and limestone cover. He also discussed the earlier work of Trueman (1965) and a photogeological study of Rivereau (1965), and in particular rationalised the interpretation of Rivereau in

accordance with his observations during field mapping. Trueman (1965) carried out petrological studies of the volcanics on Christmas Island and reinterpreted the previous petrological studies of Campbell-Smith (1926). Van Bemmelen (1949) discusses the geology of Christmas Island in the context of the Indian Ocean and Indonesia. In the earlier geophysical study, Polak (1976) briefly described the limestone cover.

2.2 General geology

Christmas Island consists of volcanic basement, covered with layers of Eocene to Recent limestone (Plate 1). Van Bemmelen (1949) considered that volcanic activity ceased in the Early Tertiary. Barrett, P. (BPC) (personal communication), from a study of the breakdown of volcanic rock into soil, considers that the main phase of volcanism finished in the Early Tertiary and that final-phase volcanism (extrusion of tuff, "frothy" lavas, and ash) continued at least into the Pliocene. Later alternating uplift and subsidence affected the island (Rivereau, 1965).

Christmas Island is located at the junction of two submarine rises: the East Christmas Rise, trending easterly, parallel to the Java Trench; a west-southwesterly trending rise terminating at Cocos Island (Jongsma, 1976). These rises may have formed as a response to the difference in spreading direction between the West Australian Basin and Late Cretaceous sea-floor to the north-west. Deep sea trenches mark the surface expressions of the consuming plate boundaries (Le Pichon & others, 1973) and seaward of the Java trench there will be a topographic bulge. This topographic bulge which theoretically is 120 to 150 km distant from the trench will be responsible for the south-southwesterly tilting of Christmas Island. This tilting, noted by Barrett P. (BPC) (personal communication), has a considerable influence on the direction of drainage in the centre of the island.

2.3 Volcanics

The volcanics form several small scattered outcrops (Plate 1). Petrographic examination shows that they are of the alkalic type, similar to others in the Indian, Atlantic, and Pacific ocean basins (van Bemmelen, 1949, p. 231) and distinct from the calcalkaline volcanics of the orogenic belts of Indonesia. Three main series of volcanics have been defined (Trueman, 1965; Table 1).

TABLE 1. VOLCANIC SERIES - CHRISTMAS ISLAND

Series	Elevation, m.	Age	Description
Upper	180 - 300	Miocene	Nepheline basalt, limburgite
Middle	90 - 180	Eocene	Basalt, limburgite
Lower	0 - 90	Eocene	Andesite, trachybasalt.

The volcanics show a general decrease in acidity from the oldest to the youngest rocks, suggesting a change in magmatic composition in the early Miocene.

Boreholes drilled through the limestone mantle (Plate 14) in earlier groundwater investigations generally penetrated only a few metres into the volcanics, except for water-bores WB4 at Grants Well and water-bore WB3 south of Grants Well. Plate 14 also shows elevation contours of the volcanic-limestone contact as deduced from all previous stratigraphic holes and water-bores on the island. Some of the volcanics may be interbedded in the limestones, but in outcrop this occurs in only two places - over Flying Fish Cove and Dolly Beach (Plate 1). Drilling in the southeastern edge of the terrace above Norris Point (Plate 1) intersected a sequence of limestone - basalt - limestone - basalt (Barrett, BPC, pers. comm.).

The character of the volcanic rocks (e.g., weathering; proportions of lavas, pyroclastics, etc.) is not well known, but we consider that the volcano is of the composite type. The cone of a composite volcano generally consists of layers of pyroclastics (scoria, ash, etc.) alternating irregularly with tongue-like lava flows (Bullard, 1962). The lava flows come through breaches in the crater wall or cracks on the flanks or base of the volcanic cone. A cone of this composite type is known as a stratovolcano; the inclination of the slope corresponds to the angle of repose of the material, and this depends on whether the material is wholly ejectamenta (slopes 35° to 42°) or mainly lava of the Hawaiian-type volcanoes (slopes of 5° to 10° ; Purbo-Hadiwidjojo, 1967).

A particularly violent eruption may blow away the top of the cone leaving a large depression known as a caldera (if its diameter is more than 1 mile; Williams & Howell, 1941). The caldera may contain several craters and vents from later eruptions. Vents located outside the caldera may form rift zones radiating from the central core. Polak

(1976) suggested that the three-pronged shape of the island is due to rift zones; the presence of known volcanic centres at Ross Hill in the southern arm and Murray Hill in the northwestern arm support this suggestion. The central plateau would then be a logical place to look for the presence of a large caldera. Andrews (1900) suggested that the central plateau area may have formed a lagoon in the later stage of the atoll.

2.4 Limestone

The limestones deposited over the island are mainly of Eocene to Miocene age. Volcanic activity continued during coral deposition. The thickness of the limestone varies from a few metres above the central plateau to over 250 m on the faulted edges of the island. The distribution of limestone cover is discussed more fully in Section 3.4.3. The island resembles the island of Guam (Ward, Hoffard, & Davis, 1965): both consist of a central volcanic core draped with large accumulations of coral limestone.

The limestones show evidence of ancient reefs near sea level and on the edges of the plateau. In places the limestones are dolomitised (Trueman, 1965).

2.5 Phosphate overburden

Most of the phosphatisation occurs in the limestone cover, but in places deep sections of C-grade phosphate occur in phosphatised volcanics. The distribution of phosphate overburden thickness is shown in Plate 3. In places the phosphate accumulations show linear trends particularly in the phosphatised volcanics, suggesting that some of the igneous rock mapped as volcanics may be intrusive dykes, however, Barrie (1967) concluded that, as the phosphatisation is confined only to the volcanics and does not extend to the surrounding limestone, the volcanics were phosphatised before the limestone was deposited. The issue is not clearly resolved, but the possibility that the linear trends of phosphate deposits reflect the presence of dykes must be considered of importance to the hydrology of the island. Karst features in the limestone have been studied in detail; in places they (e.g., Grants Well/Jane Up cavities system) reflect underlying structure in the volcanics. The relation of phosphate distribution to karst development is not well documented, but in places (of sink holes systems) accompany thick accumulation of C-grade phosphate.

3. HYDROLOGY

3.1 Literature review

The hydrology of the limestone cover of Christmas Island was discussed in the previous report (Polak, 1976), and references on karst hydrology were given in it.

Literature on the hydrology of volcanic areas is sparse (Stearns, 1942; Temperley, 1960; Davis & De Wiest, 1966; Purbo-Hadiwidjojo, 1967). Several case studies of the hydrogeology of volcanic islands have been written in recent years; these include studies of the Hawaiian Islands (Visser & Hino, 1964); Tenerife, Canary Islands (Ecker, 1976); Karkar Island, PNG (Kidd, 1976); and Norfolk Island (Abell, 1976). Christmas Island differs from a classical volcanic island because of the complication of the ubiquitous limestone capping. In this aspect it is similar to the island of Guam (Ward & others, 1965) and some of the islands of the Lesser Antilles island arc in the Caribbean (Martin-Kaye, 1969).

Because of the presence of the limestone capping a thorough hydrogeological study of the volcanics is not possible: outcrop and drilling data are limited; structure is obscured; and available hydrological data relate mainly to the limestone overburden and the limestone-volcanics contact.

In the discussion that follows, general aspects of the hydrology of volcanics considered relevant to the Christmas Island study are presented (Section 3.2) and then existing geological and hydrological data are assessed (Section 3.3).

3.2 Hydrogeology of volcanic terrains

In considering the hydrology of volcanic terrains two basic points are of importance: rock type and structure.

3.2.1 Rock type

The main volcanic rocks on Christmas Island are basaltic in nature. All basaltic flows except for massive flows are permeable (Stearns, 1942). The permeability is due to the presence of cavities, crevices within and between the lava flows, interstitial spaces, shrinkages, crags, gas vesicles, lava tubes, etc. The permeability of basaltic flows may be decreased by the presence of secondary mineralisation, or the weathering of minerals to clays, particularly montmorillonite clays. Trueman (1965) noted the presence

of montmorillonite clays in samples of volcanics he analysed. Kaolin has been noted also in volcanic samples taken near the Asian Primary School, the location of palaeomagnetic sample "1" (Plate 1).

Basaltic rocks produce two types of pyroclastic rocks: either the product of high-temperature emission comprising fine ash, pumice, spatter, and cinders, or the result of violent explosions in the form of coarse ash (bombs and lapili), agglomerate, and vent breccia (Stearns, 1942). Either of these types may be highly permeable, becoming less permeable with consolidation. There is considered to be a difference in permeability of volcanic rocks from islands which started as submarine volcanoes and islands which started as land volcanoes. Submarine volcanoes contain poorly sorted pyroclastics and are commonly laid down with ashly shales and other sediments of low permeability. The available data on Christmas Island do not indicate whether or not the final stages of volcanism were marked by an underwater explosion.

A critical consideration as to the long-term suitability of the volcanics as a source of groundwater is the proportion of pyroclastics in lava flows within the island. The model of island volcanoes proposed by Jones (1970) envisages a pyroclastic pile covered on the flanks and in the central crater by lava flows. Limited drilling data, and outcrop-mapping of the volcanics suggest that lava flows predominate.

Jones's (1970) model of a basaltic massive volcano proposes a sequence of flow breccias at or near sea level, where subaerial lavas were quenched. This sequence has been observed on Norfolk Island (Abell, 1976) and found to be a highly permeable sequence. If widespread this zone is bound to influence the flow of water at or near sea level.

3.2.2. Structure

The structure of a volcano is also important in the accumulation and distribution of groundwater. In the Hawaiian Islands a groundwater basal lens (Visher & Hino, 1964; Stearns 1940) floats on salt water according to the Ghyben-Herzberg principle, and in the classical static case attains a depth below sea level forty times the height of the groundwater table above sea level. This classical case is ideal, and assumes uniform, isotropic permeability. In practice the lens is a dynamic system as it is continuously recharging from above and discharging downwards and outwards to the sea; in addition the salt water and fresh water are

mixing at the base and side of the lens. Cooper (1959) and Henry (1964) have discussed theoretical aspects of the dynamics of a lens system. Wentworth (1947) and Palmer (1957) discuss practical aspects of the Ghyben-Herzberg lens, in particular as it affects the volcanic islands of Hawaii.

The quantity and quality of the groundwater in a basal freshwater lens depend on the distribution of permeability, the rate and distribution of recharge, and the effect of mixing of the fresh water with sea water. The second and third factors are influenced mainly by the first factor, the permeability, and it is the structure which is an important influence on permeability.

The literature gives ample evidence of the effect of structure on the distribution of groundwater, and various schematic models have been devised by different authors to illustrate the effect. Plate 2 reproduces the main models of groundwater in volcanics.

The island of Lanai in the Hawaiian group (Plate 2, fig. 1) is characterised by highly permeable basalt giving rise to a gently sloping low-level water-table on the fringes of the island. In the centre of the island near the central vent, dyke swarms provide permeability barriers to the lateral movement of water, thus impounding groundwater at high levels on the island; this results in a local deepening of the base of the freshwater lens. However geophysical evidence suggests that where the groundwater is impounded at high levels, the increase in depth of the base of the lens is only the same order as the height of the water table above sea level, and not a factor of 40 times the water table height, as given by the Ghyben-Herzberg relation.

Structure has a strong influence on groundwater circulation in highly permeable basalt typical of the Hawaiian islands (Plate 2, fig. 2), where recharge and discharge are localised owing to permeability barriers. In some Hawaiian volcanoes complex systems of galleries have been excavated to control and collect massive accumulations of high and low-level groundwater which are trapped between dykes (Stearns, 1942).

Over 1200 km of galleries have been excavated into the volcano on Tenerife (Plate 2, fig. 3), providing a unique insight into groundwater circulation within the volcanics. Ecker (1976) proposed a model of groundwater compartments connected by permeable rocks or secondary fracture leakage paths. He discussed the concept of upper and lower vadose zones

above the basal water-table. The lower vadose zone is characterised by numerous groundwater compartments separated by generally dry volcanics. Groundwater compartments range in size from a few tens of metres to more than 500 m. They are less numerous in the upper vadose zone, and are often the sources of small springs. The basal water zone (or saturated zone) is characterised by high permeability. Groundwater-table slope is less than 0.3%. On Tenerife, tidal influence extends to 5 km inland in the volcanics, and sea water mixes with the groundwater, even in places of low groundwater extraction. The permeability of clay-bearing rocks is higher in the presence of salt water than fresh water owing to the tendency of clays to take up more water molecules at lower ion concentration; this factor may promote mixing of salt and fresh water (Davies & De Wiest, 1966, p. 166).

Springs discharge from Indonesian stratovolcanoes (Plate 2, fig. 4), at changes in slope; where the groundwater encounters a less permeable formation; and where erosion or a landslide exposes the water-bearing rocks. If the slope is greater than 5° the water generally flows underground to the sea. These conditions may prevail in the rift zones of the volcano as well, though, the size of the structure may limit the quantity of the supply.

Permeability barriers can cause perched and artesian water to collect in volcanoes. Artesian water occurs in two main ways: firstly, counterbalanced by salt water, the freshwater aquifer with a constraining upper bed may discharge water under pressure; secondly an aquifer confined between two inclined impermeable beds may discharge artesian water near its base.

3.2.3 Effect of the limestone mantle

The possible sources of groundwater within volcanic islands are the springs, perched water supplies, high-level water-table supplies, and low-level basal water supplies. Additional sources on Christmas Island may include karst limestone flows, and flows over the phosphate-limestone interface and the limestone-volcanics interface. With all these sources the problem is to find a sufficiently large reservoir to exploit by high-capacity pumping.

The presence of the limestone mantle, as previously mentioned, produces special problems in groundwater search in the volcanics. In the northern part of Guam Island (Plate 2, fig. 5), for example, a thick (180 m)

sequence of permeable limestone covers a core of relatively impermeable volcanics. The limestone has a low-level water-table (less than 1.8 m above mean sea level) and supports a basal lens. The water-table in the volcanics is much higher (about 30-50 m above MSL) because of its much lower permeability. The basal lens is characterised by a wide zone of mixing in the permeable limestone (up to 2 km inland) owing to storm wave action.

Because of its high permeability, the limestone mantle on Christmas Island acts as a temporary water storage for recharge water to the volcanics. In places the flow of water in the karst follows major channels which are due to a number of factors (e.g., topography of limestone-volcanics surface; initial porosity-permeability; variations within the limestone; phosphate overburden thickness and structure; and permeability of the underlying volcanics). This channelling of runoff on or near the limestone-volcanics contact may result in selective recharge of the underlying volcanics.

3.3 Hydrogeology of Christmas Island

The hydrogeology of Christmas Island is considered with reference to Sections 3.1 to 3.3, and to the data from earlier water resources investigations on the island contained in the unpublished records of BPC. Much of the data is directed to investigating exploration targets within the limestone, and consequently a lot of data are available in small areas, whereas other areas are largely unexplored.

3.3.1 Rainfall, spring discharge, and karst flow data

Rainfall at Grants Well between 1956 and 1964 ranged from 1284 to 2964 mm (average 2250 mm) per year. For the whole of the island (area 141 km^2) this represents an average annual volume of rainfall of $3.17 \times 10^8 \text{ m}^3/\text{year}$, or $256.4 \text{ m}^3/\text{h}$ per km^2 of the island.

Present water consumption averages about $260 \text{ m}^3/\text{h}$ and additional maximum requirements are $200 \text{ m}^3/\text{h}$ if a second washing and screening plant is introduced, giving a total of $460 \text{ m}^3/\text{h}$. The known water sources on the island are listed in Table 2 and shown in Figure 1. Present supplies come from the Grants Well/Jane Up cavities system and Waterfall. Previously the Ross Hill Gardens springs provided the water supply. The remaining supplies are widely dispersed around the island and either too difficult or too expensive to develop. Almost all supplies, except Waterfall, are

markedly seasonal, indicating that they come from subsurface runoff. The Waterfall source is constant, suggesting that it is from within the volcanics (Temperley, 1960) and thus giving some optimism for water search in the volcanics.

Table 2 lists only the known, measurable springs on land. Several freshwater springs have been noted in Flying Fish Cove (Fig. 1) down to the 200 m depth contour, and several outflows of water rise in limestone caves just below sea level around the coast. Most of the coastline is unexplored in this regard, and because of the wave action the chances of detection of small freshwater outflows around the coast are limited.

Utilizing flow data for Grants Well-Jane Up cave system, Ross Hill Gardens springs and Freshwater cave, the water balance of the central plateau is calculated as follows: rainfall on the catchment, at 256.4 m^3/h per km^2 , is 6410 m^3/h ; assuming a conservative estimate of 70% for evapotranspiration and allowing for no surface runoff, groundwater recharge is 1923 m^3/h ; measured discharge from springs and water-extraction points is 324 m^3/h , leaving some 1600 m^3/h of groundwater to be accounted for. Present known outflow, therefore, constitutes a little more than 5% of rainfall input. The remainder will be divided between unknown outflows along the volcanics-limestone contact (these will be mainly in the Smithsons Bight area, see Fig. 1) and water infiltrating to the volcanics.

3.3.2 Water-table and the volcanics-limestone boundary

The water-table on the island is strongly influenced by the location of the top of the volcanics. Resistivity depth probing has given much information on the water-table surface. Generally the water-table on the plateau area is just above the volcanics-limestone contact and fluctuates seasonally. Resistivity evidence (Section 5.3.3.) suggests that the basal water lens and the water-table are hydraulically connected. The water-table rises within the volcanic centre of the island owing to the relatively low permeability of the volcanics. At the edge of the island, where large thicknesses of limestone occur and the volcanics are close to sea level, the water-table drops to just above sea level because of the high permeability of limestone.

Plate 14 shows contours of the top of the volcanics for the central and northern part of the island. The contours are derived from borehole data and from resistivity depth probing. Estimates of depth from resistivity depth probing may be in error, but not critically as the

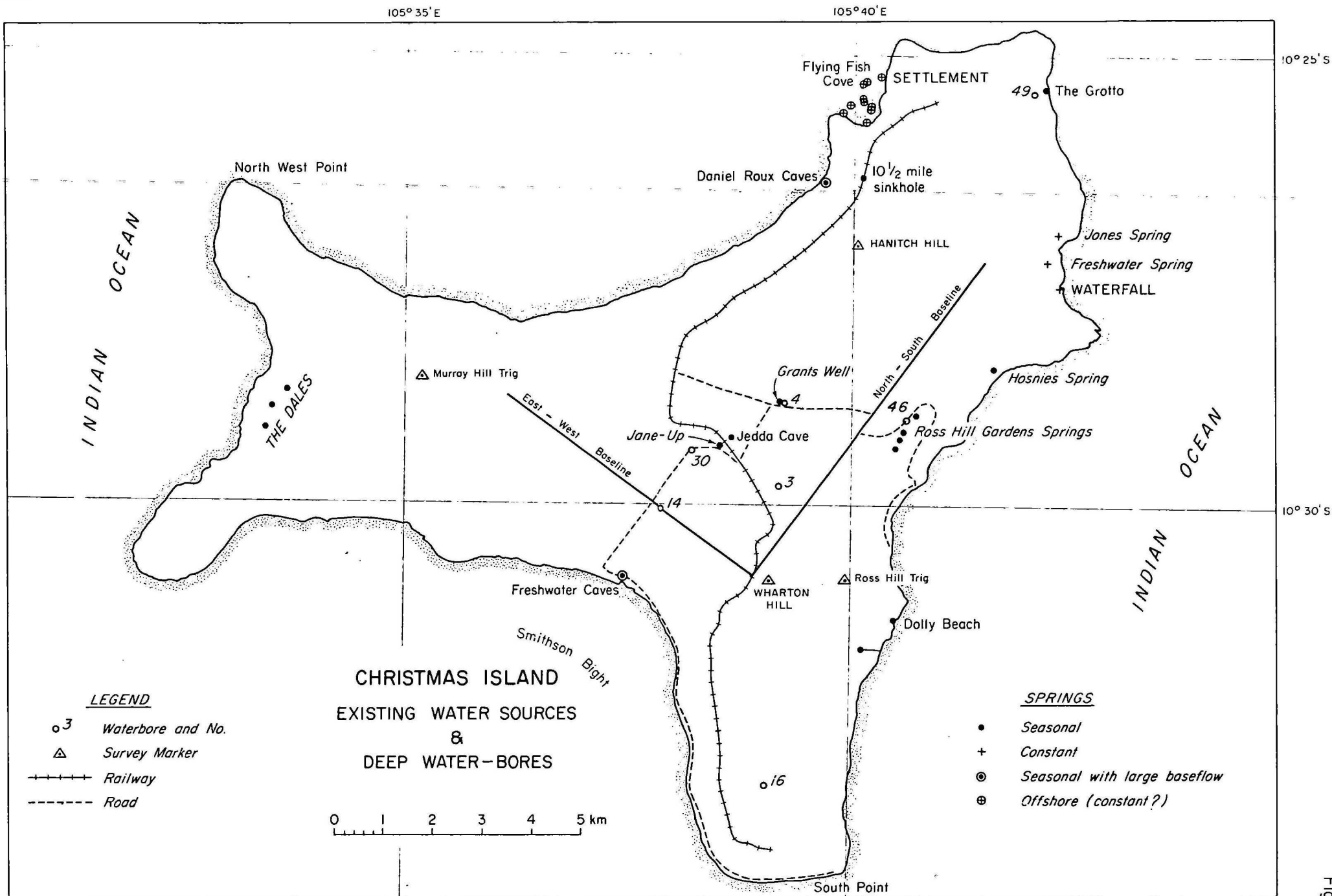


TABLE 2. SOURCES OF WATER ON CHRISTMAS ISLAND

(SOURCE BPC DRAWING NO. 67-X9E/X33A)

SOURCE	FLOW						COMMENTS
	Minimum		Maximum		Average		
	m ³ /hr	galls/hr	m ³ /hr	galls/hr	m ³ /hr	galls/hr	
Waterfall					53.2	11 700	Constant supply, volcanic -limestone interface near sea level
Grants Well	7.3	1 600	109.1	24 000	45.5	10 000	volcanic-limestone interface, flow direction 279°N
Jedda Cave	50.0	11 000	318.2	70 000	97.7	21 500	volcanic-limestone interface, flow direction 225°N Flow rate 320 m/sec.
Jane Up					18.2	4 000	branch of Grants Well system
Ross Hill Springs	22.7	5 000	527.3	116 000	40.9	9 000	four springs, volcanic-limestone interface
Daniel Roux Cave Clunies Cave					136.4	30 000	In tidal zone, volcanic-limestone interface flow direction 120°N
Freshwater Cave					68.2	15 000	volcanic-limestone interface at sea level, flow direction 15°N
10½ mile Sink hole			36.4	8 000	9.1	2 000	volcanic-limestone contact, 160 m above sea level, flow direction 175°N, fault controlled
The Ravine			25.0	5 500	9.1	2 000	volcanic-limestone contact
230' contour stream			36.4	8 000	13.6	3 000	
Dolly Beach					22.7	5 000	volcanic-limestone contact
Dales					46.6	10 300	volcanic-limestone contact
TOTAL					561.2	123 500	

volcanics are on a steep slope. Borehole data suggest that the volcanics are not underlain by limestone.

In some places the volcanics are dry and relatively unweathered. Water bore No. 3 (WB3) intersected 88 m of dry volcanics between Grants Well and Wharton Hill. At Grants Well, water bore No. 4 (WB4) penetrated 82 m into saturated, moderately fresh basalts with a low permeability (pump testing showed yields of $0.6 \text{ m}^3/\text{h}$). The present resistivity survey results suggest that WB3 results are not representative of the volcanics of the island.

3.3.3 Limestone distribution

Plate 11 shows the thickness of limestone based on interpretations of resistivity depth probes and borehole data in the central and north-eastern part of the island; it should be studied in conjunction with the levels of the top of the volcanics (Plate 14). In the South Point area (to the South of the plate) limestone extends to at least 8 m below sea level. In the west of the island no borehole data are available. The present survey results throw some light on the thickness of limestone.

3.3.4 Phosphate distribution - central area

Plate 3 shows distribution of the phosphate. Between the railway line and the bore line 210 EW (EW BASELINE) the phosphate is thick and shows linear trends, suggesting structural control. Barrandite (phosphatised volcanics) has been identified in an area of thick limestone near WB14. A vertical magnetic intensity anomaly indicates a possible volcanic plug 100 m south east of this barrandite deposit. The barrandite is 15 m thick in this area, though elsewhere the phosphate is up to 50 m thick. In places isolated deep pockets of phosphate less than 100 m in diameter occur and may indicate small volcanic plugs.

The barrandite is thought to be residual dykes (Barrie, 1967; Section 2.4) but may represent post-Miocene lava flows and intrusions. If there are dykes they may influence water flows over the older volcanic surface, and hence recharge of the volcanics in localised areas.

Barrett (internal BPC report dated 7/5/75) concludes that major water flows occur at the phosphate-limestone contact rather than the limestone-volcanics contact.

3.3.5 Chemical and conductivity analyses of water

Polak (1976) gives water analyses for samples from Grants Well, Jedda Cave, Jane Up and Waterfall. All samples show similar composition, high HCO_3 content (212-277 ppm), Ca content (64-81 ppm), and pH from 7.6 to 8.0.

Resistivity measurements show values from 21.9 to 28.1 ohm-m.

4. METHODS AND EQUIPMENT

During the survey resistivity, gravity, and magnetic geophysical methods were used.

4.1 Resistivity method

The resistivity method measures the resistivity variation of the rocks for an interpretation of the subsurface lithology.

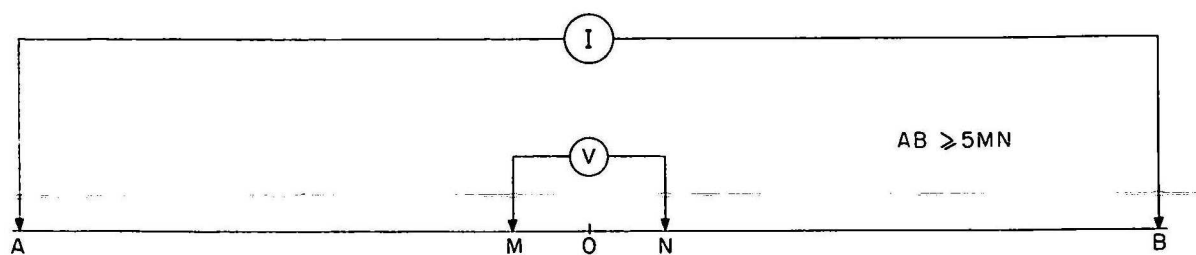
In the Christmas Island survey, both vertical depth probing and gradient array techniques were used. The vertical depth probing determines the vertical variations of resistivity, whereas the gradient array measures the lateral variations in resistivity in a particular range of depths. For all measurements four electrodes were used - two current and two potential electrodes.

4.1.1. Resistivity depth probing

Three main electrode configurations were used (Fig. 2). The Schlumberger and half-Schlumberger (or pole-dipole) configurations were used for depth probing. In the Schlumberger depth probing technique the separation of two potential electrodes M and N is kept small with respect to the current electrode separation AB. Generally MN separation is less than 0.2 AB. For each reading the outer current electrodes are progressively moved farther apart, while the inner potential electrodes are kept fixed until the voltage (V) between MN is small. Then the distance between the potential electrodes is extended, the reading repeated and the outward movement of the current electrodes is continued until the voltage between MN is again small; the process is repeated until the desired maximum current electrode spacing is reached. At each electrode spacing $AB/2$, a measurement of current (I) and voltage (V) is taken, and apparent resistivity of the medium for that particular electrode spacing is calculated according to the formula in Figure 2a. In this manner a curve of apparent resistivities versus current electrode separation is obtained. For interpretation purposes the curve is a log-log plot of apparent resistivity (ρ) versus $AB/2$.

(a) SCHLUMBERGER CONFIGURATION

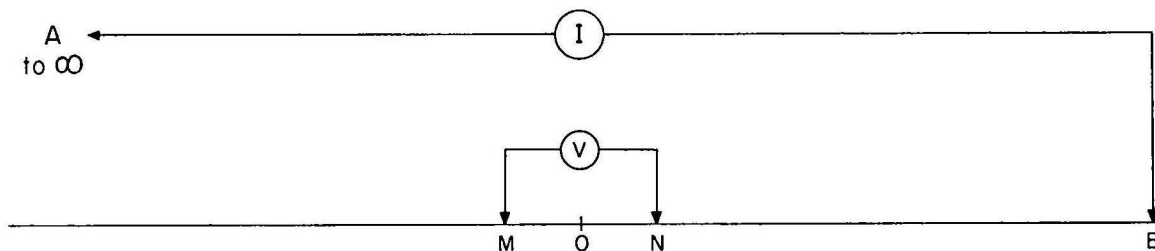
Fig. 2



Apparent resistivity $\rho = \pi \frac{AM \times AN}{MN} \times \frac{V}{I}$

Plot $\text{LOG } \rho$ versus $\text{LOG } \left(\frac{AB}{2} \right)$

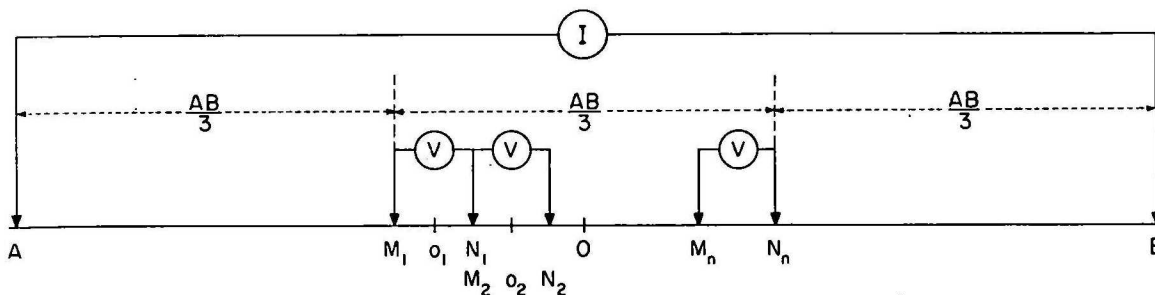
(b) HALF SCHLUMBERGER CONFIGURATION



Apparent resistivity $\rho = 2\pi \frac{BM \times BN}{MN} \times \frac{V}{I}$

Plot $\text{LOG } \rho$ versus $\text{LOG } (OB)$

(c) GRADIENT ARRAY



Apparent resistivity $\rho = \pi \left(\frac{1}{AM_i} - \frac{1}{AN_i} - \frac{1}{BM_i} + \frac{1}{BN_i} \right) \times \frac{V}{I}$

$i = 1 \text{ to } n$

\approx Schlumberger apparent resistivity
(if $M_i, N_n \leq \frac{1}{3} AB$)

Plot ρ versus Distance along traverse

ELECTRODE ARRANGEMENTS
USED ON CHRISTMAS
ISLAND

For the half-Schlumberger depth probing, one of the current electrodes, say A, is placed a long way from the other three electrodes (effectively at infinity) and only one current electrode (in this case B) is moved progressively outwards. In practice in this survey the maximum distance OB was as large as $\frac{1}{3}$ of OA, but this possible source of error was offset by expanding OB perpendicular to line OA as in the pole-multipole technique (Merrick, 1974). The apparent resistivity is calculated according to the formula in Figure 2b, and the depth probing curve is interpreted in the same manner as Schlumberger curves, OB is equivalent to AB/2.

Initially, Schlumberger depth probing was carried out to OB = 300 m, but this was increased to 1 km when it was realised that larger spacings were needed to penetrate the limestone cover and define the resistivity of the volcanics. Dipole spacings of up to 120 m were employed for voltage measurements. The large electrode spacings hampered the areal coverage by depth probing in the limited time available for the survey. Two deep depth probes were made to obtain deeper information; S8 near Grants Well to AB/2 = 2072 m and S19 on the 460 NS baseline to 2400 m. S19 was repeated with the half-Schlumberger arrangement to OB = 1 km to test the accuracy of the half-Schlumberger depth probing with a finite remote electrode separation; with the remote electrode at 4 km offset perpendicular to the line of other electrodes the half-Schlumberger resistivities were higher than the Schlumberger resistivities by a maximum of 8 percent on the logarithmic scale at maximum OB = 1 km. This is acceptable considering the time and field effort it saved.

Currents up to 2 amp were used and voltages as low as 100 microvolts were measured.

4.1.2. Gradient array

In the gradient array (Fig. 2c), a potential dipole M_1M_1 is used in the interval M_1N_1 , and readings are taken within the central third of the electrode spread. For a uniform medium the apparent resistivity ranges from the Schlumberger resistivity at the centre of the spread to 1.4 times the Schlumberger resistivity at the extremities of the central third of the current electrode separation (Kunetz, 1966, p.32); this then enables variations of resistivity laterally to be detected. These variations will be superimposed on an increase in apparent resistivity on either side of the centre of the separation. Generally AB is chosen to

focus at a particular depth of investigation. In this survey AB was chosen so that $AB/3$ was equal to an electrode spacing where the depth probe curve was asymptotic to the resistivity of the volcanics. This ensured that the variations in apparent resistivity reflected the variation within the volcanics.

In the survey two gradient array measurements were taken (Plate 14). One of these was along gridline 410EW, where current electrodes were placed at stations 380-410 and 460-410 - equivalent to $AB/2 = 1219$ m. Dipole lengths of 61 m were used with a 61-m interval between readings over the interval 409-410 to 439-410. A current of 1.2 amp gave voltages of 0.4 to 1.2 mV. Results are shown in Plate 15.

The other gradient array was along the new powerline road from Grants Well to the railway line (Plate 14). Electrode spacing was $AB/2 = 2072$ m, and the current electrodes were placed at the intersections of the new powerline road with the railway (roughly 338-289) and of Grants Well road with the 460 gridline (roughly 460-345). A dipole length of 122 m and station intervals of 61 m were used. The area close to the Grants Well pumping station had to be omitted owing to electrical interference. A current of 0.9 amps gave voltages of 0.3 to 1.2 mV. Results are shown in Plate 15.

4.1.3. Equipment

The resistivity transmitter used on this survey was a Geotronics model FT10 IP transmitter capable of 850 volts and 10 amps. The transmitter was used in the time domain mode in 2-second duty cycle.

The voltage measurements were taken with a Scintrex IPR-8 time domain IP receiver with manual or automatic spontaneous potential back-off capability.

4.1.4. Interpretation methods

The interpretation of the depth probe data was carried out by an inversion technique using a computer program developed by Zohdy (1975). This program automatically generates a layered-earth model which fits the field data. The program smooths any distortions in the field curve. Because of the large resistivity contrast between the high-resistivity limestone and underlying low-resistivity volcanics, the forward modelling component of Zohdy's program had to be modified to accept higher resistivity contrasts. The original version used Ghosh's (1971) 3-point per decade linear filter method to generate theoretical depth probe curves for layered

models; this can accept resistivity contrasts up to about 50:1.

O'Neill (1975) has published coefficients for a 6-point per decade linear filter; these are capable of modelling contrasts up to 1000:1, which is generally slightly greater than the average (500:1) for the Christmas Island environment. These coefficients were used in the modified Zohdy program.

But still some difficulties were experienced. The Zohdy inversion often modelled a series of steps for a large resistivity decrease rather than a single boundary. Consequently the Zohdy interpretation was further simplified manually by accepting the simplest possible layer interpretation unless independent evidence (drilling, gravity, magnetic, etc.) or the shape of the depth probing curve suggested otherwise.

The final adjustment was carried out using a forward modelling program, on the Wang 600 desk calculator and plotter employing O'Neill's coefficients in the linear filter method.

4.1.5. Errors in interpretation

A major source of error in the method of interpretation of the depth probe data is the assumption of horizontal layering in the limestone and volcanics. In practice vertical structure and lateral resistivity changes occur so the interpretations represent equivalent layered models of the real structure. The limestone in particular appears to have large lateral variations in resistivity which distort the maximum in the depth probe curves (see examples on Plate 17).

In resistivity depth probing, the problem of equivalent models frequently occurs. For a horizontally stratified medium, every layered model produces a unique depth probe graph, but the differences between some graphs are not recognizable owing to the limited accuracy of the field measurements (say 1 to 5 percent). The laws of equivalence (Kunetz, 1966, p.58) state that, as on Christmas Island, where a high resistivity bed (limestone) occurs between two low resistivity layers (soil and underlying volcanics), it will be difficult to distinguish between two resistive beds of different thickness and resistivity if the product of the thickness and resistivity (so-called transverse resistance) for one layer is the same as the other. This is known as T equivalence, where T is transverse resistance (in ohm m^2).

The T equivalence in the Christmas Island depth probe curves means that it is theoretically possible for the interpreted limestone thicknesses to be in error by as much as 100%, however, in practice, with the available geological control in the central area of the island, it is estimated that errors are less than 50% in areas of thin limestone (say less than 20 m thick) and probably less than 20% in other areas.

The interpretation of intermediate layers between the high-resistivity limestone and saturated low-resistivity volcanics at depth is hampered by the high resistivity contrast. In such cases the effect on the resistivity curve by any intermediate layers is masked and their presence or absence cannot be verified by resistivity alone. This ambiguity means that the resistivity depth probing in places is incapable of resolving vertical variations in resistivity which might reflect karstification at the base of the limestone or low-resistivity or high-resistivity layers within the volcanics.

4.1.6. Transverse resistance of the limestone

The resistivity method has delineated the areas of thick and thin limestone, and this will be reflected to a certain extent in the variation of transverse resistance over the central area.

Accordingly a transverse resistance map of the central area has been prepared (Plate 13) as a further guide to limestone thickness and should be viewed in conjunction with the map of interpreted thickness (Pl. 11). The interpretation of this map is discussed further in Section 5.3.2.

The values of transverse resistance (T) were derived from the depth probes from the present survey and Wenner depth probes carried out by BPC before 1973.

Following the method of Zohdy, Eaton, & Mabey (1974 p. 35) an estimate of T can be derived from a Schlumberger depth probe curve by drawing a line at 45° of negative slope, on the bilogarithmic plot of the depth probing curve, tangentially to the maximum of the curve. This tangential line has the equation:

$$\log \rho = -\log t + T$$

$$\rho = T/t$$

$$\text{or } T = \rho t$$

where t = thickness

ρ = resistivity

Also T can be obtained from the product of resistivity and electrode spacing for any point on the line. This is generally an overestimate of the true value of T by less than 10%. The method is illustrated schematically in the inset in Plate 13. For Wenner configuration the value of T derived in this manner needs to be multiplied by a factor of 1.4 to compensate for the fact that Wenner curves are, to the first approximation, equivalent in shape to Schlumberger curves shifted by a factor of 1.4 to the right on the electrode spacing axis (abscissa; Koefoed, 1968, p. 30).

Plate 13 shows the location of the BPC Wenner depth probes that investigated the thin limestone cover and therefore only obtained a maximum electrode spacing of 122 m (equivalent to a Schlumberger spacing of 171 m). Occasionally, particularly in the areas of thicker limestone the curve maximum was not reached, or more commonly, only partly defined. Therefore many of the T values derived from the Wenner curves are minimum values.

Further the Wenner depth probes show consistently lower resistivities and hence lower transverse resistances for the limestone than those obtained during the BMR survey. This may be due to two factors: firstly, the different times of the surveys (hence different groundwater conditions); and secondly the fact that the BPC Wenner measurements were conducted using a low-frequency AC instrument (Evershed and Vignoles, Geophysical Megger) compared with the BMR survey's DC instrument. Andrew & Wainwright (1965) also noted that Megger instruments yielded lower resistivities.

4.2 Gravity Method

4.2.1. Field procedures, data reduction, and map compilation

The gravity survey undertaken in the 1976 investigation extended the 1973 survey. Polak (1976) described the survey method and the reduction of gravity data.

Appendix 1 summarises the gravity survey statistics for both surveys. In compiling the gravity map, several conflicting sources of information were available as to the correct latitude and longitude grid of the island. The grid accepted as correct for the purpose of this survey (latitude corrections, station positioning, etc.) was taken from the National Mapping 1:50 000 coloured map of the island (X782, Edition 5, DNM; 1972). The latitudes and longitudes for this map are based on a satellite fix of the Christmas Island Radio Tower by US survey ship Bartlett in 1971.

In addition, to aid in an interpretation of the total gravity field of the Christmas Island atoll, a bathymetry map of the ocean floor to a depth of 5000 m was compiled at 1:100 000 scale. The bathymetry is based on a map by Barrie (1967), which gives bathymetry to 2700 m; admiralty charts and RAN hydrographic charts with bathymetry to 5000 m; and ocean sounding charts at 1:1 000 000 scale. The navy charts are based on pre-aerial photograph and pre-satellite fix maps of the island. The bathymetry compiled from the navy data has been fitted as well as possible to existing topographic maps of the island and to the shallow bathymetry of Barrie (1967). The resulting map at 1:100 000 scale is shown in Plate 5.

The 1976 gravity survey established regional stations and detailed traverse stations. The detailed traverse stations were along gridlines and roads in the central area (station spacing 61 m). Plate 14. shows the Bouguer anomaly map (without terrain correction) for a density of 2.67 g/cm^3 . Plate 6 shows the detailed gravity traverse profiles.

4.2.2. Sources of error in the gravity map

Appendix 1 outlines the main sources of error in the Bouguer anomaly. The largest errors are due to terrain and elevation effects.

The Bouguer anomalies have been produced for a local survey only. Accordingly they have been obtained using the old international gravity ellipsoid formula, for theoretical gravity and the absolute value of the observed gravity of the base station is not rigidly tied to an isogal station. However, errors in observed gravity base level are probably less than 0.1 mGal (Wellman, BMR, 1978, personal communication) for the whole island.

Terrain corrections have not been applied to the Bouguer anomalies, but approximate terrain corrections are shown in schematic sections (inset, Plate 4). The corrections range from almost zero in the middle of the central plateau to between 5 and 6 mGal at the top and base of the cliffs around the island. Terrain corrections have been estimated using a 2-dimensional approximation for the three arms of the island. The 2-dimensional modelling was carried out using a 2-dimensional density profiling program developed by Anfiloff (1975).

The Bouguer anomalies also reflect an error in the estimation of Bouguer reduction density - an effect which has a maximum value of 1.43 mGal per 0.1 g/cm^3 error for a maximum elevation of 343 m on the island, but is proportionally less for stations at lower elevations.

The Bouguer anomaly contains a large effect due to the seafloor topography around the island which has not been corrected for. This effect dominates the gravity field of the island and obscures anomalies due to smaller bodies at shallower depths because of the large gravity gradients in the regional field of the island. The detailed traverse profiles show small wavelength anomalies due to shallow geological features; these are generally only separable from the regional field in the centre of the plateau. Towards the edges of the plateau, terrain corrections increase and regional gradients steepen, obscuring small wavelength features.

4.2.3. Interpretation procedures

Interpretation of the gravity data is qualitative, though simple quantitative estimates have been made in places. The regional field is analysed by attempting to separate gravity effects due to topography, geological structure, and the submarine pedestal of the island was simulated using a 3-dimensional gravity program written by Spies (1975), and using the recently compiled bathymetry map (Plate 5) to construct the 3-dimensional gravity model. The analysis was carried out in a preliminary sense only to obtain the average gravity gradient between the central gravity maximum and the extreme arms of the island. This gradient is diagnostic of the bulk density of the island, and also indicates whether the island is of uniform density or has a dense inner core. This analysis is similar to that carried out by Robertson (1967a) for gravity surveys of the Cook Island group of oceanic volcanic islands (Robertson, 1967b). A full gravity simulation of the island was not carried out as it is beyond the scope of this report.

The detailed gravity profiles (Plate 6) show small anomalies generally less than 1.5 mGal superimposed on larger regional gradients. Choice of the regional gradient is a subjective process, and accordingly the regional gradients have not been removed from the original profiles. Because of the small density contrast in the volcanics and the lack of geological control or reliable independent geophysical information, the gravity anomalies are not analysed quantitatively, but are interpreted in terms of their correlation with magnetic anomalies, topography, and resistivity variations.

4.3 Magnetic method

4.3.1. Field procedures, data reduction, and presentation

Polak (1976) described the field procedures and data reduction for the vertical magnetics and continuous profile total field magnetics. In this survey the total field coverage was extended along major grid lines and roads covered by detailed gravity stations in the central area. Traverses were also carried out on the western area of the island as shown in Plate 10. Plate 8 shows total and vertical field magnetic profiles along EW grid lines and Plate 9, the NS grid lines.

4.3.2. Interpretation methods

Quantitative interpretation is hampered by the high and variable remanent magnetisation of the volcanics on Christmas Island. Remanent intensity can be as high as 20 times induced intensity, but generally is 5 to 10 times higher. In addition normal and reversed magnetisation has been recorded on samples around the island. Generally only simple depth estimates can be made from the magnetic profiles. Because of the presence of remanence, mathematical modelling of magnetic bodies cannot be carried out with any accuracy. Consequently, dip, susceptibility, and geometry of the bodies cannot be estimated from the magnetic profiles without better geological control. The magnetics indicate remanence variation and structure within the volcanics in a qualitative manner only, and the total field data complement the vertical field data in this regard.

5. INTERPRETATION OF THE GEOPHYSICAL RESULTS

5.1 General

In discussing the results of the 1976 geophysical investigation, previous work has been incorporated, and an integration of all geophysical methods has been attempted. The interpretations are subject to the errors and limitations discussed in Section 4.

Data from the different geophysical methods are presented in separate plates in the report, and are also incorporated in an interpretation map (Plate 18). The interpretation begins with a preliminary analysis of the regional gravity field of the island, and the bathymetry, to delineate gross structure in the island (Section 5.2). The groundwater study is examined in four major sections: firstly, the limestone mantle and topography of the limestone-volcanic contact is discussed; secondly, the evidence for

vertical structure in the volcanics is considered; thirdly, the resistivity data for the central area of the island are analysed; and finally the results of the Ross Hill Garden tests are presented.

5.2 Gravity and bathymetry

This section describes the gross structure of Christmas Island inferred from the recently compiled bathymetry map (Plate 5) and the 1973-76 gravity survey of the island (Plate 4). As this subject is only of marginal importance to the immediate problems of groundwater supply, which is the main consideration of this report, only a preliminary analysis of the regional gravity and bathymetric data is attempted.

5.2.1. Bathymetry

The bathymetric expression of Christmas Island (Plate 5) is similar to the shape of the island, though the main feature is an elongation of the 3000 and 4000-m contours in a NE-SW direction, parallel to the trend of the northeast area of Christmas Island. The fault lineament associated with Tait's Vale (Plate 4) also parallels this trend.

5.2.2. Gravity evidence for the bulk density of Christmas Island

Using the 3-dimensional gravity modelling program of Spies (1975) the gravity effect of the mass of the island has been modelled for gravity stations both within the central gravity maximum on the central plateau of the island and on the extreme arms of the island. Based on the topography of the island, and the surrounding bathymetry to a depth of 3000 m, an average gravity difference between the centre and extreme edge of the island has been calculated. By incorporating the effect of the attraction of the mass of the island, and assuming that the karst limestone mantle has a negligible density contrast with the volcanic core, we can equate the observed and calculated gravity differences to obtain an average density of the island, according to the following formula:

$$(\Delta BA) + (UBRF) \times 2.67 = (\Delta UIE) \times (D - 1.04) + (UBRF) \times D$$

where ΔBA = observed average Bouguer anomaly difference (density 2.67 g/cm^3)
between central gravity maximum and extreme edge of island

UBRF = Unit density Bouguer plate reduction factor for the central
plateau of the island (elevation 213 m)

ΔUIE = Calculated unit density island effect difference between centre
and extreme

D = Equivalent uniform density of island

Substituting values of $\Delta BA = 60(\pm 5)$ mGal, $UBRF = 8.9$ mGal, $\Delta UIE = 8.7(\pm 0.5)$ estimated) mGal and carrying out a first-order differential error analysis the following density is obtained.

$$D = 5.3 (\pm 0.5) \text{ g/cm}^3$$

In the first order the density determination is insensitive to error in a determination of the gravity effect of the mass of the island.

The value of density obtained is unrealistically high, and suggests that the observed average gravity difference of 60 mGal is too high for the assumption of a uniform density island. Polak (1976) listed density determinations of samples of limestone ($2.54\text{--}2.64 \text{ g/cm}^3$) and basalt ($1.97\text{--}2.94 \text{ g/cm}^3$). To obtain a density of less than 3.0 g/cm^3 in the above analysis the observed Bouguer anomaly difference would need to be less than 20.7 mGal.

The high observed Bouguer anomaly difference can only be explained by postulating a high-density body at depth within the island. Robertson (1967 a, b) noted similar results with the circular volcanic islands of the Cook Island group in the Pacific.

The analysis is not taken any further at this stage because it is beyond the scope of this report.

5.2.3. Gravity and geological structure

The main N to NE trend in the bathymetry is evident also in the regional gravity map of the island (Plate 4) particularly on the northeast arm of the island. The gravity trend is superimposed on the strong radial gravity gradient of the island.

On the southern arm of the island, the gravity results suggest that a major fault is associated with the photolineament in Tait's Vale (Plate 4). This evidence is based only on one gravity station (7604-5951 at Tait's Point), and must be considered tentative until further stations are established. The evidence suggests a northeasterly trend in gravity contours on the southern arm of the island.

On the western arm of the island a marked gravity gradient is evident 400 m east of Murray Hill, between gravity stations 7309-0604 and 7604-5917, corresponding to the major fault flanking Murray Hill (Plate 1). Resistivity evidence (Section 5.5.2) suggests that this fault is a major discontinuity in the island.

5.3 Limestone mantle and the limestone-volcanics contact

5.3.1. Thickness of the limestone mantle

The variation in thickness of the limestone in the central area as inferred from depth probing is shown in Plate 11. Plate 12 shows an interpreted section together with the transverse resistance of the limestone, along the Grants Well road and new powerline. In places where high-resistivity volcanics underlie the limestone it is impossible to determine the limestone-volcanics contact from the resistivity data alone.

5.3.2. Topography of the top of the volcanics

The generalised topography of the limestone-volcanics contact as derived from the resistivity and borehole data is shown in Plate 14. Where the slope of the contact is steep, the direction of the slope is well defined; but, where the contact is roughly level, errors in the interpretation of the thickness of the limestone may influence the slope direction. Further, detailed flow patterns may not follow the lines of steepest slope, but karst channels instead; these karst channels may be influenced by small-scale topography and structure in the limestone-volcanics contact. The distribution of data is too sparse to delineate this fine detail.

The features of the topography of the volcanics are firstly the three major ridges: one paralleling the Hanitch Hill ridge, trending northeast; another towards the west; and the less well-defined ridge towards Wharton Hill, to the south. The features were previously known, but the resistivity data have delineated them more definitively.

The second principal feature is the inferred fault separating the plateau area from the terrace behind the Ross Hill Gardens. This fault was defined by earlier resistivity data. The terrace is characterised by high transverse resistance values (Plate 13) related to the large (roughly 100 m) thickness of limestone to the east and southeast of this fault (Plate 14). The fault is contoured as a steep slope, but may be an abrupt step in elevation of the volcanics.

The third feature is the inferred groundwater flow directions shown by arrows. Of interest is the possibility of flow to the east-southeast from the Grants Well-Jedda Cave area over into the terrace area. The flow to the west north of Grants Well is of doubtful validity, being based mainly on one depth probe (S36, Plate 11) where the limestone-volcanics contact interpretation is uncertain.

The most interesting feature of this map is the evidence that the known Grants Well-Jedda Cave flow represents only a minor slope surface of the volcanics, and that, unless the water flow is diverted to the southwest, most of the water from Hanitch Hill ridge should be flowing to the southeast rather than towards Grants Well.

The Grants Well karst system is the only major karst system known on the plateau area. It is controlled by an interpreted dyke system (Polak, 1976), which is shown on the map of the vertical magnetics (Plate 7) and the interpretation map (Plate 18). The dyke system is interpreted to extend only 1400 m northeast of Grants Well, as far as line 358 EW, which is well away from the major topographic high of the volcanics surface. If the Grants Well cavities system follows these dykes northeast from Grants Well it will have little chance of intercepting most of the runoff from the Hanitch Hill ridge, and therefore the existence of either sheet flow or a major karst flow system or systems to the southeast from Hanitch Hill ridge must be postulated. The evidence for such a feature is discussed in Section 5.3.4.

5.3.3: Relation of the water-table to the top of the volcanics

Implicit in the above discussion are the assumptions that the volcanics are relatively impermeable; that subsurface runoff is on the volcanics-limestone contact; and that the water-table follows closely the topography of the volcanics.

These assumptions are certainly true on a broad scale on Christmas Island (Section 3.4.2), though if permeable ash is present at the surface of the volcanics the water-table may be below the top of the volcanics. The major ridge in the top of the volcanics associated with Hanitch Hill ridges is defined by resistivity soundings S29, S31, and S32, and to a lesser extent S27, S23, and S33. Gravity lows associated with the Hanitch Hill ridge and shown on the interpretation map (Plate 18) are considered evidence for the presence of ash, particularly on the southeast side of Hanitch Hill ridge (Section 5.4.2), but no borehole data or independent geophysical data are available to verify this. The gravity lows are tentatively interpreted to trend east-west. If present, ash will certainly have a strong influence on the water-table, and on the flow of water on and below the volcanics surface. The gravity lows are bounded by gravity highs which from resistivity evidence (S34 and S33, Plate 12) correspond to high-resistivity volcanics and most probably represent dyke structures.

The difference in elevation of the volcanics throughout the central area is considerable - over 100 m between the highest point and the vicinity of WB30. The possibility of artesian water in permeable sections of the volcanics should not be overlooked; water from the volcanics may be entering the limestone, particularly at lower elevations in the catchments. Powell (unpublished BPC report, undated) cites the presence of old gardens which are saturated in the lower part of the catchment between the railway and EW baseline 210; evidence for artesian conditions in the lower catchment.

5.3.4. Transverse resistance map

The map of minimum transverse resistance (Plate 13) shows contours, at logarithmic intervals, of transverse resistance (T) in units of 1000 ohm-m^2 . T is the product of resistivity and thickness of the limestone (and underlying high-resistivity volcanics if any), and variation in T can be caused by either, or both, resistivity and thickness variation. Limestone thickness variation is from 20 m to 100 m, a factor of five. Observed T values range from less than $30\,000 \text{ ohm-m}^2$ at the BPC Wenner soundings on lines 366EW to over $3\,600\,000 \text{ ohm-m}^2$ at BPC Wenner depth probe 18, a factor of 120 at least. Accordingly variations in T can be assumed to represent mainly variation in the limestone resistivity. T values have been contoured in preference to interpreted limestone resistivity because the T value is not subject to large errors due to equivalence, as is interpreted resistivity (Section 4.1.5).

For aquifers, T can be correlated empirically with transmissibility (Duprat, Simler, & Ungemach, 1970) if no clay is present and if sufficient joint permeability exists. Vincenz (1968), investigating limestone aquifers in Jamaica, found an empirical linear relation between pumping yield and resistivity in porous limestone. On Christmas Island, however, the water-table is at or near the base of the limestone mantle, and the limestone resistivity will be related to the amount of residual water and clay in joints and on the degree of karstification. Polak (1976) discussed the factors affecting resistivity of limestone. In general, however, lower resistivity and T values indicate damp cavities, and higher values represent solid limestone or limestone with dry cavities.

The features of the transverse resistance map are firstly low values of T at Grants Well and also near lines 366 EW and 378; secondly, the high T values on depth probes S52, S53, S54, S55 (shown in profile form in Plate 12); thirdly, the area of high T values corresponding to thick limestone over the terrace west and southwest of Ross Hill Gardens; and fourthly the high variability of T, evident in areas where data distribution is dense.

The last feature should be considered to show the limitation of this T map in areas of sparse data density. The contours are generalised and a logarithmic contour interval has been chosen to delineate only major T variations.

The low T values at Grants Well indicate the presence of the Grants Well karst system. The only other area of low T values (less than 30 000 ohm-m²) is on the BPC Wenner depth probe on lines 366 EW and 378 EW. This is the only evidence pointing to a possible karst system trending southeast from Hanitch Hill (as mentioned in Section 5.3.2).

The high T values (600 000 to 1 160 000 ohm-m²) at depth probes S2, S3, S4 and S5 correspond to an area of little or no phosphate (Plate 3), which is underlain by higher resistivity volcanics (40 to 200 ohm-m). Further, the feature correlates with a gravity high (Plate 18) which is bounded by the faulted region between the central area and the terrace to the west, and southwest Ross Hill Gardens. The high T values represent either solid limestone which is relatively unweathered due to the absence of phosphate or the existence of underlying denser, higher-resistivity and presumably less permeable volcanics. An alternative interpretation is that the limestone is dolomitised, but geological data are lacking. The high T values do not appear to correlate with areas of pinnacle limestone.

The area of high T values over the terrace behind the Ross Hill Gardens reflects both the increased thickness of the limestone and the presence of dry cavities above the water-table.

5.4 Vertical structure in the volcanics

The evidence for vertical structure within the volcanics comes from the gravity, magnetic, and resistivity data, as well as some existing geological information such as the distribution of phosphate and faults (Plate 3). In general the complexity of the volcanic structure is such that only preliminary conclusions can be drawn from the geophysical results, mainly because of the limited data coverage, lack of continuity of geological features, limitations in interpretation techniques, and most importantly limited geological control.

The geophysical interpretation is presented in Plate 18. To consider the overall view of structure in the central area it is necessary to review first the vertical field magnetic map (Plate 7) reproduced from Polak (1976).

5.4.1 Interpretation of the magnetic data

Polak's (1976) interpretation is briefly reviewed below, and elaborated in terms of the further data gathered in the 1976 survey.

The magnetic map can be divided into two separate areas on the basis of magnetic trends; firstly southwest of line 282 EW, magnetic features trend roughly NW-SE. Northeast of line 282 EW, magnetic features trend roughly NE-SW, perpendicular to the trend in the other area. This trend difference is reflected also in the phosphate distribution map (Plate 3). This does not suggest a one to one relation between magnetics and phosphate distribution, but indicates that the phosphate is reflecting basic structural trends. Further, as previously suggested, areas of thick C-Grade phosphate accumulation may be phosphatised volcanics (Sections 2.5 and 3.44). The magnetic trend in the Grants Well area also parallels the basic structural direction of the northeast arm of this island (Section 5.2.1).

Polak (1976) postulated the notion of a central caldera in the Grants Well area, outlined roughly by the large circular feature on the magnetic map. Radiating from the central caldera are three major rift zones (Section 2.3). The large linear magnetic feature extending from line 306 EW roughly parallel to the NS baseline 460 is bounded by the fault between the central plateau and the Ross Hill Gardens terrace. This fault is considered to be the southeastern margin of the original caldera. Elsewhere the original caldera wall is not as well defined. The southwestern rim may be represented by the magnetic feature between Jane Up well and Jedda Cave through Camp 4, roughly along grid lines 270 EW and 274 EW. The northwestern and northern margins are not exactly defined in the magnetics.

The postulated caldera area is intersected by the major dyke system (previously mentioned in Section 5.3.2) which apparently controls the Grants Well-Jedda Cave karst system.

Southwest of the railway, various dykes defined by magnetics - particularly the feature between 258 and 262 EW grid lines - may divert groundwater flow. The southwestern rim of the caldera postulated above is considered an important magnetic feature controlling groundwater flow to the top of the volcanic terrace area directly south of Grants Well near lines 282 to 298 EW. Depth probes S40 and S41 (Plate 11) show low-resistivity volcanics on this feature.

Northwest of Grants Well three prominent dykes are confirmed by gravity data (Section 5.4.2) and may represent the northern rim of the postulated caldera.

The total field magnetic profiles have further delineated magnetic features, particularly where remanent magnetisation of the volcanics is such that the vertical field expression of a body is relatively flat (e.g., line 410, Plate 8; line 388 NS, anomaly at grid line 362 EW, Plate 9), however, the original interpretation based on the vertical magnetic map is unaltered.

5.4.2 Detailed gravity profiles

The detailed gravity profiles are presented in Plate 6. Plate 18 shows a qualitative interpretation of the data in conjunction with all other available geophysical data. The gravity anomalies considered of significance are discussed in three sections.

5.4.2.1 Gravity anomalies associated with Hanitch Hill ridge

Immediately west of Grants Well on the new powerline road a series of three gravity highs alternating with two gravity lows of peak-to-peak amplitude of 1 mGal (maximum) and wavelength from 60 to 300 m can be traced from the new powerline road traverse through line 294 EW to line 314 EW. These three gravity highs correlate exactly with dykes interpreted in the vertical magnetic map referred to above (Section 5.4.1).

Farther northeast on lines 366 EW and the old powerline traverse north from Grants Well, a major gravity low associated with the peak of the topographic ridge is defined. This low is present even if terrain corrections are applied (see terrain corrections for section BB¹ Plate 4). The anomaly after terrain corrections is about 0.9 mGal amplitude and wavelength greater than 700 m. It is also well defined on the powerline traverse (stations 0920 to 0930, Plate 6) but not on line 346 EW. The gravity low correlates well with a small area of low magnetic intensity (Plate 7); line 346 is just outside this area. The low is postulated to indicate the presence of low-density ash material; this may represent a cinder cone of the old volcanics.

Farther to the northeast of this area at the intersection of NS baseline 412 and line 410 EW a series of low-amplitude (0.6 mGal) high and low anomalies trend east-northeasterly. These anomalies are located at least 600 m from the peak of Hanitch Hill ridge. The gravity anomalies for line 410 are also plotted in Plate 15 along with magnetics and gradient array data. No clear magnetic expression is evident except for a 100-nT anomaly in the total field data at NS chainage 415. The gravity anomalies correlate with high resistivity volcanics below chainages 418 NS.

5.4.2.2 Gravity expression of Grants Well dyke system

The powerline gravity traverse (stations 0833 to 0800, 1100 to 1134, Plate 6) crosses the major Grants Well dyke system. Plate 15 shows the gravity, magnetic, and gradient array results for the area immediately northwest of Grants Well.

A small bilobed gravity high (0.25 mGal) is evident between stations 0800 and 0805. This high can be traced also on the powerline road north of

Grants Well stations (0903 to 0913, Plate 6). Although the anomaly is small the gravity is further evidence for a dyke system as originally interpreted from magnetics. An abrupt decrease in resistivity of the volcanics between stations 0800 and 0803 (Plate 15) is evident, and this provides further evidence for a major discontinuity just west of Grants Well.

5.4.2.3 Gravity high on the southeastern margin of the postulated caldera

Gravity profiles along line 298 EW (stations 1534 to 1563), Grants Well road (1100 to 1132), line 322 EW (1001 to 1020), line 266 EW (1310 to 1356), line 346 (1844 to 1860) have delineated a broad gravity high feature bounded on the southeast by the faulted margin of the postulated caldera wall. The gravity high (maximum amplitude 1.4 mGals, width approximately 800 m) follows closely the magnetic feature in this area (Plate 18). It extends farther west than the magnetic feature and the existing survey has traced it as far as line 298 EW. To the northeast the gravity high is not readily identifiable on line 410 EW (stations 1400 to 1440, Plate 6).

This gravity high corresponds to the area of high transverse resistance limestone (Section 5.3.4, Plate 12) and part of it may be explained by an increase in the density of the limestone. Using a simple formula and the standard slab correction (41.7 mGal/km thick slab of unit density), 30 m of limestone would give a 1.25 mGal anomaly for an increase of 1.0 g/cm^3 in density. Such an increase in limestone density is unlikely; 0.5 g/cm^3 maximum is a more realistic value giving a maximum anomaly of 0.63 mGal. The observed anomaly of 1.4 mGal is much larger, which is evidence for higher-density volcanics in this area. As previously mentioned (Section 5.3.4), higher-resistivity and presumably less permeable volcanics are noted on the interpretation of soundings S2, S3, S4, S5 (Plate 12).

5.4.3 Resistivity gradient array results

The limited amount of gradient array work carried out has shown the potential of this method for delineating vertical structures on Christmas Island, but more time would have been needed to do the gradient array work necessary for a complete study of all major vertical structures in the volcanics.

The gradient array data are presented in Plate 15 for line 410 EW and the new powerline road. The two areas have been previously referred to in discussions of the gravity results (Sections 5.4.2.1 and 5.4.2.2).

The principal finding of the gradient array work is the existence of a major change in resistivity of the volcanics at gravity station 0803, 182 m west of Grants Well. This corresponds to the middle point of the two possible

dykes controlling the Grants Well karst system, shown in the magnetic interpretations (Plate 7). The potential dipole length (122 m) used in the gradient array has poor resolution and the resistivity low at station 0803 is probably more pronounced than shown. The $\frac{AB}{2}$ spacing (2072 m) is large, suggesting that the resistivity discontinuity extends to well over a depth of 1 km (see Section 5.5) and thus represents a major discontinuity in the island.

Resistivity depth probes (Section 5.5.1), in particular S8 (Plate 12) and S42 (Plate 11) show evidence also of low resistivities at other places close to this dyke system.

The resistivity low at station 0803 is recommended as a prime drilling target for testing for groundwater in the volcanics. The results of a drilling survey across this feature will be crucial to the success or otherwise of the volcanics as a suitable water supply source. Closely spaced drillholes are recommended along the power-line road extending from depth probe S8 (300 m west of Grants Well) to Grants Well. If water is present in the volcanics the vicinity of station 0802 to 0805 is certainly the best hope uncovered by the present geophysical survey.

5.5 Interpretation of resistivity depth probes

5.5.1 Central area

The resistivity depth probe interpretations are presented in Plate 11. The Grants Well Road section depth probes S0 to S14, and S45 to S48, are shown in Plate 12. All interpretations are subject to errors as outlined in the limitations of the interpretation method (Section 4.1.5).

The results have been correlated with the geology by classifying the interpreted resistivities into preliminary ranges of resistivities for the volcanics and a bulk classification of high-resistivity limestone. The arbitrary ranges for the volcanics shown by contrasting hachures in Plate 11 are, firstly, less than 25 ohm-m, interpreted to be highly weathered or fractured volcanics of high water-bearing potential; secondly, 25 to 60 ohm-m, representing moderately weathered or fractured volcanics; and thirdly slightly weathered to hard, fresh volcanics with resistivities greater than 60 ohm-m. The classification presented is tentative and needs testing further by drilling.

As a further guide to the interpretation of the results the resistivities of the volcanics are shown on the interpretation map (Plate 18) in sequence from shallowest to deepest at each depth probe location: the symbol LHI, for example, indicates that a sequence of low-resistivity volcanics immediately beneath the limestone overlies high-resistivity and then deeper still intermediate-resistivity volcanics.

Several features of the interpretation are discussed herein. Sections 5.3.1 and 5.3.3 previously discussed the limestone mantle and the relation of the water-table to the top of the volcanics.

The first and most important feature of the resistivity interpretations in the volcanics (Plate 18), is the persistence of intermediate (I) and high (H) resistivity volcanics underlying the northern area of the catchment, where the elevations are higher. In the southeastern area of the catchment, lower resistivity volcanics are more frequent particularly on the terrace. These data suggest that groundwater recharge to the volcanics is generally greater in the lower catchment, where the limestone cover is thicker. The data are also consistent with the notion of upper and lower vadose zones put forward by Ecker (1976; Section 3.2.2, fig. 3 in Plate 2) to explain the increase in degree of saturation with depth in the volcanic island of Tenerife.

The second feature is the location of low resistivities at depth probes S8, S42, and to a lesser extent S36, along the Grants Well dyke feature. As discussed in Section 5.4.3 the area between S8 and S7 holds the most promise for high-level groundwater in the volcanics.

The third feature is the low resistivities of the volcanics immediately underlying the limestone near depth probes S40 and S41, where the volcanics are at depths of about 28 to 41 m (Plate 13). The depth probes are located over the broad magnetic feature, postulated (in section 5.4.1) to be the magnetic expression of the southwestern margin of the caldera. The surface at the top of the volcanics (Plate 14) suggests that water might flow southeast along this feature into the downfaulted terrace (Section 5.3.2). The marked contrast in the resistivity of the volcanics at depth probes S40 and S41 on the one hand and S43 on the other is further evidence for a rapid change in the character of the volcanics in this area. The area between S40 and S41 is recommended as a second prime target for drilling for high-level groundwater in the volcanics. A line of drillholes is recommended to ensure maximum chance of intersection of water-bearing zones.

The fourth feature is the general low resistivity of the volcanics over the downfaulted terrace area, where the great thickness of limestone makes the economics of drilling in this area prohibitive.

In summary the results of the resistivity work indicate two prime drilling targets for water search: the possible high level water-bearing volcanics between S7 and S8 on the new powerline road west of Grants Well, and on the magnetic feature through S40 and S41. In both these areas the volcanics are at shallow depths (less than 40 m), and will be more economical to drill than the deeper volcanics in the terrace area.

5.5.2 Resistivity evidence for basal groundwater

5.5.2.1 General

Basal groundwater will form a continuous lens only if the permeability is high enough to sustain it. Offshore springs in Flying Fish Cave (Fig. 1; Section 3.4.1) down to depths of 200 m suggest that groundwater with a hydraulic head of at least 5 m is sustaining them (according to the classic Ghyber-Herzberg relation - Section 3.2.2). This is direct evidence for the existence of basal groundwater; the permeability of the volcanic rocks containing it can be inferred from the resistivity data.

5.5.2.2 Relation of resistivity of volcanics to permeability and groundwater salinity

Any investigation of the resistivity of volcanic rocks at sea level must consider that they may contain

indicate slightly jointed to fresh volcanics. Ambiguity arises in the intermediate and low resistivity ranges (say 10 to 60 chm-m): slightly jointed volcanics saturated with saline water will be of similar resistivity to porous volcanics saturated with fresh water.

Thus resistivity data can distinguish areas of saline water intrusions, areas of low permeability and areas of intermediate porosity/permeability where the basal groundwater could be sustained. The above classification of resistivities is generalised only, and, as no supporting drilling data are available, must be considered tentative.

A decrease in resistivity interpreted at or near sea level may be further evidence of basal groundwater, but, because the depths determined for resistivity discontinuities in the volcanics may have a wide margin of error (Section 4.1.5), this evidence must be considered statistically.

5.5.2.3 Possible evidence for saline intrusion - central area

In the central area, evidence of salt-water intrusion is evident at depth probes S62 and S19. At S62, 1.8 km inland from the coast, where the depth control to volcanics is good (WB14 is 940 southeast of S62), the steep descending branch of the depth probe curve suggests a resistivity in the range 1-10 chm-m for the volcanics at sea level, but the asymptotic resistivity value is not reached on the depth probe curve. S19, a deep depth probe ($\frac{AB}{2}$ maximum = 2400 m), is interpreted to show possible salt-water intrusion (7 ohm-metre layer)

extending to a depth of 380 m below sea level, where resistivity increases to 30 ohm-m. The deeper 30 ohm-m layer is uncertain because of the effect of topography on the depth probe curve and the deep valley of limestone beneath S19 (Plate 17).

5.5.2.4 Areas of low permeability

Areas of low permeability are suggested by high resistivity; below sea level these are near depth probe S17, S18, S32, S41, S45, and possibly S1 and S16. Gradient array data at S7, at Grants Well (Section 5.4.3, Plate 15), show that resistivities for $\frac{AB}{2} = 2072$ m increase from less than 40 ohm-m to greater than 100 ohm-m at gravity station 0800 at Grants Well. This shows, as previously mentioned, a major near-vertical discontinuity extending deep into the island. A conventional layered interpretation of S8 suggests that the 38 ohm-m layer extends to a depth of at least 3 km, or 2.8 km below sea level. However, this interpretation must be considered tentative because of the deviation of the rock structure from a layered model. Thus permeability exists at depth below S8, but not S7.

5.5.2.5 Areas of possible basal groundwater in the central area

Areas of low to intermediate resistivity (less than 60 ohm-m) at sea level with no evidence of a resistivity decrease below or near sea level have been delineated on depth probes S0, S2, S3, S4, S8, S9, S10, S11, S22, S23, S24, S26, S28, S30, S31, S33, S38, S39, S40, S42, S43, S44, S46, and S48. Depth probes S5, S6, S13, S15, S19, S21, S29, S35, S36, S37, and possibly S1, S12, and S47 show low to intermediate resistivities at sea level with a decrease in resistivity at or near sea level.

At all these depth probes the low resistivity must persist for at least several hundred metres below sea level - that is, about 85 percent of the 45 depth probes in the central area show low resistivities which may indicate a permeability capable of sustaining basal groundwater. Owing to the poor depth resolution of the resistivity depth probing technique; errors in assuming horizontal layering in an environment where vertical discontinuities are numerous; and the inability to distinguish between salt water and fresh water - the geometry of a basal freshwater body cannot be determined. Drilling alone can resolve this.

5.5.3 Resistivity depth probes outside the central area

Resistivity depth probing was also carried out on the western arm of the island along the new railway: S45, S46, S47, S48; then along Toms Ridge: S49, S50, S51; and also at the Dales: S52. The interpretations of S45, S46, S47, and S48 are shown in Plates 11 & 12, and of depth probes S49, S50, S51, and S52 in Plate 18, where locations are shown in the inset.

Depth probes S45 to S48 show that limestone forms a thick cover on the northern margin of the island. The principal result of interest, however, is the contrasting resistivities of the volcanics between the group of depth probes S45 to S48 (Plate 12) and S49 to S51 (Plate 18).

A major north-northeasterly trending fault passes through Murray Hill, between S48 and S49, roughly 400 m east of S49. This fault (shown in Plate 1) is subparallel to the main northeasterly structural trend on the island, which is in the bathymetry (Plate 5, Section 5.2.1), phosphate distribution (Plate 3), magnetics (Plate 7, Section 5.4.1), and gravity (Plate 4, Sections 5.2.2 and 5.2.3). Depth probes S49, S50, and S51 consistently show low resistivity (less than 5 to 20 ohm-m) volcanics at depth below sea level, whereas depth probes S46 to S48 show intermediate-resistivity volcanics 38 to 55 ohm-m and S45 shows high-resistivity volcanics 70 to 300 ohm-m.

The above findings suggest that the fault through Murray Hill is a major discontinuity dividing areas of different permeability: lower permeability to the east, and higher permeability - and possibly salt-water intrusion - to the west.

Depth probes S52 at the Dales and S61 at Norris Point on the northeast of the island (Plate 18) were both taken near the edge of the limestone cliffs on the coast and both show salt-water intrusion owing to wave action beneath the cliff.

5.6 Ross Hill Gardens - geophysical results

The Ross Hill Gardens area is on a terrace at an elevation of 90 to 110 m. The area was used as a vegetable garden until phosphate was mined there. It contains four major springs (Fig. 1, Table 3) which are located on a change of slope from the limestone cliff to the terrace. The site is extensively covered by fans of calcareous sinter. The springs are wide soaks on the contact of volcanics and limestone. The water from the springs flows over the sinter to disappear underground among the pinnacles of the mined area.

TABLE 3

FLOW DATA FOR ROSS HILL GARDEN SPRINGS

	elevation (m)	maximum flow (m ³ /h)
Harrisons	104	231
Hendersons	100	
Hewans	98	136
Hudsons	92	164

The total flow of the springs depends on the rainfall: during the dry season it may be as low as 20 m³/h, reaching 527 m³/h in the wet. The main increase in the flow in the wet season is from Hudsons spring, but after prolonged dry weather this spring dries up, while the other springs still produce considerable flows of water. These facts suggest the following conclusions:

- a) Hudsons spring is really an overflow from other springs;
- b) Hudsons spring is fed by groundwater at a higher level than other springs in the area.

The supply of water is inferred to come from the northwest across the baseline. As the area southeast of depth probe S0 is part of a much larger terrace, which is covered by thick limestone and extends southwest roughly parallel to the 460 baseline (see Plate 14), water may come from the southeast also. It is not known whether the water flow on the limestone-volcanic contact is channelled or a 'sheet' flow.

Some novel geophysical techniques were used in an attempt to determine the source of the springs. The groundwater and weathered volcanics cropping out at the springs are more conductive (20-30 ohm-m) than the limestones (1000-30 000 ohm-m). Groundwater flows through the limestones will form conductive paths through the high-resistivity limestone also. By placing a current electrode at the springs, current density within the low resistivity material can be maximised, and current will flow either in concentrated zones or uniformly, depending on groundwater and resistivity distribution. Concentration of the current flow can be detected by surface voltage methods or by measuring the changes in magnetic field from the normal when no current is flowing.

5.6.1 Resistivity measurements

For the surface voltage measurements four pairs of half-Schlumberger or pole-dipole depth probes (S54 to S60, Plate 16) were placed along EW gridlines between Ross Hill Gardens Road and the baseline.

In each pair of depth probes, measurements were made with two different positions for the 'infinite' electrode, one in Hudsons Spring and the other in Harrisons Spring. If there is a change in current concentration for a particular current electrode spacing in the area near a depth probe it will show up as a change in resistivity; higher current concentration produces a lower resistivity.

Only in one depth probe pair (S59, S60) is there a change in apparent resistivity, at an electrode spacing of 80 m. This suggests that a conductive path for current flow from Hudsons Spring is close to grid line 330 EW. Other channels for Hudsons Spring may exist in areas not investigated by the other depth probe pairs. The change in resistivity at $AB/2 = 80$ m is at the point on the depth probe curve which shows maximum influence of the high-resistivity layer, suggesting that the concentration of current flow is within the limestone and possibly within a narrow range of depths.

Because the quantitative interpretation of depth probe curves is based on the theory which assumes that all electrodes are on the same elevation and on horizontal bedding, it is not possible to take the interpretation much further than the above comments because these assumptions are violated in this experiment.

5.6.2 Magnetic measurements

If a DC current flows in the ground it produces a small change in the Earth's magnetic field. For current flow in a uniform medium between two grounded electrodes this change is very small (less than 0.4 nT/amp) at the centre of the two electrode configuration. However, if current flow is concentrated in narrow high-conductivity paths the change in the magnetic field may be enhanced locally above the conductivity path.

For the experiment at Ross Hill Gardens one electrode was placed in Hudsons Spring and the second electrode was positioned west of the NS baseline. Measurements were taken along Ross Hill Garden Road with no current flowing. Then measurements were repeated with a current of 2 amps flowing through the ground. The two magnetic profiles show major differences in two places (Plate 16). One is over a section about 50 m wide at position

1070 m on the profile. This corresponds to roughly midway between the extension of 366 EW and 370 EW grid lines on Ross Hill Gardens Road. The difference observed between the two profiles is 75 nT, and occurs at an elevation of about 100 m above sea level, close to the limestone-volcanics contact. The other anomaly is a difference of up to 20 nT over a section 100 m wide centred at the 230-m position on the profiles. This anomaly is between depth probe S19 and S59-S60 (Plate 18). The change is consistent with that indicated by the electrical depth probe pair S59-S60 (Section 5.6.1).

The magnetic and resistivity measurements suggest that a conductivity path from Hudsons Spring within the limestone passes close to depth probes S59-S60 and S19.

6. CONCLUSIONS

The conclusions presented herein are based on preliminary interpretations, and are subject to the limitations of data coverage and interpretation methods discussed in Section 4. The major limitation, however, is the lack of hydrogeological control of the volcanics owing to the ubiquitous limestone capping. Accordingly the interpretation should be re-examined as further geological control, pump-test results, and other data become available.

Experience with geophysics in karst and volcanic terrains is limited, probably because geophysical methods are difficult to apply in these environments which are characterised by extreme changes in both hydrological and physical properties. Accordingly quantitative interpretations of geophysical data based on simple models (e.g., layered media in resistivity depth probes) may be of limited validity. Generally the approach used in this report has been to delineate anomalous areas rather than emphasise quantitative interpretations.

With the above in mind the conclusions are presented in five main sections: structure; the limestone mantle; high-level groundwater in the volcanics; Ross Hill Garden springs; and basal groundwater.

6.1 Structure of Christmas Island

Bathymetry, gravity, magnetics, and phosphate distribution together provide evidence which suggests that a northeast structural trend, delineated by geological mapping, is the main structural trend in the island. Resistivity evidence at Grants Well and Murray Hill show that this structural trend may have hydrological significance. The northeasterly trending Grants Well dyke system is characterised by low-resistivity volcanics to

the northwest and higher-resistivity volcanics to the southeast; this discontinuity probably extends to a depth of several kilometres. A major north-northeasterly trending fault just east of Murray Hill represents a discontinuity in volcanics resistivity at sea level; resistivity is low to the east and higher to the west.

6.2 Limestone mantle

Resistivity depth probing has delineated the gross topography of the top of the volcanics (Plate 14) and areas of thick limestone cover (Plate 11). Detailed topography and groundwater flow patterns on the volcanics cannot be determined. Structure is known to influence flow also.

A downfaulted terrace of thick limestone (80 m+) lies southeast of the faulted southeast margin of the postulated caldera. The edge of the central plateau above the terrace is characterised by a zone of high resistivity limestone representing either a possible ancient reef, or unkarstified or dolomitised limestone.

The topography of the volcanics suggests a major slope from Hanitch Hill ridge to the faulted terrace. Unless runoff to the southeast is diverted towards Grants Well, a major southeasterly trending flow system may be located northeast of Grants Well. Data coverage is sparse, but the low transverse resistance of limestone on lines 366 EW and 410 EW (Plate 13) may provide a starting point for further investigation.

A possible flow direction trending southeast from Camp 4 corresponds to a magnetic feature which is postulated as the southwest margin of the original caldera. This feature is also characterised by low-resistivity volcanics. If this flow exists, it may represent a major diversion of the Grants Well/Jedda Cave cavity system.

Minor flow directions inferred from slopes on the top of the volcanics are to the southeast along the Grants Well cavity system, and a possibly northerly flow starting north of Grants Well.

6.3 High-level groundwater in the volcanics

Detailed gravity traverses and continuous total field magnetic traverses have reinforced the previous vertical magnetic interpretation. The gravity anomalies associated with magnetic features are further support for the possible geological interpretation of these features as vertical dykes. Resistivity data combined with the magnetics and gravity

have shown that vertical structures in the volcanics are of prime importance in the distribution of potential water-bearing zones in the volcanics.

Gravity highs are associated with the Grants Well dyke systems - a dyke swarm northwest of Grants Well near the railway and the postulated southeast margin of the caldera. A gravity low on line 366 EW corresponding to an area of low magnetic intensity at the top of Hanitch Hill ridge may be an area of volcanic ash. Gravity anomalies at the intersection of lines 410 EW and baseline 412 NS correspond to an area of high-resistivity volcanics delineated by gradient array investigations.

Gradient array data and resistivity depth probing have delineated a zone of low-resistivity volcanics associated with the Grants Well dyke system, between resistivity depth probes S7 and S8. This is considered to be the main finding of the 1976 survey.

The second important finding of the 1976 survey is the low-resistivity volcanics at depth probe S40 and S41 over the magnetic feature which is postulated as the southwest margin of the original caldera. This and the Grants Well dyke system represent the main hope for finding high-level groundwater in the volcanics.

The downfaulted terrace appears to be underlain by uniformly low-resistivity, potentially water-bearing volcanics. This is consistent with an increase in water saturation with depth within elevated volcanic islands. The depth of the low-resistivity volcanics beneath the terrace (80 m) may be too great for economic development of the volcanics as a groundwater source in the terrace area.

6.4 Ross Hill Gardens springs

Experiments with mise-a-la-masse resistivity and the magnetic resistivity method using electrodes placed in the Ross Hill Garden Springs suggest that a conductivity path extends from Hudsons Spring and passes close to depth probes S59-S60 and S19. This may represent a groundwater flow in the limestone to Hudsons Spring.

6.5 Basal groundwater

The resistivity method has delineated areas of possible saline intrusion, areas of low permeability, and areas of low to intermediate resistivity at or below sea level; the areas of low to intermediate resistivity below sea level occupy 85 percent of the central area, and are likely to

have the permeability to sustain basal groundwater. Because of the difficulty in distinguishing between saline and fresh groundwater, it is impossible to determine the geometry of any basal groundwater body. There is, however, no evidence of any uniform low-resistivity layer which could be interpreted as salt water underlying fresh water.

West of Grants Well, low-resistivity volcanics (38 ohm-m) may persist to at least 2.8 km below sea level.

7. RECOMMENDATIONS

The need for future water supplies will be determined by future prospects for the phosphate industry. In making recommendations in this report, we have taken into account three possible options for future water supplies; firstly, if existing seasonal water sources and springs (e.g., Ross Hill Gardens springs, Daniel Roux Caves) are developed in such a way that minimum flows of seasonal sources will meet predicted demands, further exploration for groundwater will be unwarranted; secondly, exploration for and development of new seasonal sources of water in the karst of the central plateau; and thirdly, investigation of low yield, but relatively constant sources of water within the volcanics either at high levels or at sea level.

The first option is presently being implemented by BPC; it is likely that the recommendations of this and the previous report (Polak, 1976) will not have to be considered any further. However, until the first option has been proved viable, particularly after prolonged dry seasons, the second and third alternatives remain open. Accordingly in view of these considerations the following recommendations are made.

7.1 Limestone - further investigations

Polak (1976) has outlined recommendations for further work on the Grants Well/Jedda Cave/Jane Up karst systems near WB30. From the results of the 1976 survey the following recommendations are made.

The possibility of a major karst system northeast of Grants Well between Hanitch Hill ridge and the NS baseline 460 should be investigated. The low transverse-resistance limestone area on line 366 may serve as a starting point. Flow could be expected in a southeasterly direction. Geophysics and drilling should be considered. To facilitate the investigation BPC should consider installing auxiliary NS baselines between lines 338 NS and 460 NS to ensure a better chance of intersecting any southeasterly flows.

The magnetic feature trending southeast from Camp No. 4 should be investigated for a possible karst flow (see also Polak, 1976); this may be a diversion of the Grants Well/Jedda Cave flow into the terrace area. Magnetism and resistivity data and the topography of the top of the volcanics included in this report provide strong evidence for its existence. Again auxiliary baselines should be considered.

Where possible, further geophysical investigations in the karst should make greater use of the mise-a-la-masse technique, especially with potential measurements on a grid rather than profiles, (Arandjelovic & Milosevic, 1965). The exploration for new unknown karst sources by resistivity profiling focussed at average depths in the karst should be considered. This could be supported by gradient array investigations focussed at the underlying volcanics to determine volcanic structure which may influence water flow in karst.

7.2 Volcanics - further investigations

If the volcanics are to be developed as a long-term groundwater source, drilling will have to be done and more hydrological data accumulated. The interpretations in this report should be regarded as preliminary, subject to reassessment as new hydrological data on the volcanics become available.

Because water is difficult to extract from volcanics, and is expensive drilling, it is strongly recommended that future hydrogeological investigations (drilling programs, aquifer testing, well development, etc.) in the volcanics be supervised by a qualified hydrogeologist with experience of fractured-rock environments.

Two lines of test bores are recommended: firstly, between resistivity depth probe S7 and S8 immediately west of Grants Well; and secondly, across the postulated southwest rim of the caldera delineated by the magnetic feature trending from Camp No 4 through depth probe S40 and S41. The second line should extend from the railway to line 282 EW between S40 and S41. It is further recommended that all holes be drilled at least 30 m into the volcanics to ensure the maximum chance of intersection of water-bearing zones. If both these areas prove unsuitable for groundwater development, prospects of the volcanics providing high-level groundwater from boreholes are likely to be limited, and alternative sources of water should be considered.

If high-level groundwater sources in the volcanics are found they should be monitored for at least one year to ensure that supplies are not seasonal. Any high-level supplies being recharged from the karst immediately above may reflect the seasonal fluctuations of the karst also. Low-level sources in the volcanics such as Waterfall and the offshore springs in Flying Fish Cove should be less subject to seasonal effects than high-level sources.

If several low-yield bores on the central plateau are needed to sustain the supply of groundwater, and these are expensive to develop, an alternative would be to excavate a gallery similar to that on Tenerife, Canary Islands (Ecker, 1976). A suitable place to excavate a gallery might be via a tunnel extending from Ross Hill Gardens into the volcanics, possibly as far as the postulated faulted edge of the caldera (about 1500 m), or extending only as far as required to ensure adequate supply. The volcanics beneath the limestone terrace behind Ross Hill Gardens show uniformly low resistivities, suggesting high saturation. Barounis (1965) has discussed the hydrogeological, design, and construction aspects of infiltration galleries.

If further geophysical investigations in the volcanics are to be considered, depth probing should use shallow audiofrequency magnetotelluric techniques, rather than time-consuming DC resistivity, to penetrate the high-resistivity limestone mantle. Resistivity (or more appropriately conductivity) detail in the volcanics should be less obscured in the magnetotelluric data. The main investigation technique should be DC resistivity gradient array using grid measurements (the rectangle method, Kunetz, 1966, p. 31) focussed at the volcanics to investigate the trend of vertical structure. Use of induced polarisation measurements (taking into account possible surface effects due to phosphate) with the rectangle method should also be considered.

8. ACKNOWLEDGEMENTS

We thank the staff of the British Phosphate Commissioners, in particular: J. Hoare of the Melbourne Office; D. Powell and members of the island surveying office for their generous assistance.

Peter Barrett, BPC geologist, especially ensured that the survey ran smoothly, and provided valuable geological information.

Within BMR, D. Hsu assisted with magnetic interpretation; A. Murray and B. Barlow assisted in reduction and analysis of the gravity results; W. Anfiloff carried out two-dimensional gravity modelling of terrain, and K. Barrett and B. Holden drafted the illustrations for the report. Their efforts are gratefully acknowledged.

We thank the following individuals and organizations for permission to reproduce the five figures in Plate 2: Department of Land and Natural Resources, Hawaii (Fig. 1); John Wiley and Sons Inc., New York (Fig. 2); Amos Ecker of the Geological Survey of Israel and Elsevier Scientific Publishing Company, Amsterdam (Fig. 3); International Association of Hydrogeologists (Fig. 4); and the U.S. Geological Survey, Water Resources Division, California (Fig. 5).

9. REFERENCES

- ABELL, R.S., 1976 - Groundwater investigation of Norfolk Island
Bureau of Mineral Resources Australia Record 1976/62 (unpublished)
- ANDREW, T. & WAINWRIGHT, M., 1965 - Lae resistivity survey for
underground water, Territory of Papua and New Guinea, 1964
Bureau of Mineral Resources Australia Record 1965/207 (unpublished)
- ANDREWS, C.W., 1900 - A MONOGRAPH OF CHRISTMAS ISLAND (INDIAN OCEAN)
British Museum of Natural History
- ANFILOFF, W., 1975 - Automated density profiling over elongate topographic
features. Bureau of Mineral Resources Journal of Australian Geology
and Geophysics 1(1), 57-61
- ARANDJELOVIC, D., and MILOSEVIC., 1965 - Hydrogeological investigations in
Yugoslav karst areas by application of geophysical methods. International
Association of Hydrogeologists Memoires, 7, Congress of Hannover 247-54.
- BAROUNIS, A.N., 1965 - Infiltration galleries, hydrogeological study,
hydraulic design and construction. International Association of
Hydrogeologists Memoires, 7, Congress of Hannover, 323-31.
- BARRIE, J., 1967 - The geology of Christmas Island. Bureau of Mineral
Resources Australia Record 1967/37 (unpublished)
- BULLARD, F.M., 1962 - VOLCANOES IN HISTORY, IN THEORY, IN ERUPTION
University of Texas Press.
- CAMPBELL-SMITH, W., 1926 - The volcanic rocks of Christmas Island
Quarterly Journal of Geological Society of London, 82, 44
- COOPERS, H.H., 1959 - A hypothesis concerning the dynamic behaviour of
fresh water and salt water in a coastal aquifer Journal of Geophysical
Research 64, 461-7
- DAVIS, S.N., & DE Wiest, R.J.M., 1966 - HYDROGEOLOGY. J. Wiley & Sons Ltd,
New York.

- DOBRIN, M.B., 1960 - INTRODUCTION TO GEOPHYSICAL PROSPECTING. McGraw-Hill Book Co., New York.
- DUPRAT, A., SIMLER, L., & UNGEMACH, P., 1970 - Contribution de la prospection electrique a la recherche des caracteristiques hydrodynamiques d'un milie aquifere. Terres et Eaux, 23, 23-31.
- ECKER, A., 1976 - Groundwater behaviour in tenerife, volcanic island (Canary Islands, Spain). Journal of Hydrology, 28(1), 73-86.
- GHOSH, D.P., 1971 - Inverse filter coefficients for the computation of apparent resistivity standard curves for a horizontally layered earth. Geoph. Prosp. 19(4), 769-75.
- HENRY, H.R., 1964 - Interfaces between salt water and fresh water in coastal aquifers In Seawater & Coastal Aquifers. US Geological Survey Water-Supply Paper 1613, 35-70.
- JONGSMA, D., 1976 - A review of the geology and geophysics of Christmas Island and the Christmas Rise Bureau of Mineral Resources Australia Record 1976/37 (unpublished)
- KIDD, C.H., 1976 - Hydrogeology of Karkar Island - Preliminary study Geological Survey of Papua New Guinea Report 74/9 (unpublished).
- KOEFOED, O., 1968 - The application of the Kernel function in interpreting geoelectrical resistivity measurements. Geoexploration Monographs 1(2), Gebruder Borntraeger Berlin-Nikolassee.
- KUNETZ, G., 1966 - Principles of direct current resistivity prospecting. Geoexploration Monographs 1(1), Gebruder Borntraeger Berlin-Nikolassee.
- LE PICHON, X., FRANCHETEAU, J., & BONNIN, J., 1973 - PLATE TECTONICS. Elsevier Scientific Publishing Co. Amsterdam.
- MARTIN-KAYE, P.H.A., 1969 - A summary of the geology of the Lesser Antilles. Overseas Geology and Mineral Resources 10(2), 172-206.
- MERRICK, N.P., 1974 - The Pole-Multipole method of geoelectrical sounding. Australian Society of Exploration Geophysicists Bulletin 5(2), 48-64.

- O'NEILL, D.J., 1975 - Improved linear filter coefficients for application in apparent resistivity computations. Australian Society of Exploration Geophysicists Bulletin 6(4), 104-9 (errata 7(1), p 48)
- PALMER, H.S., 1957 - Origin and diffusion of the Herzberg principle with especial reference to Hawaii. Pacific Science 11, 181-189.
- POLAK, E.J., 1976 - Christmas Island (Indian Ocean) geophysical survey for groundwater, 1973. Bureau of Mineral Resources Australia Record 1976/100 (unpublished).
- PURBO-HADIWIDJOJO, M.M., 1967 - Hydrogeology of strato-volcanoes, a geomorphic approach. International Association of Hydrogeologists, Memoires, Congress of Hannover, vol. 7, p. 293-8.
- RIVEREAU, J.C., 1965 - Notes on a geomorphological study of Christmas Island, Indian Ocean. Bureau of Mineral Resources Australia Record 1965/116 (unpublished).
- ROBERTSON, E.I., 1967a - Gravity effects of volcanic islands. New Zealand Journal of Geology and Geophysics 10(6), 1466-83.
- ROBERTSON, E.I., 1967b - Gravity survey in the Cook Islands. New Zealand Journal of Geology and Geophysics 10(6), 1484-98
- SPIES, B.R., 1975 - A fortran program for calculating the gravity effect of a three dimensional body of arbitrary shape. Bureau of Mineral Resources Australia Record 1975/4 (unpublished)
- STEARNS, H.T., 1940 - Geology and groundwater resources of the islands of Lanai and Kahoolawe, Hawaii. Territory of Hawaii, Division of Hydrography Bulletin 6, p. 137.
- STEARNS, H.T., 1942 - Hydrology of volcanic terrains In MEINZER, O.E., (Editor) Physics of the Earth Volume 9, McGraw Hill, New York
- TEMPERLEY, B.N., 1960 - A study of the movement of groundwater in lava-covered country. Overseas Geology and Mineral Resources 8(1), 37-52.

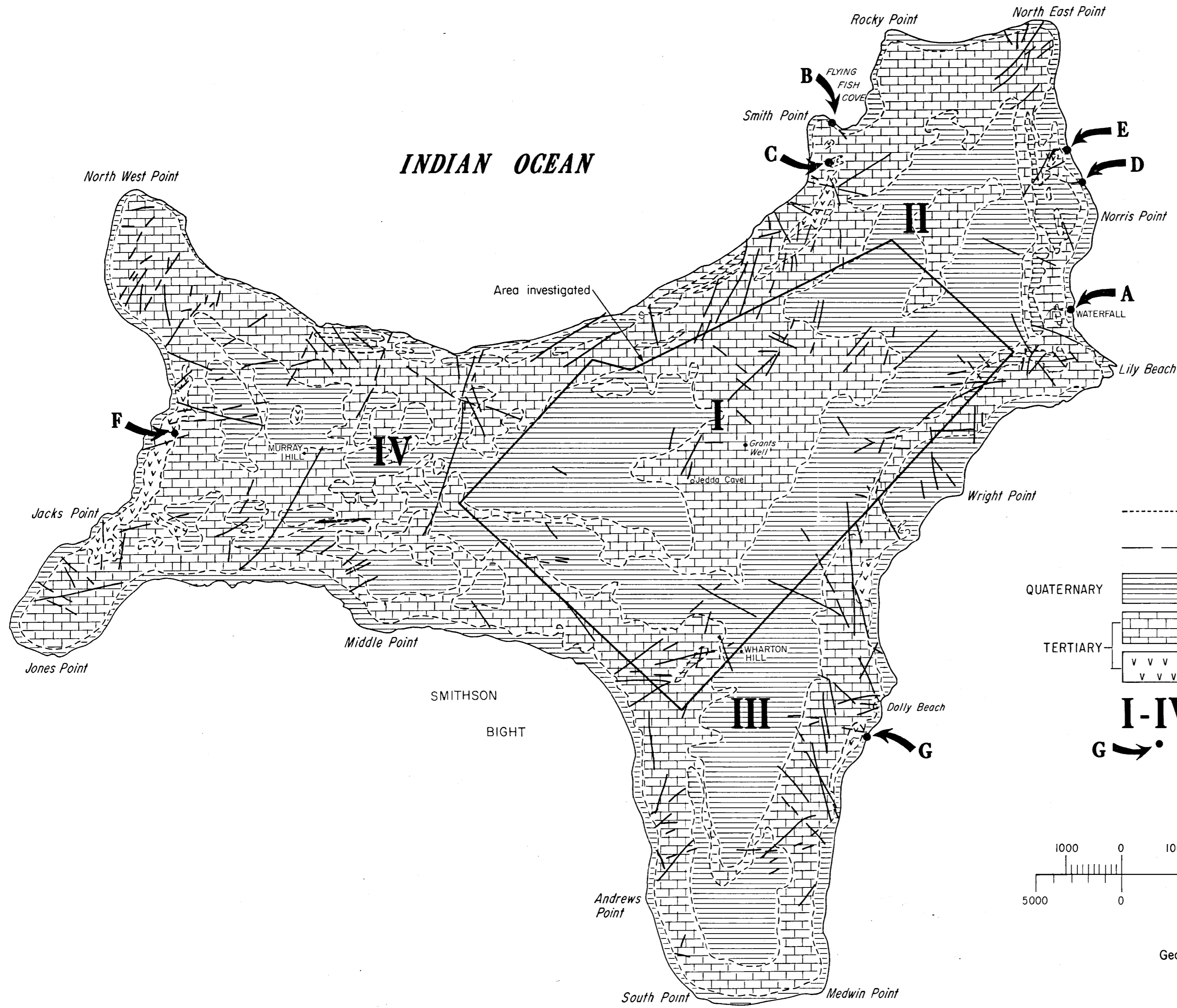
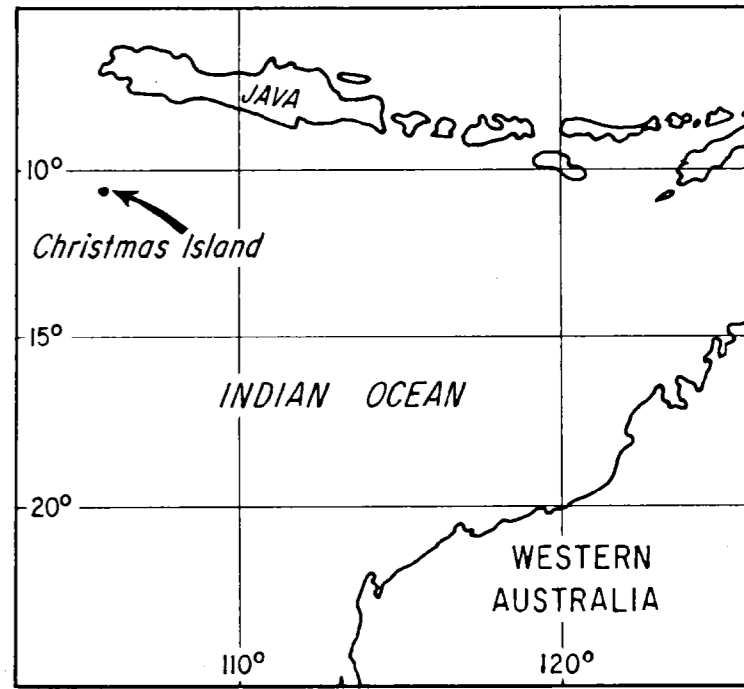
- TRUEMAN, N.A., 1965 - Geological and Mineralogical Investigation - Christmas Island, Indian Ocean, Volume 1 AMDEL Report 399, 1 (unpublished).
- VAN BEMMELEN, R.W., 1949 - THE GEOLOGY OF INDONESIA. Martinus Nijhoff, The Hague.
- VINCENZ, S.A., 1968 - Resistivity investigations of limestone aquifers in Jamaica. Geophysics, 33(6), 980-94.
- VISHER, F.N., & HINO, J.F., 1964 - Groundwater resources in Southern Oahu, Hawaii. US Geological Survey Water-Supply Paper, 1778.
- WARD, P.E., HOFFARD, S.H., & DAVIS, D.A., 1965 - Hydrology of Guam. US Geological Survey Professional Paper 403-4.
- WENTWORTH, C.K., 1947 - Factors in the behaviour of groundwater in a Ghyben-Herzberg system. Pacific Science 1, 172-84.
- WILLIAMS & HOWELL, 1941 - CALDERAS AND THEIR ORIGIN University of California Publication, Bulletin of the Department of Geological Sciences 25, 239.
- WOOLARD, G.P., 1951 - A gravity reconnaissance of the island of Oahu Transactions of the American Geophysical Union 32(3), 358-67.
- ZOHDY, A.A.R., EATON, G.P., & MABEY, D.R., 1974 - Techniques of water resource investigations of the United States Geological Survey. Book 2 Chapt. D1: Application of surface geophysics to groundwater investigations. US Geological Survey
- ZOHDY, A.A.R., 1975 - Automatic interpretation of Schlumberger sounding curves using modified Dar Zarrouk functions. US Geological Survey Bulletin 1313-E.

APPENDIX 1

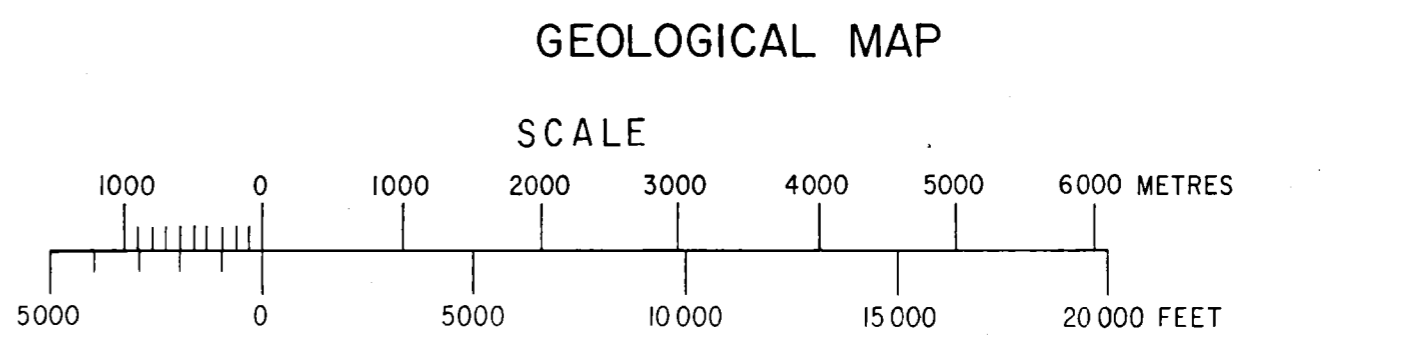
GRAVITY SURVEY STATISTICS

Time of survey and (BMR survey no.):	Sept-October 1973	(7309)	
	Aug-October 1976	(7604)	
	E.J. Polak (1973, 1976)		
	G.R. Pettifer (1976)		
1976 survey and 1973 survey recomputation based on:	Station No 7309 - 0002		
	Observed gravity (preliminary) value		
	978, 488.32 mGal		
Meter calibration factors:	LaCoste-Romberg G20 (1.0487 ± 0.0001 est)		
	LaCoste-Romberg G101 (1.0452 ± 0.0001 est)		
Bouguer reduction density:	2.67 g/cm ³		
Base map:	(DNM, X782 Edition 5, 1972)		
Terrain correction:	Not applied. Maximum terrain correction estimated at 6 mGal. No corrections applied for bathymetry		
No. of stations:	<u>1973</u>	<u>1976</u>	<u>Total</u>
Detailed traverses	576	469	1045
Regional	<u>35</u>	<u>92</u>	<u>127</u>
Total	611	561	1172
Bouguer anomaly relative errors (in mGal):	<u>Traverse</u>	<u>Regional</u>	
Height	± 0.01	± 0.1 (maxm)	
Latitude	± 0.006	± 0.02	
Observed			
Gravity	<u>± 0.05</u>	<u>± 0.05</u>	
RMS	<u>± 0.05</u>	<u>± 0.1</u>	
Detailed traverse station spacings:	1973	10 m to 30 m	
	1976	61 m	

-9 SEP 1980



- LEGEND**
- Geological boundary
 - Fault or fracture (airphoto-interpretation)
 - QUATERNARY: [Pattern of horizontal lines] Unconsolidated phosphate, phosphatic soil and boulders, etc.
 - TERTIARY: [Pattern of vertical lines] Limestone
 - [Pattern of 'V' shapes] Volcanics - basalt
 - I-IV Postulated cone and rift zone areas (Polak, 1976)
 - G Palaeomagnetic and geochronology sample location (Polak, 1976)



Geology after Barrie, 1967

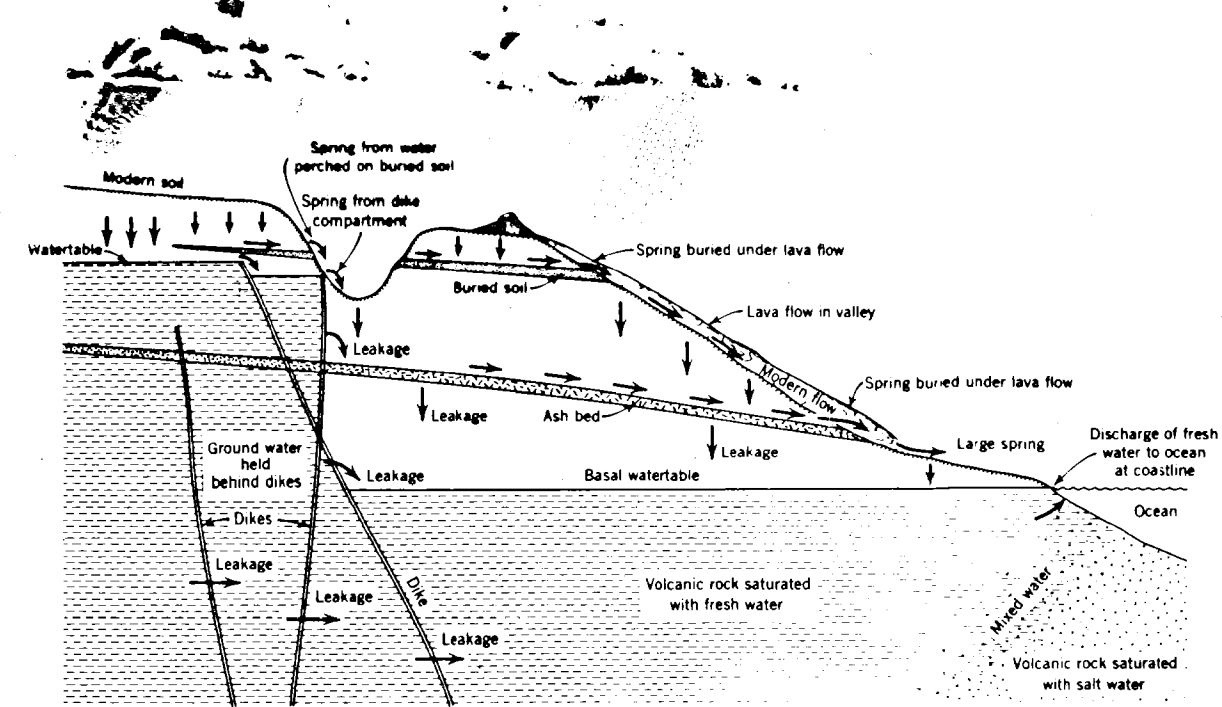


Fig.2 HAWAIIAN ISLANDS GROUNDWATER SCHEMATIC MODEL
FROM DAVIS & DE WIEST, 1966

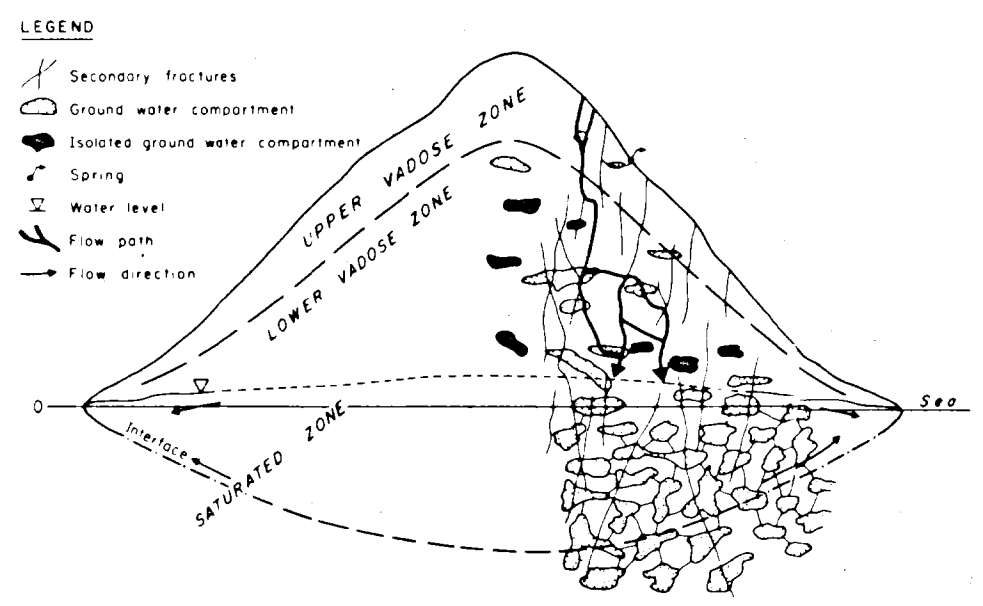


Fig.3 TENERIFE, CANARY ISLES GROUNDWATER SCHEMATIC MODEL
FROM ECKER, 1976

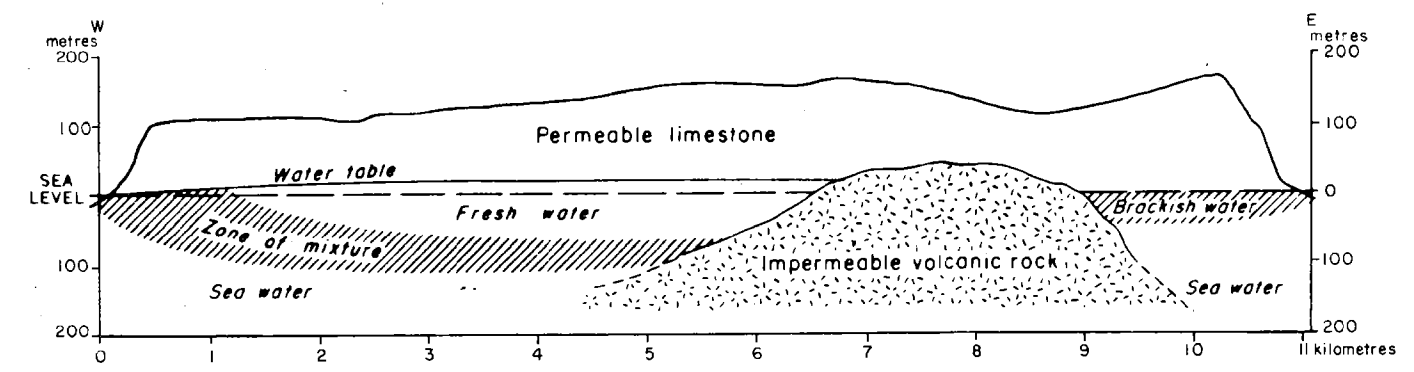


Fig.5 GUAM ISLAND CROSS SECTION
FROM WARD & OTHERS, 1965

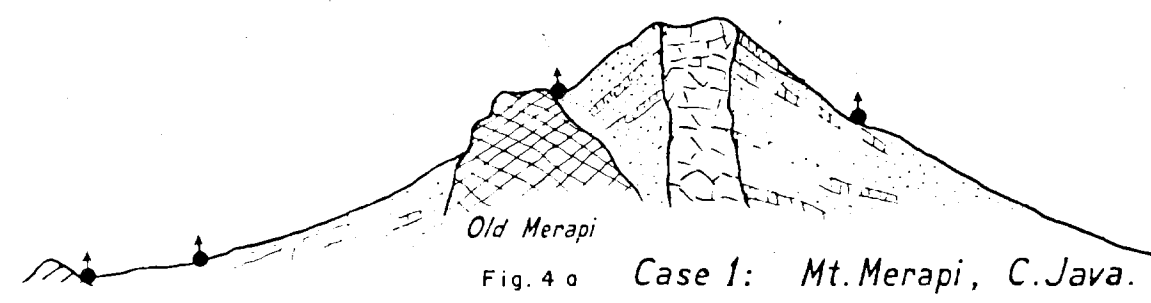


Fig. 4 a Case 1: Mt. Merapi, C. Java.

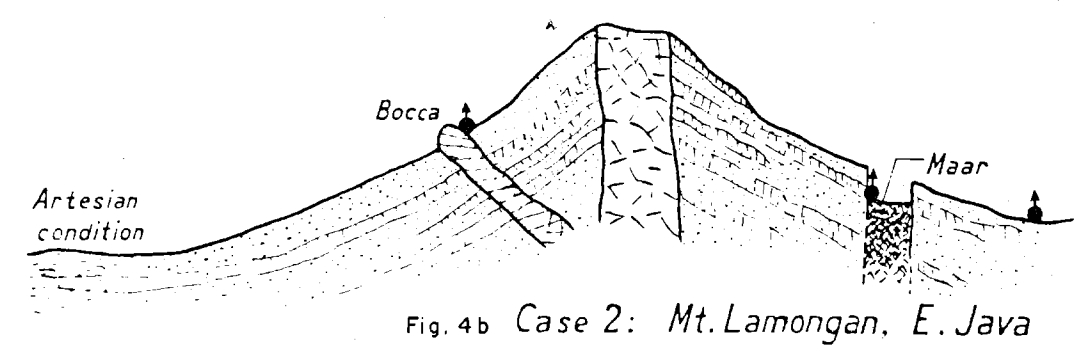


Fig. 4 b Case 2: Mt. Lamongan, E. Java

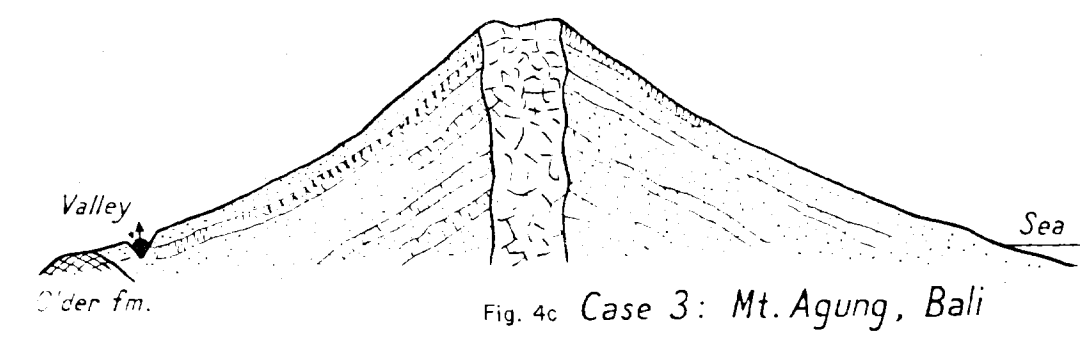


Fig. 4 c Case 3: Mt. Agung, Bali

SCHEMATIC GROUNDWATER MODELS
OF VOLCANIC ISLANDS

INDONESIAN STRATOVOLCANOES GROUNDWATER SCHEMATIC MODEL
FROM PURBO-HADIWIDJOJO, 1967

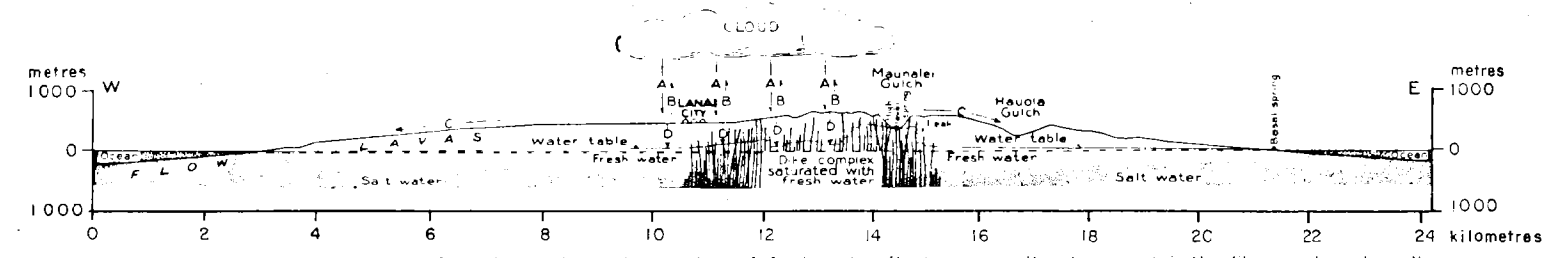


Fig. 1 LANAI ISLAND, HAWAII GROUNDWATER SCHEMATIC MODEL
FROM STEARNS, 1940

90000 E 100000 110000 120000 E

CHRISTMAS ISLAND

DISTRIBUTION OF PHOSPHATE (CENTRAL AREA)

(SOURCE : BRITISH PHOSPHATE COMMISSIONERS)

0 1 2 km

INDIAN OCEAN

INDIAN OCEAN

SMITHSON BIGHT
INDIAN OCEAN

10°26'S

100000

90000

10°30'S

80000 N

Daniel Roux Cave

Radio Station

Norris Point

Jones Spring

Freshwater Spring

WATERFALL

Low Pt

Steep Point

Allan Point

Hosnies Spring

Wright Point

Deans Point

John D. Point

Dolly Beach

McMicken Point

WHARTON HILL
284

Ross Hill Trig
319

Camp 4

Jane-Up

WB 30

WB 14

WB 46

Ross Hill Gardens Springs

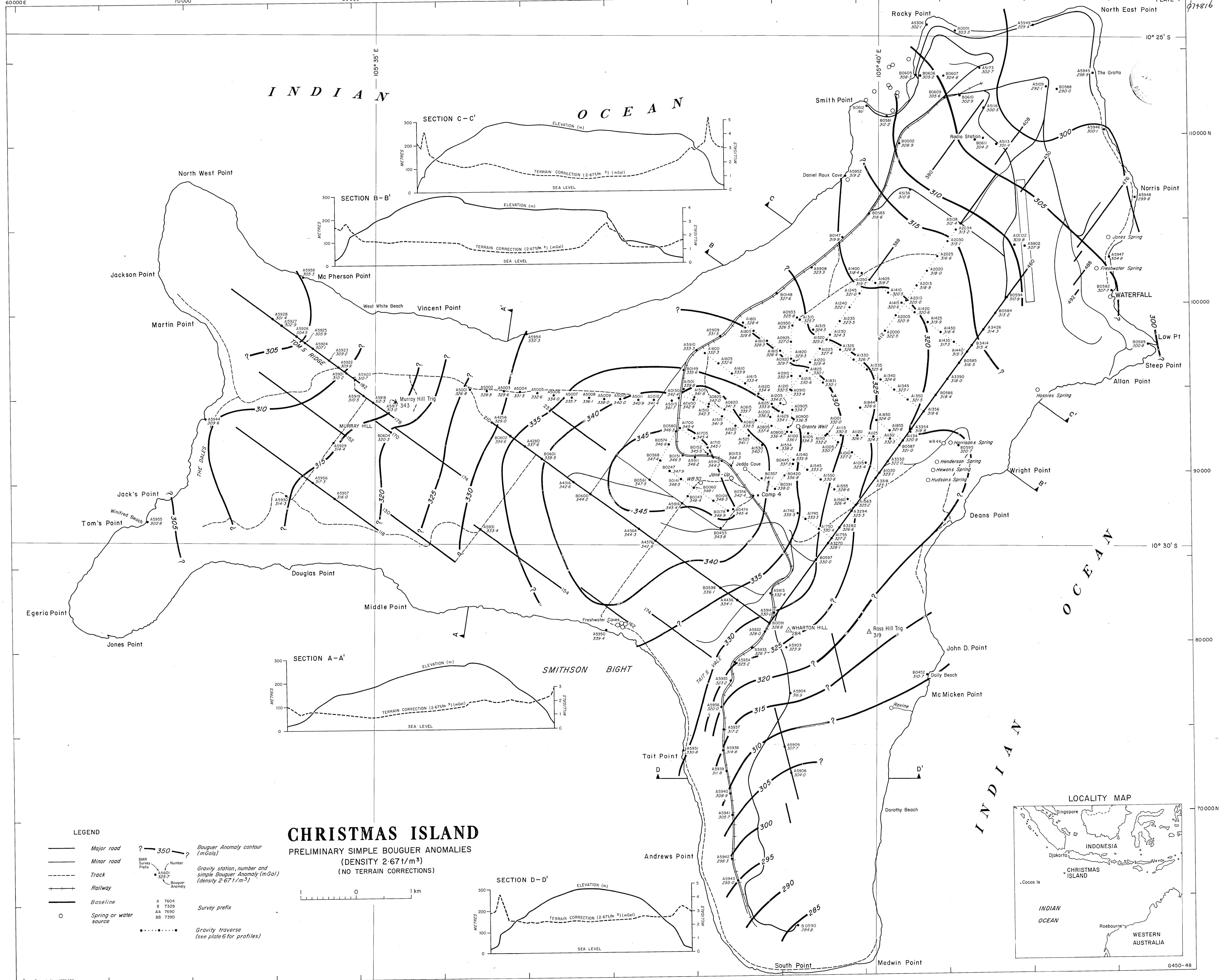
Grants Well

Jedda Cave

Freshwater Caves

LEGEND

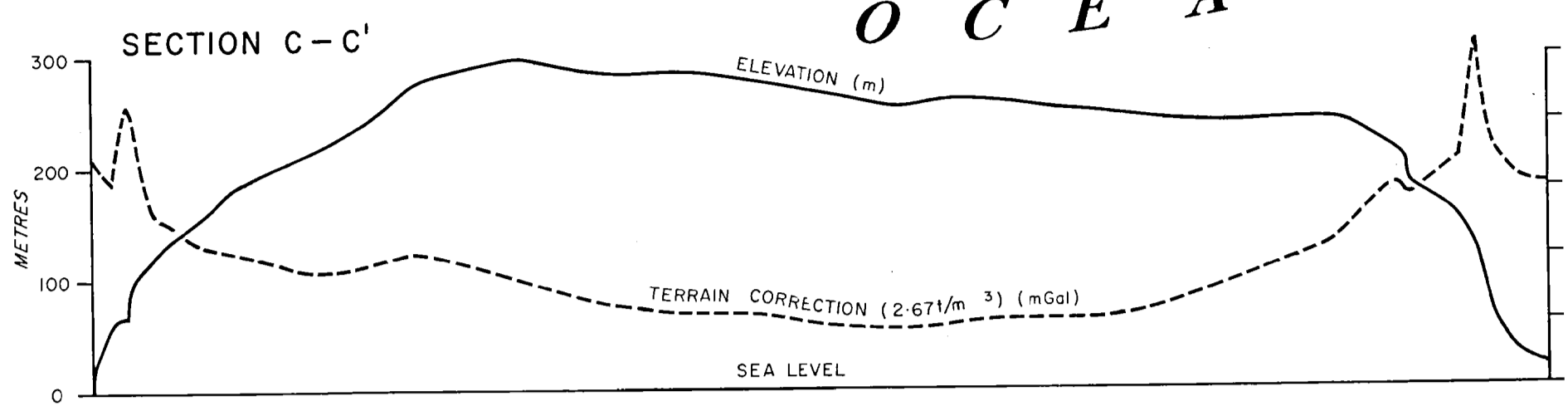
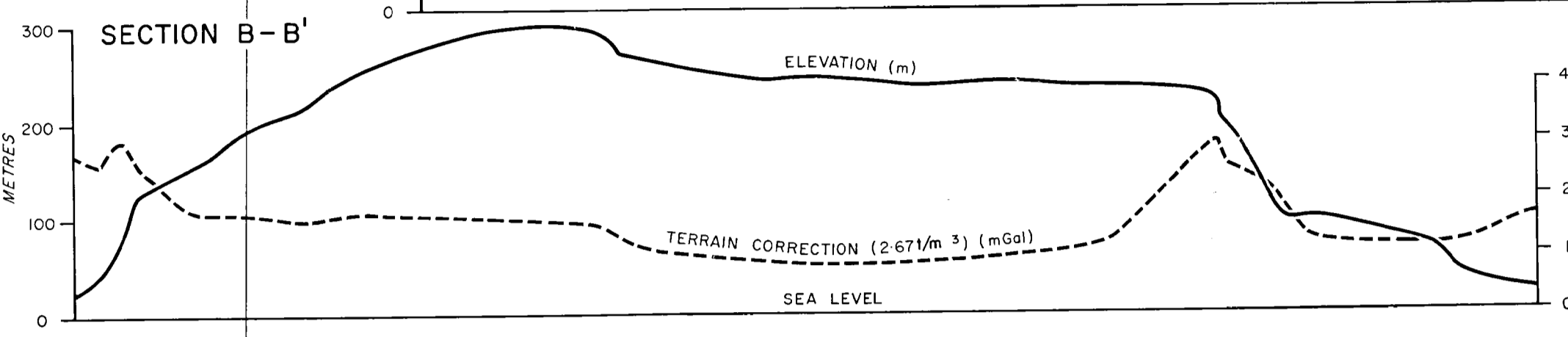
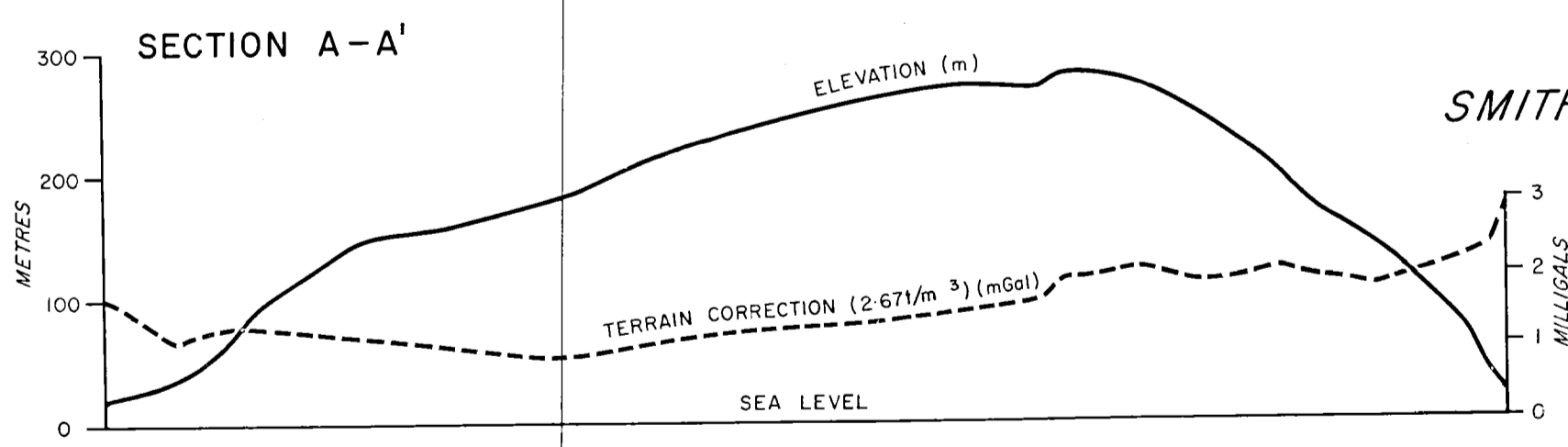
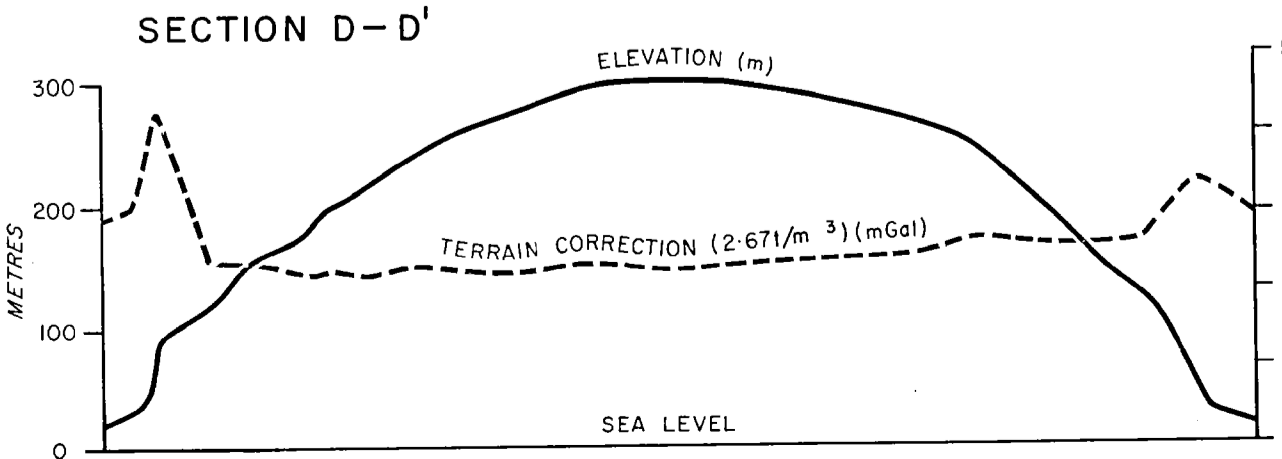
- Traverse line
- - - Interpreted fault (after Barrie, 1967)
- - - Road
- + + + Railway
- Spring, well, cave
- Water-bore
- △ Control point
- ▨ 3-10 metres depth
- ▨ 10-30 metres depth
- ▨ > 30 metres
- 29 Maximum depth of phosphate (metres)

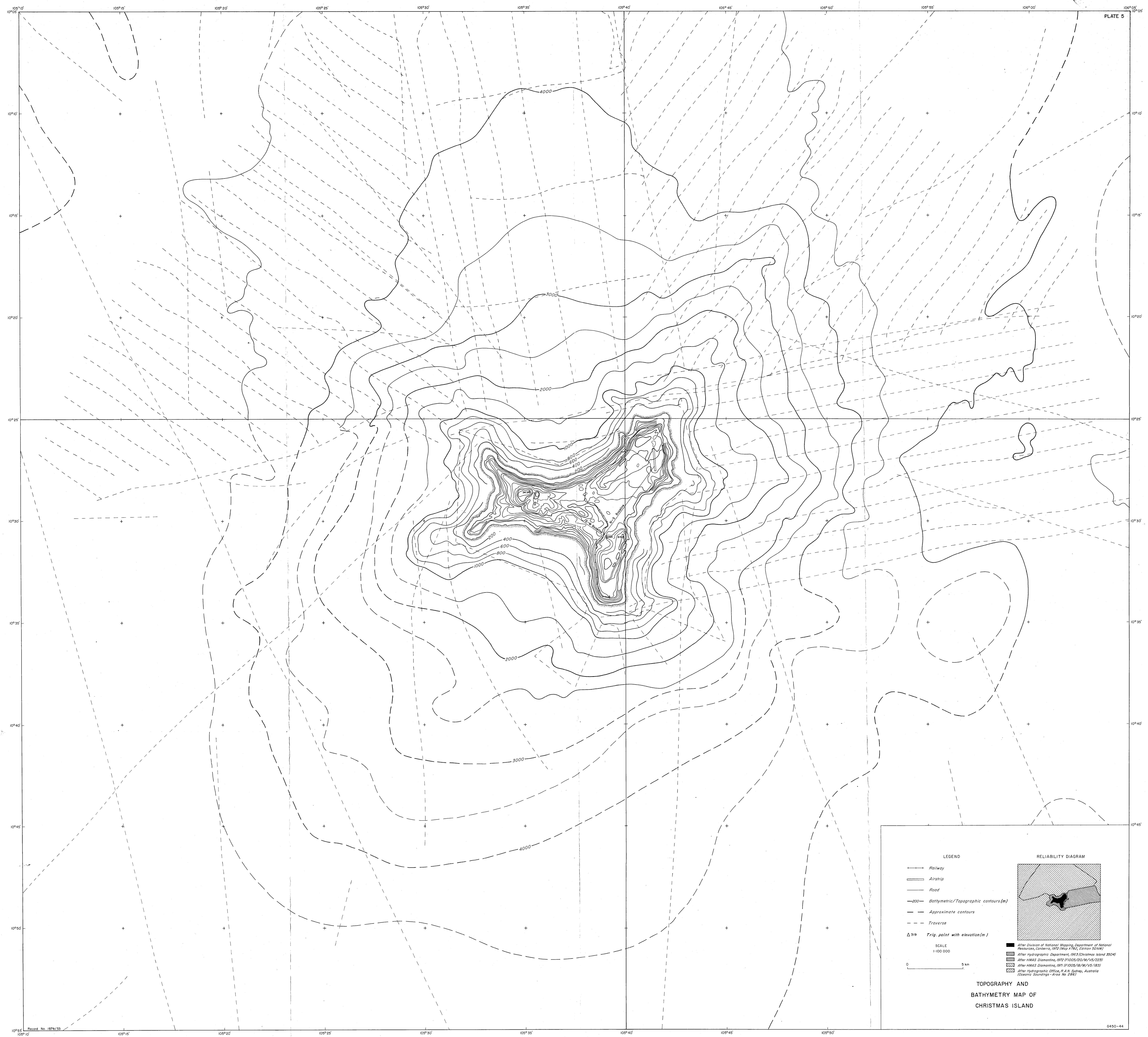


- LEGEND
- Major road
 - Minor road
 - Track
 - Railway
 - Baseline
 - Spring or water source
 - Bouguer Anomaly contour (mGal)
 - Gravity station, number and simple Bouguer Anomaly (mGal) (density 2.671/m³)
 - Survey prefix
 - Gravity traverse (see plate 6 for profiles)
- BMR Survey Prefix
- | Prefix | Number |
|--------|--------|
| A | 7604 |
| B | 7309 |
| AA | 7690 |
| BB | 7390 |

CHRISTMAS ISLAND
PRELIMINARY SIMPLE BOUGUER ANOMALIES
(DENSITY 2.671/m³)
(NO TERRAIN CORRECTIONS)

1 0 1 km





LEGEND

- +— Railway
- Airstrip
- Road
- 200— Bathymetric/Topographic contours (m)
- - - Approximate contours
- - - Traverse
- Δ 319 Trig point with elevation (m)

RELIABILITY DIAGRAM

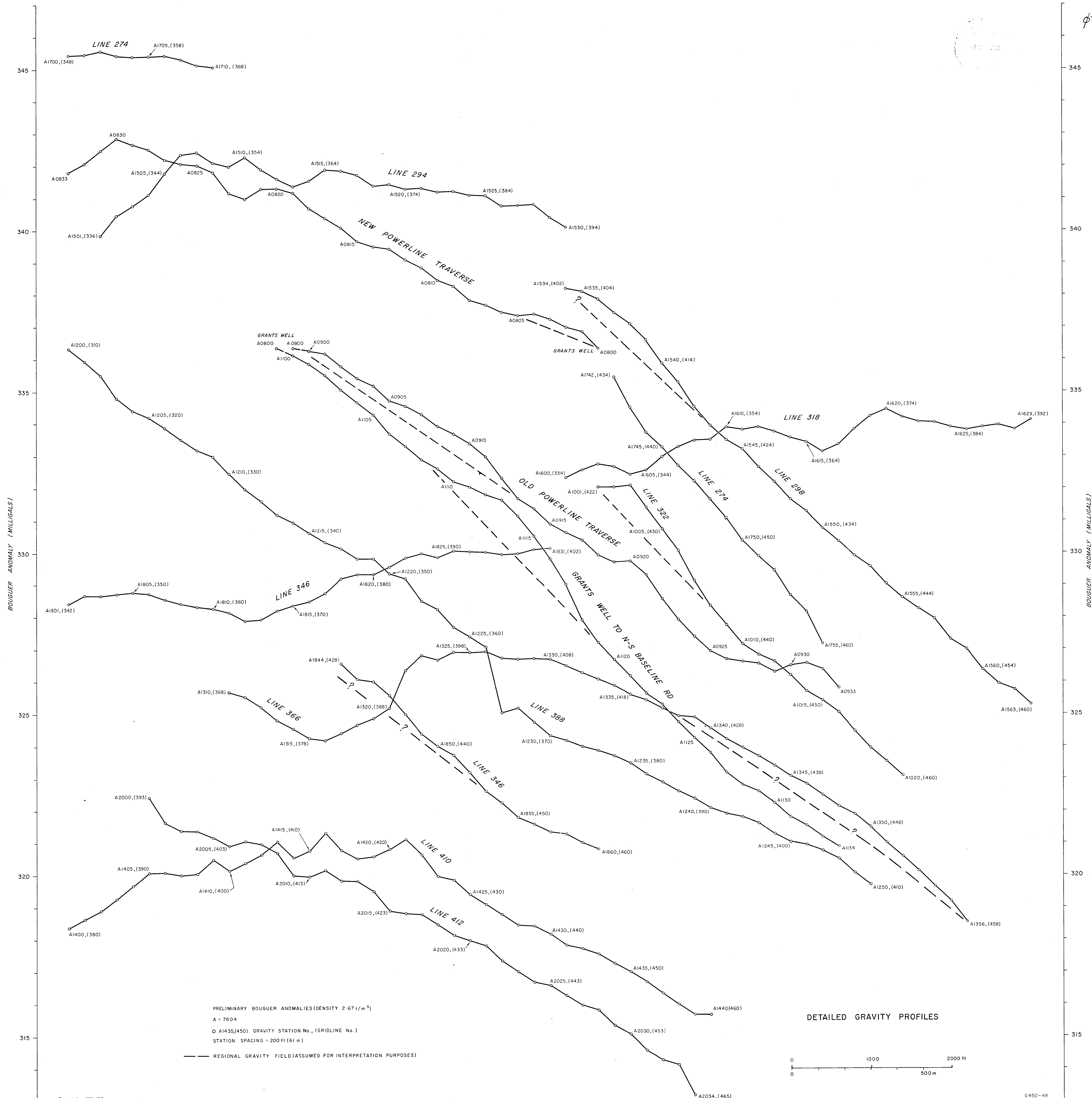
SCALE
1:100 000

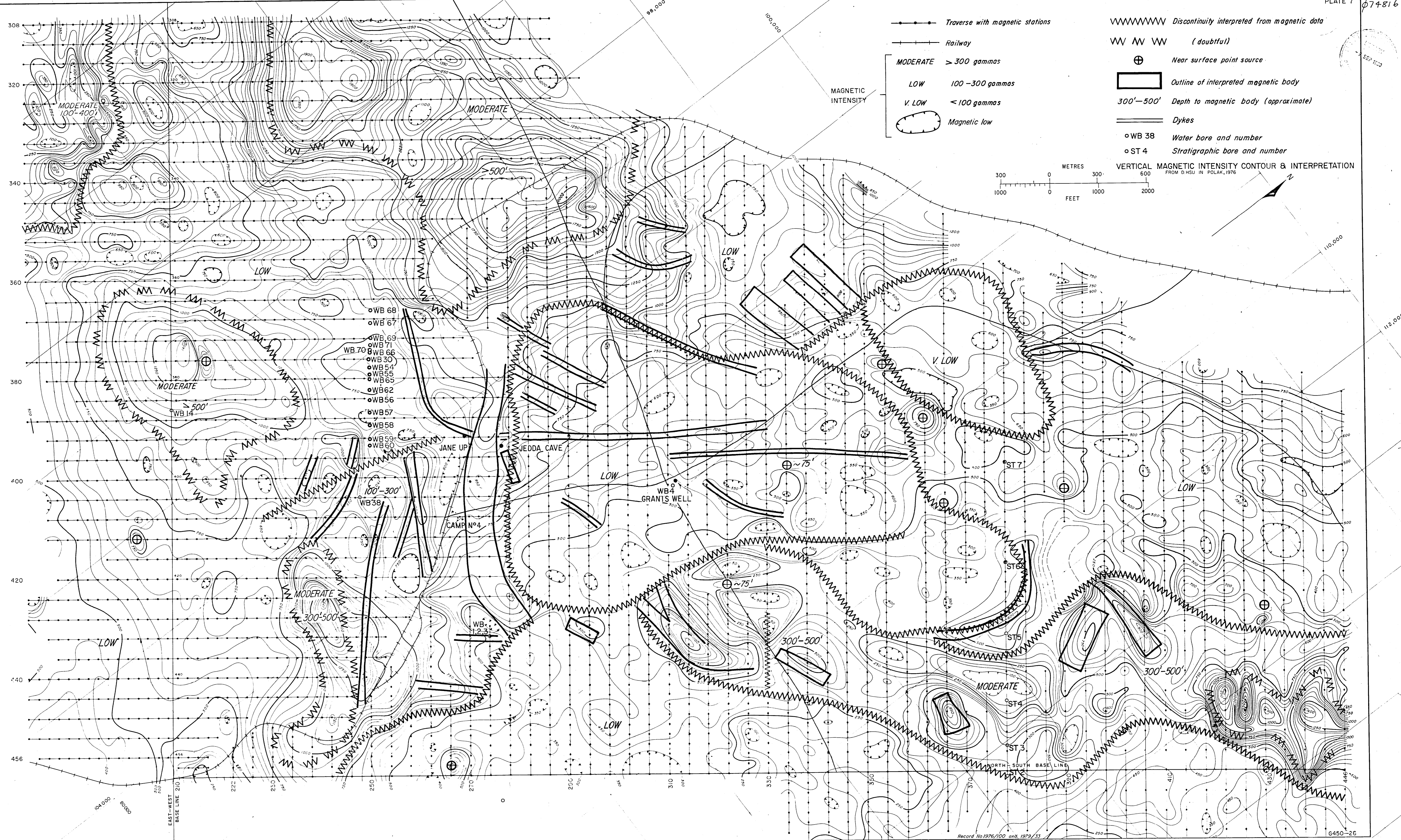
0 5 km

**TOPOGRAPHY AND
BATHYMETRY MAP OF
CHRISTMAS ISLAND**

After Division of National Mapping, Department of National Resources, Canberra, 1952 (Ship 1782, Chart 52141)
After Hydrographic Department, 1963 (Christmas Island 3504)
After HMAS Diamantina, 1972 (11005/20/M/V/5/223)
After HMAS Diamantina, 1971 (11005/18/M/V/5/183)
After Hydrographic Office, R.A.N. Sydney, Australia
(Oceanic Soundings - Area No. 286)

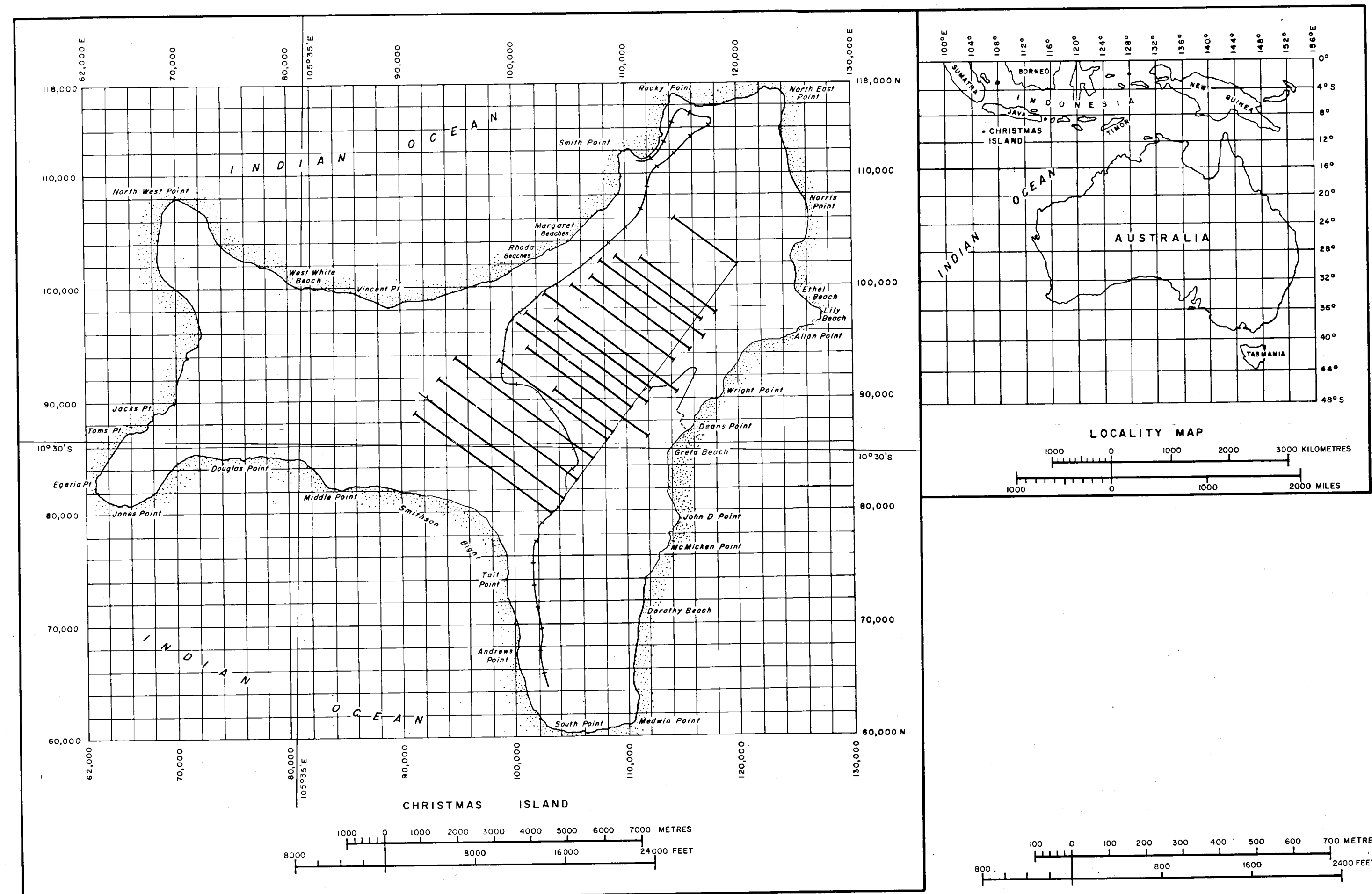
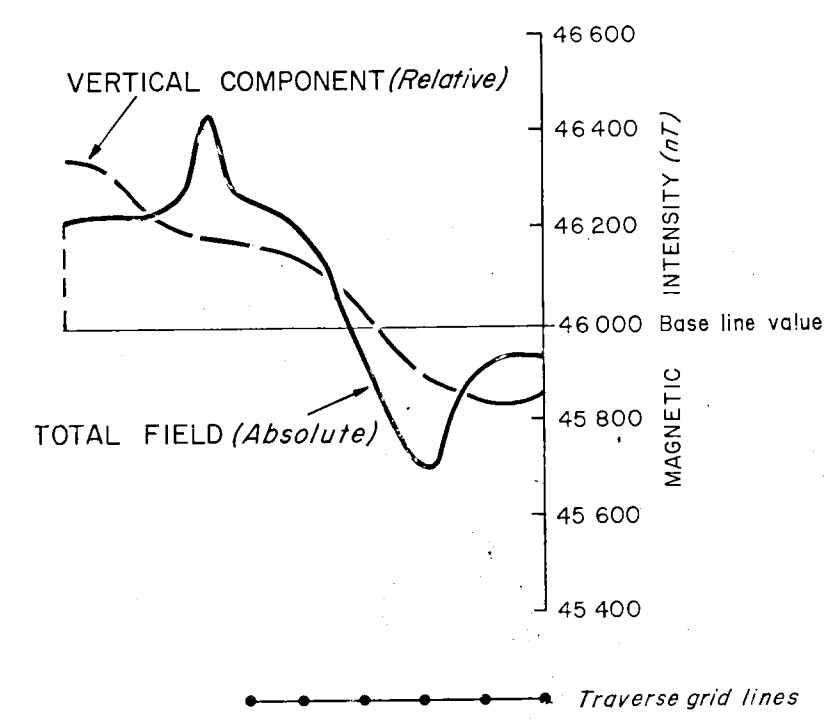
074816





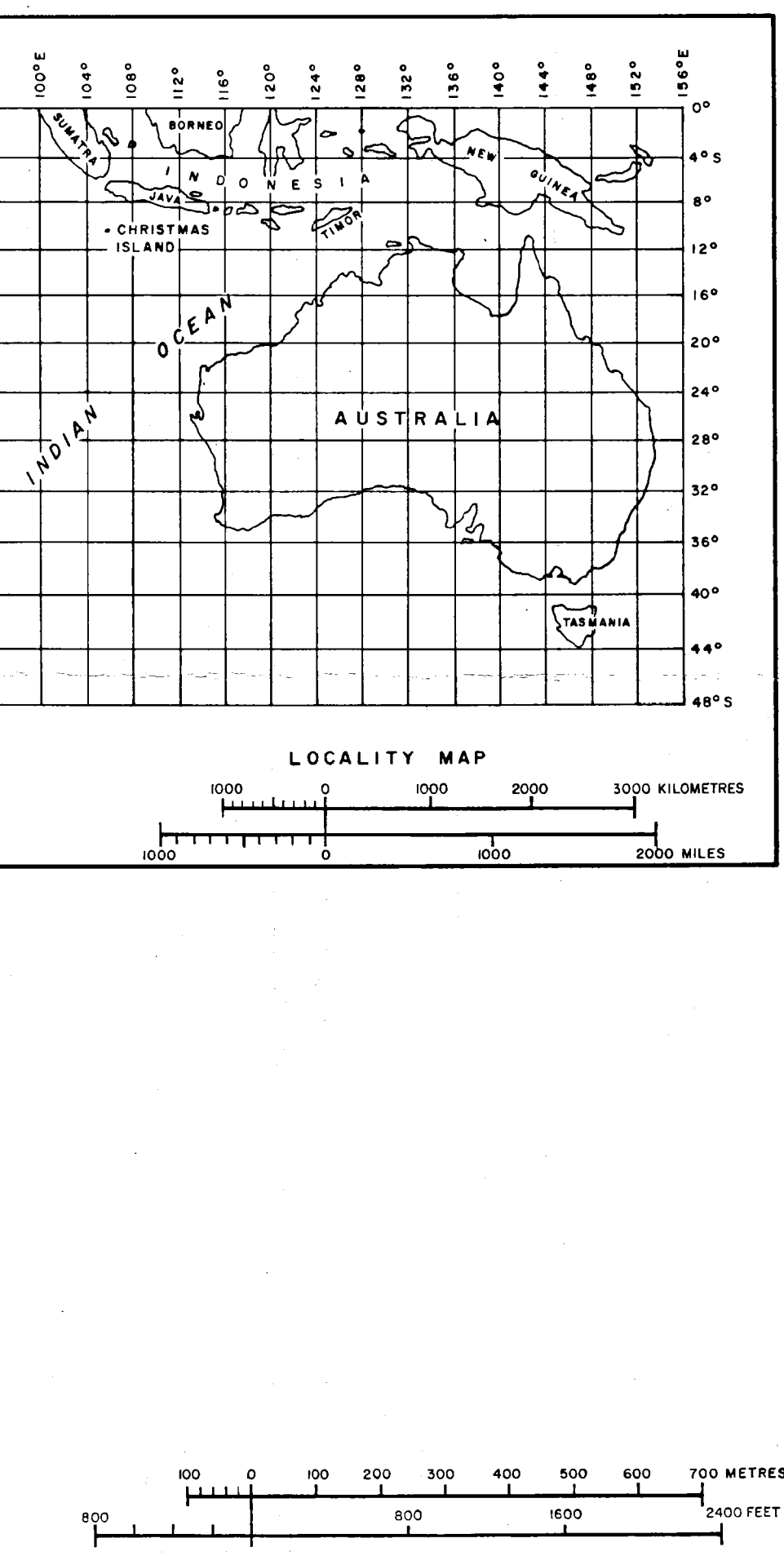
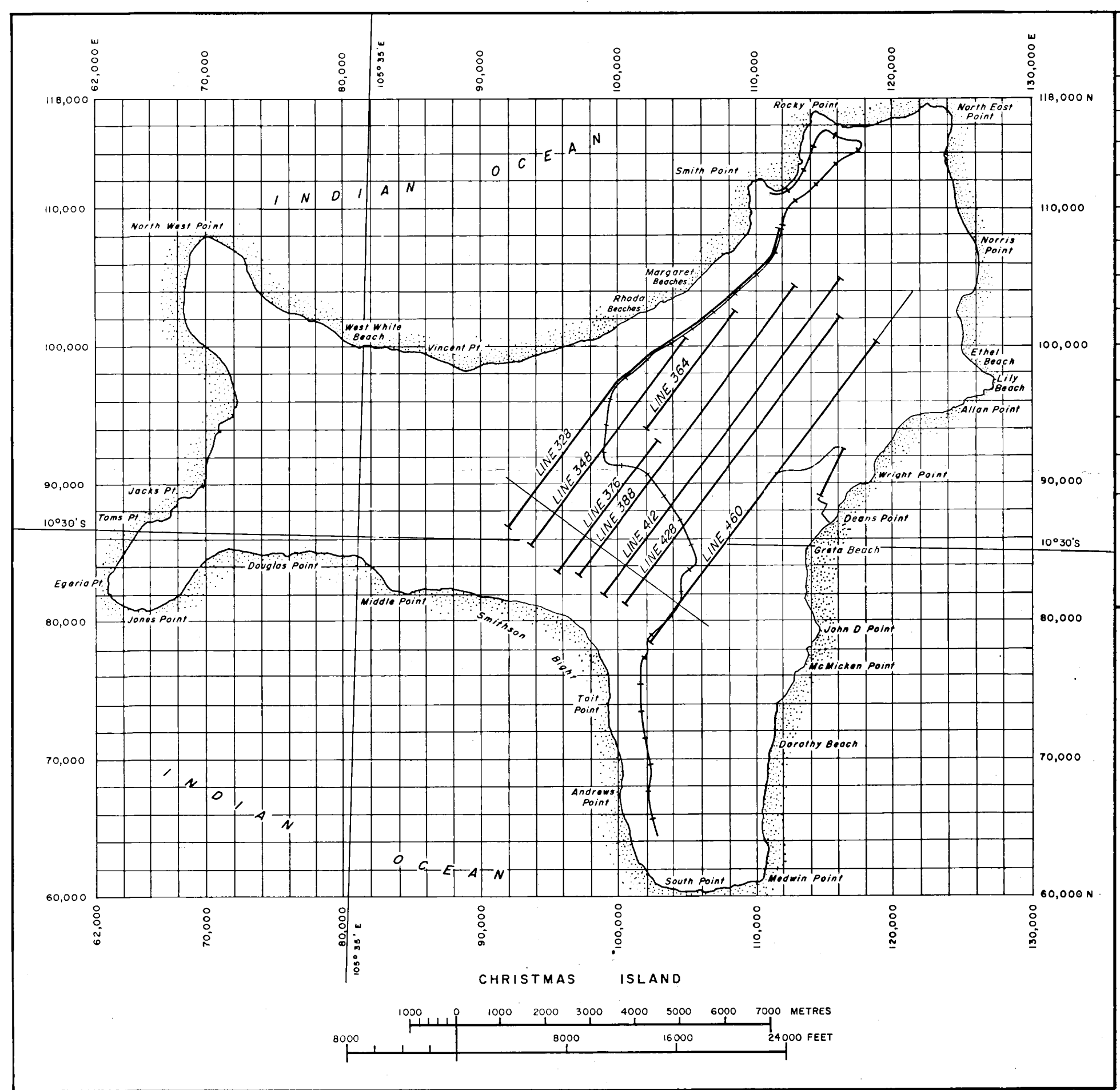
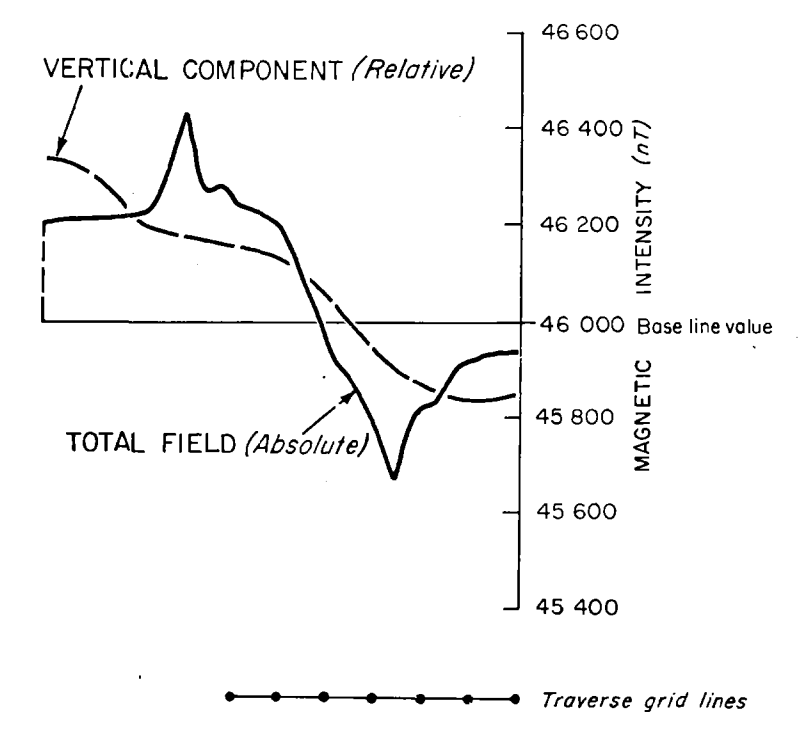


MAGNETIC INTENSITY PROFILES
(ALONG EAST-WEST GRID LINES)

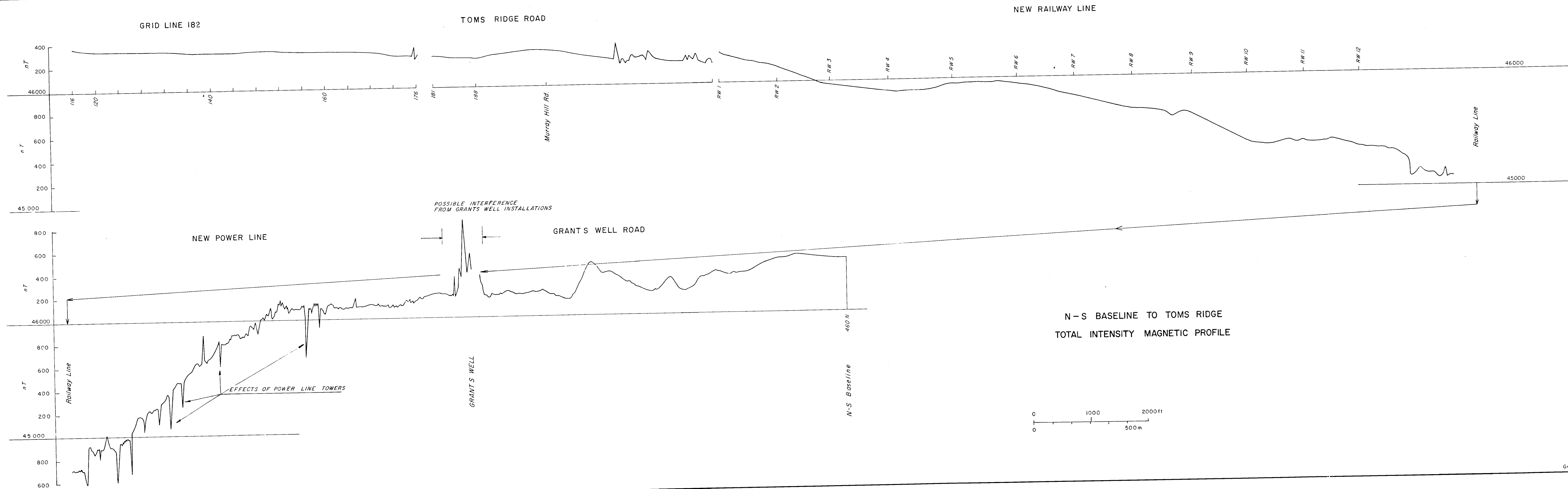


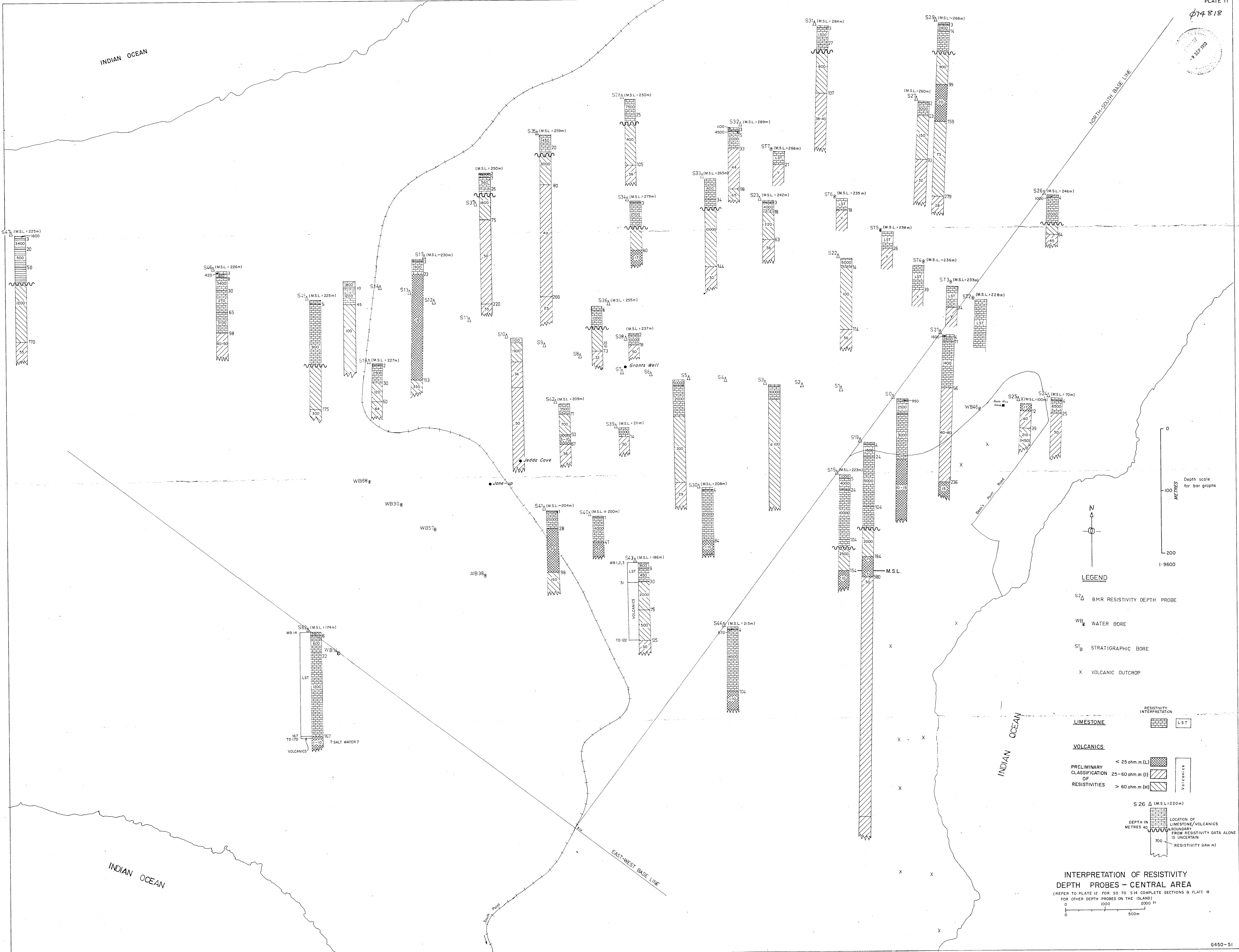


MAGNETIC INTENSITY PROFILES
(ALONG NORTH-SOUTH GRID LINES)



074818





LEGEND

S2 Δ BMR RESISTIVITY DEPTH PROBE
WB WATER BORE
ST STRATIGRAPHIC BORE
X VOLCANIC OUTCROP

RESISTIVITY INTERPRETATION

LIMESTONE LST

VOLCANICS

PRELIMINARY CLASSIFICATION OF RESISTIVITIES

< 25 ohm.m (L)
25-60 ohm.m (I)
> 60 ohm.m (H)

LOCATION OF LIMESTONE/VOLCANICS BOUNDARY FROM RESISTIVITY DATA ALONE IS UNCERTAIN

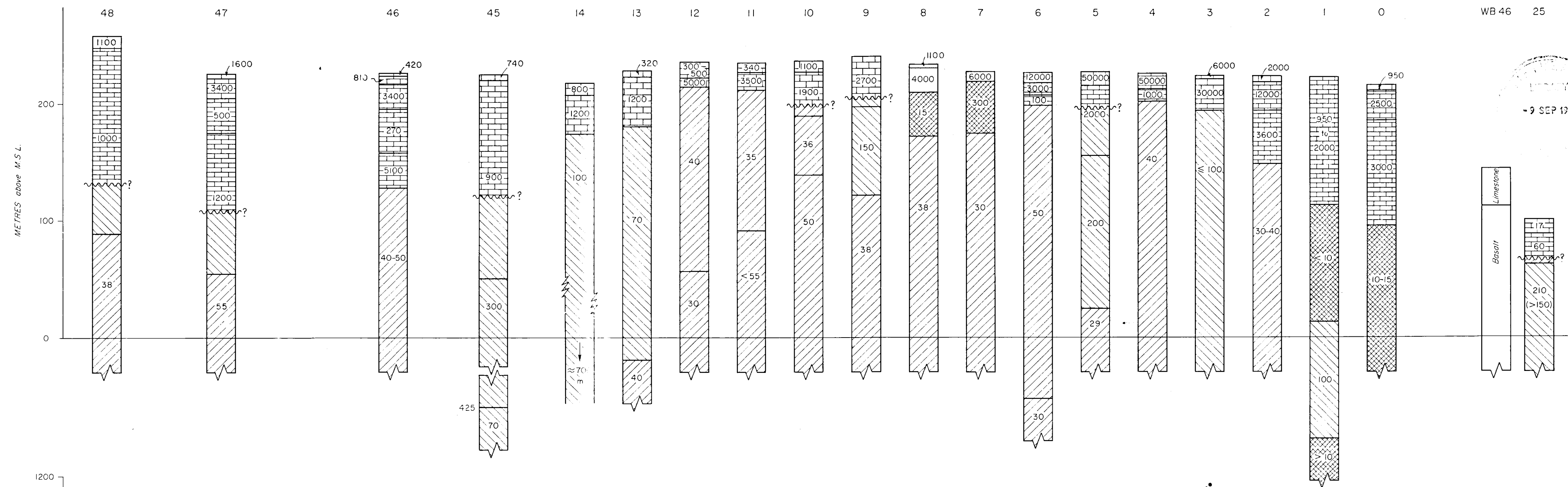
DEPTH IN METRES 40 700

RESISTIVITY (ohm.m)

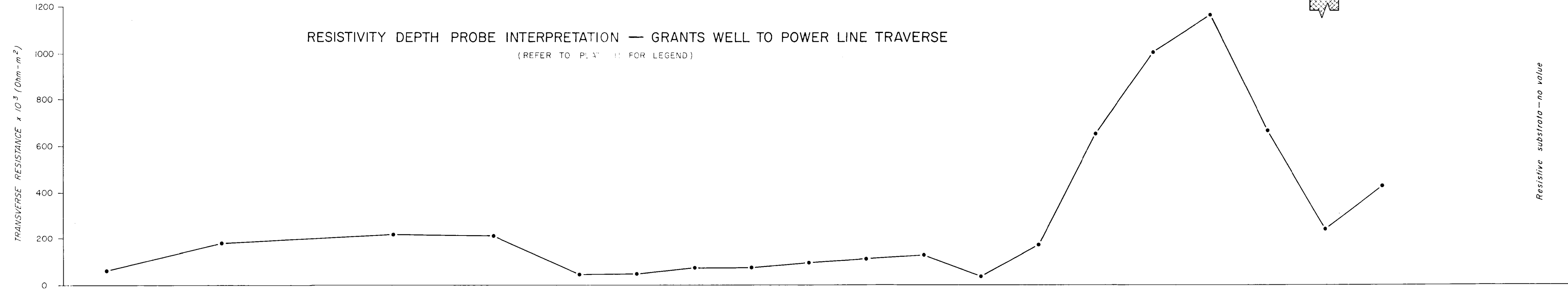
INTERPRETATION OF RESISTIVITY DEPTH PROBES - CENTRAL AREA

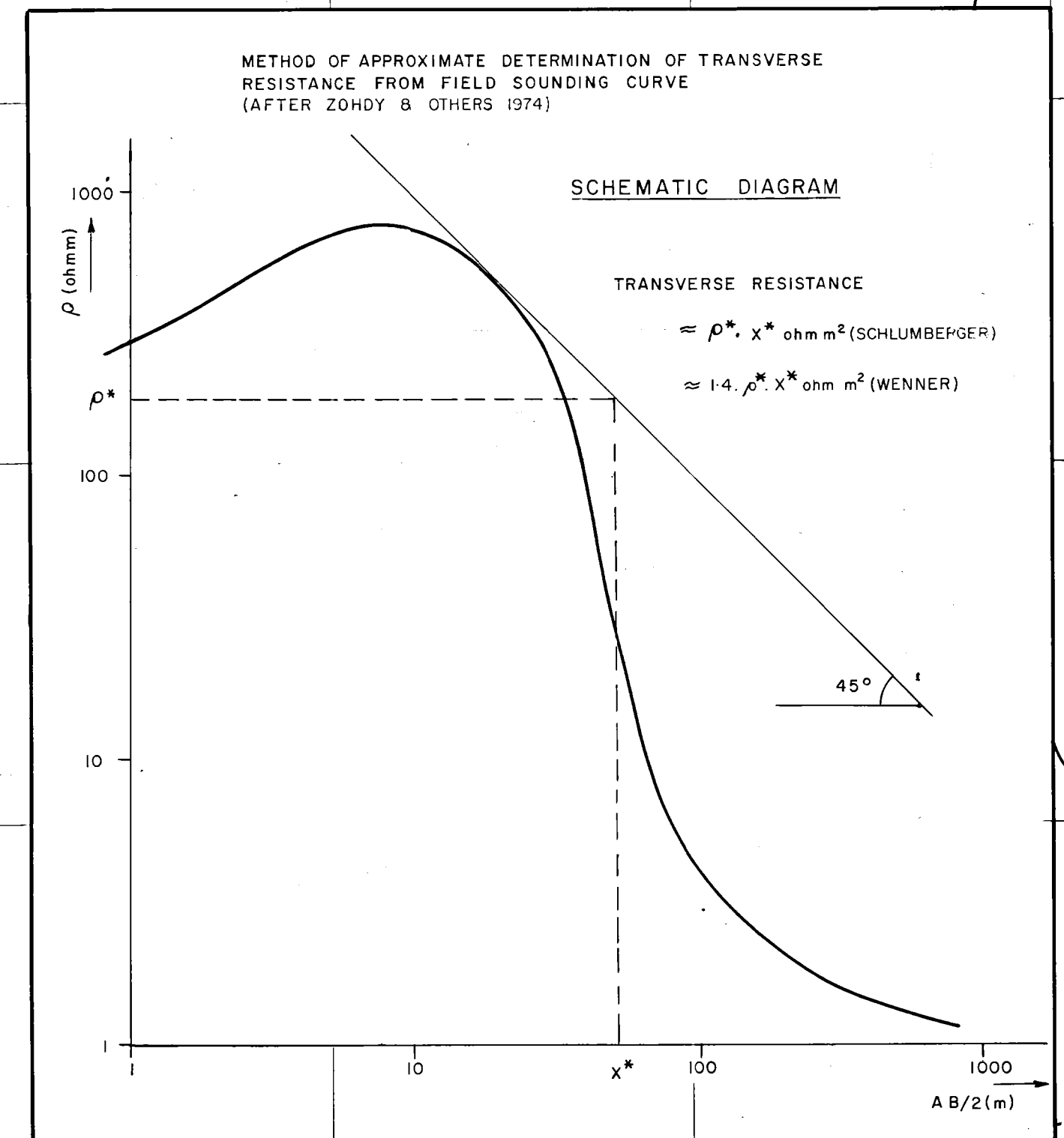
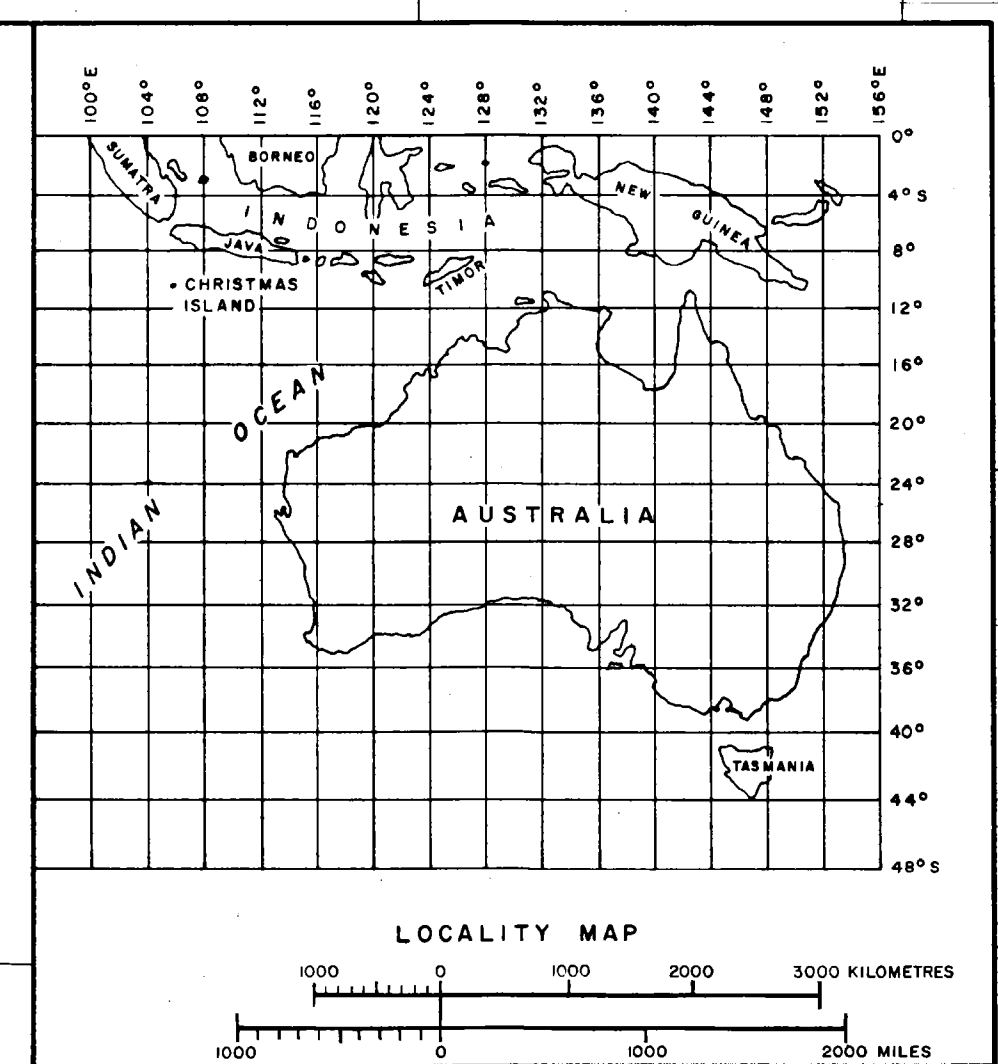
(REFER TO PLATE 12 FOR SO TO S14 COMPLETE SECTIONS & PLATE 18 FOR OTHER DEPTH PROBES ON THE ISLAND)

0 1000 2000 ft
0 500m



RESISTIVITY DEPTH PROBE INTERPRETATION — GRANTS WELL TO POWER LINE TRAVERSE
(REFER TO PLATE 11 FOR LEGEND)

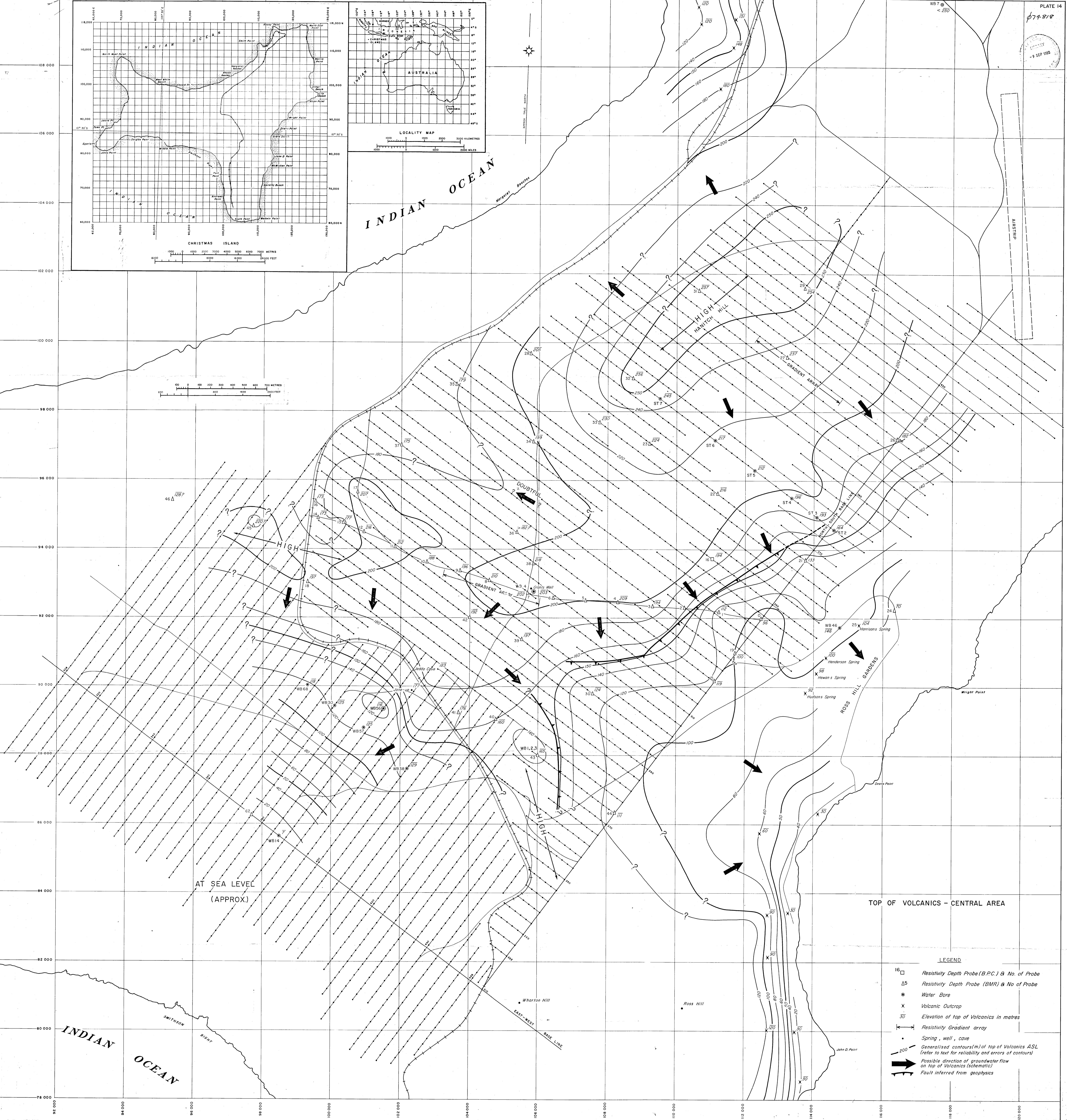
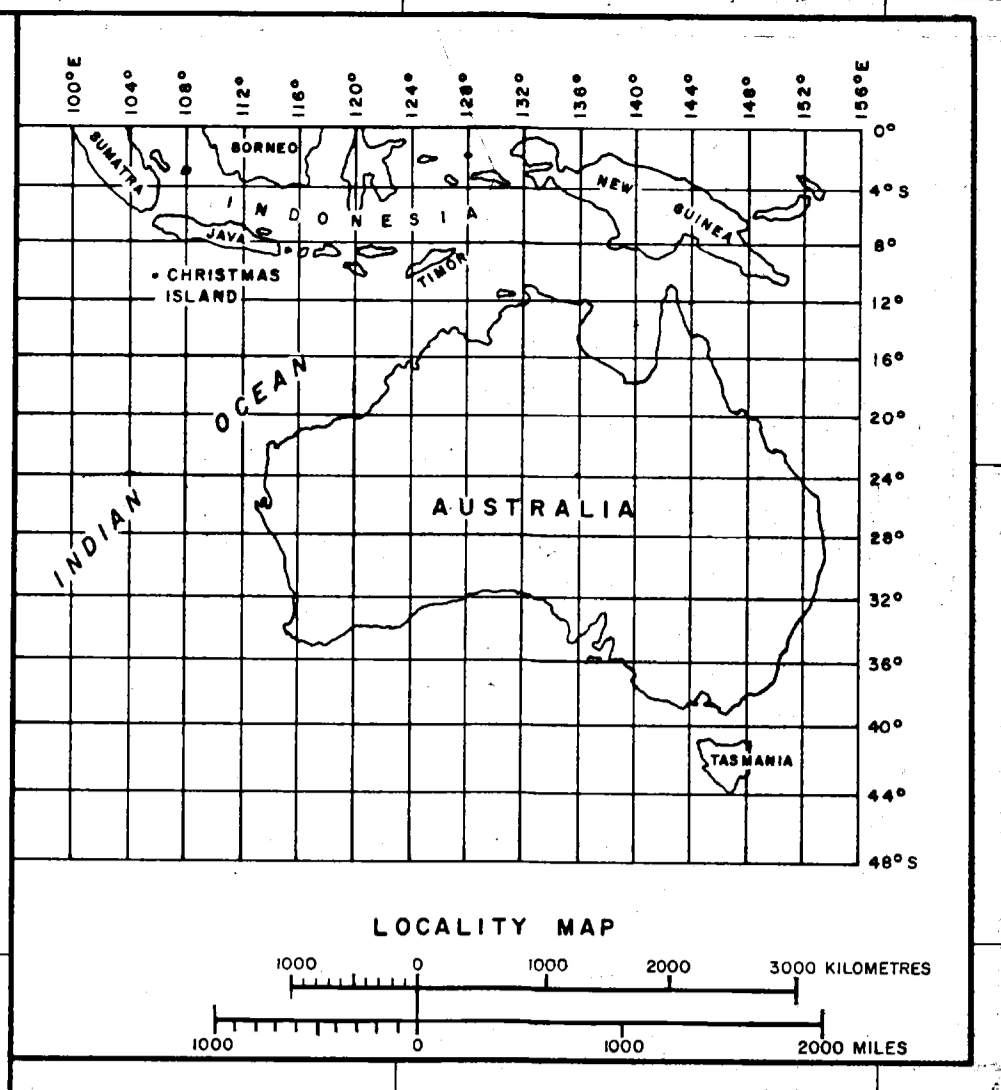
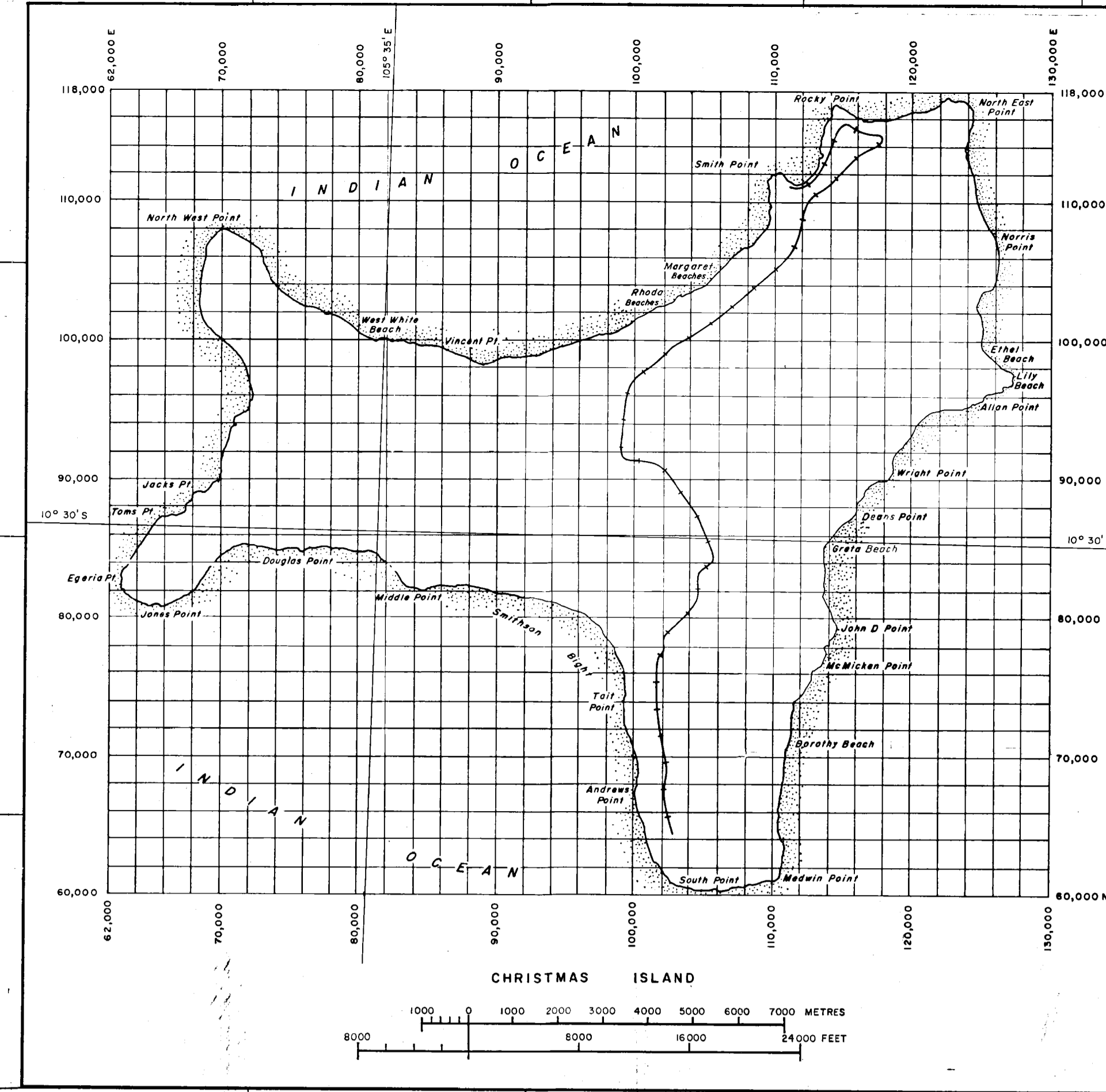




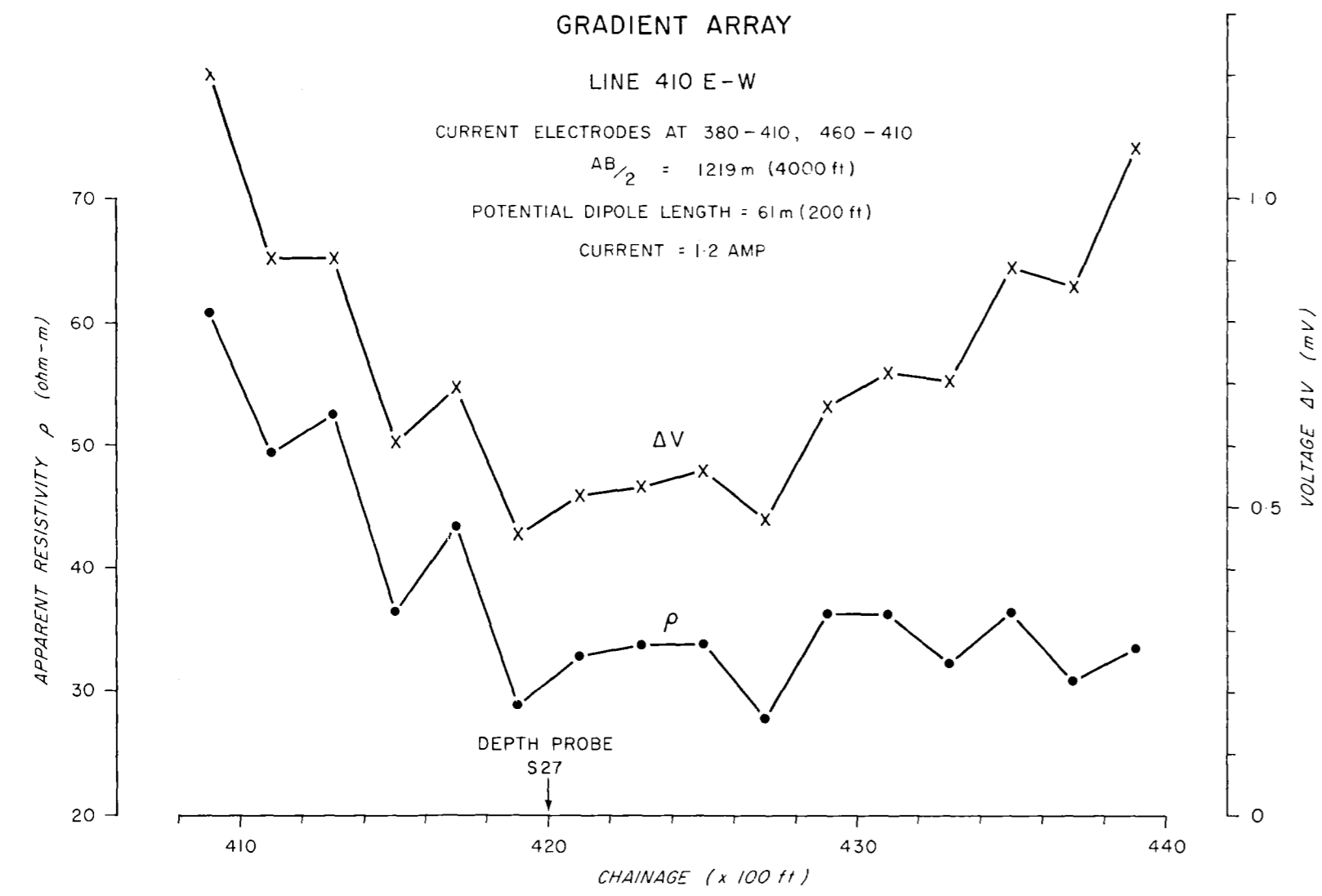
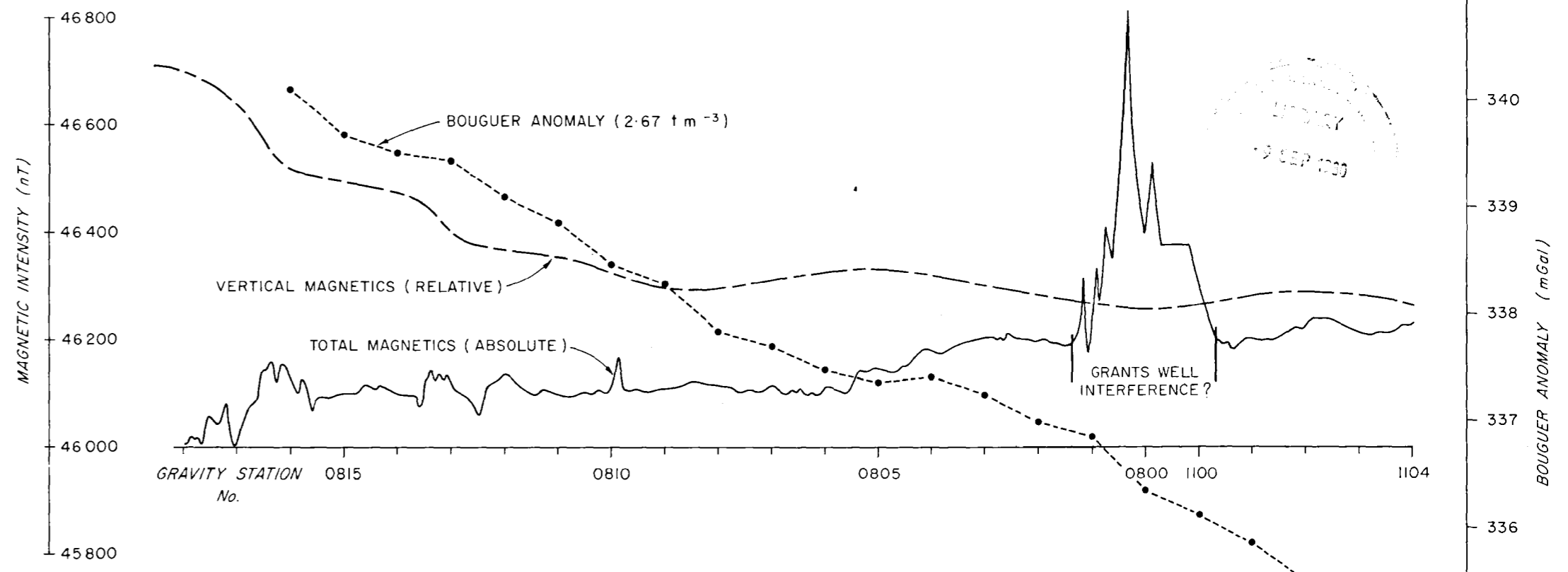
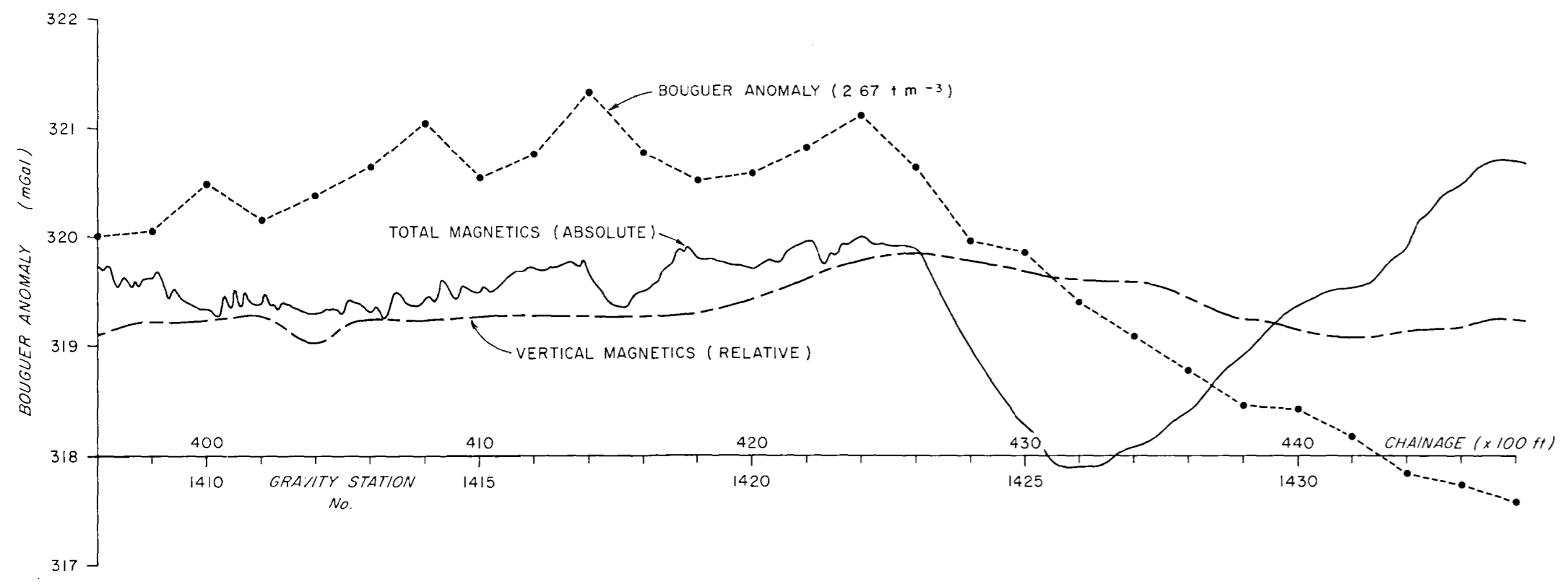
LEGEND

+	B. P. C. depth probe (Wenner)
□	BMR depth probe (Schlumberger)
△	BMR depth probe (1/2 Schlumberger)
—1000—	Generalised contour of transverse resistance

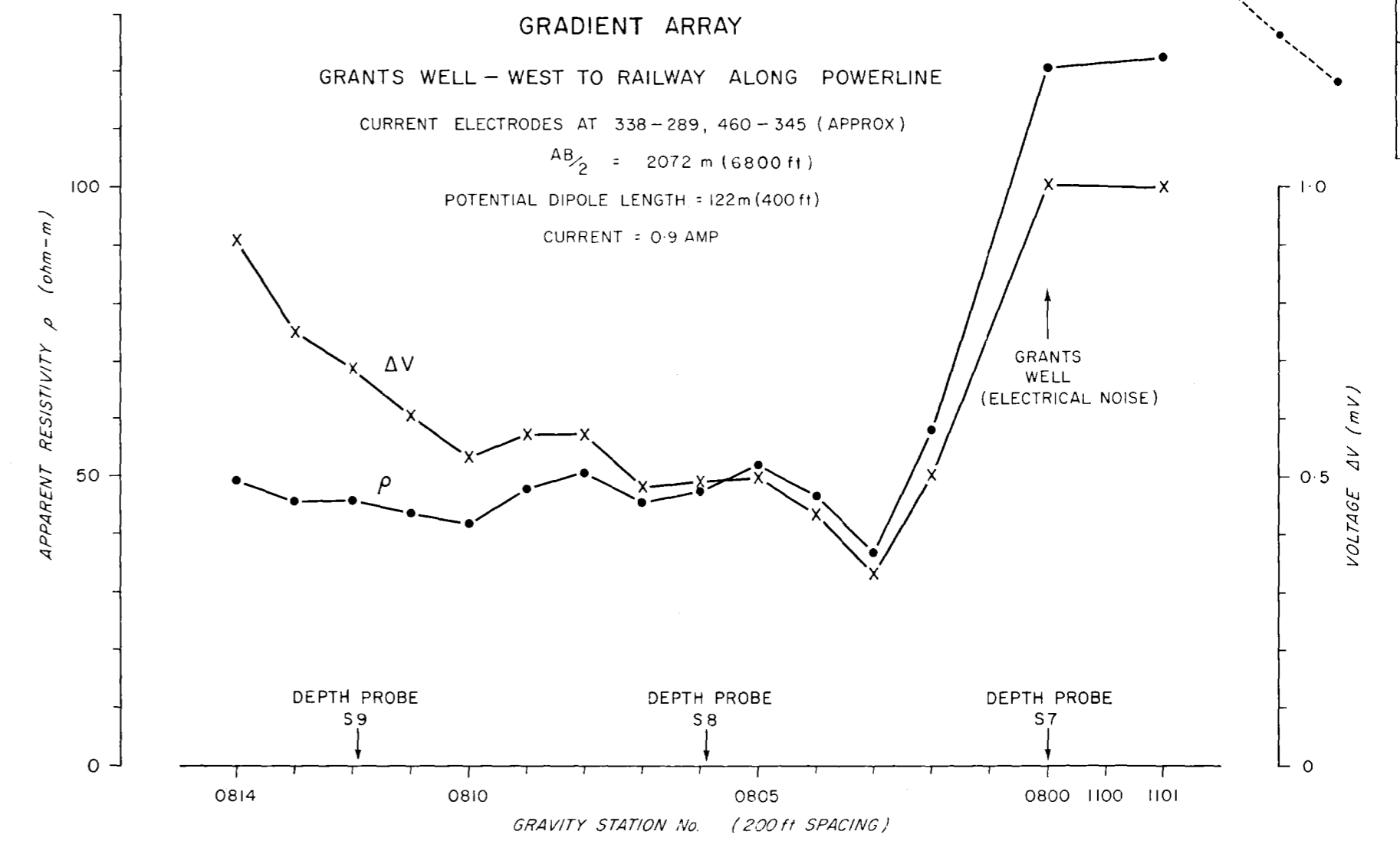
SEP 1950

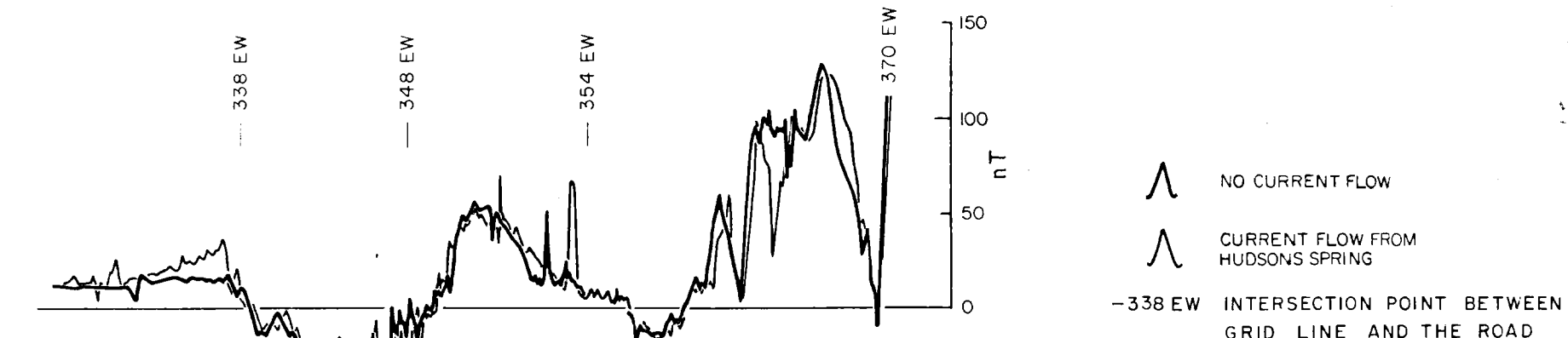
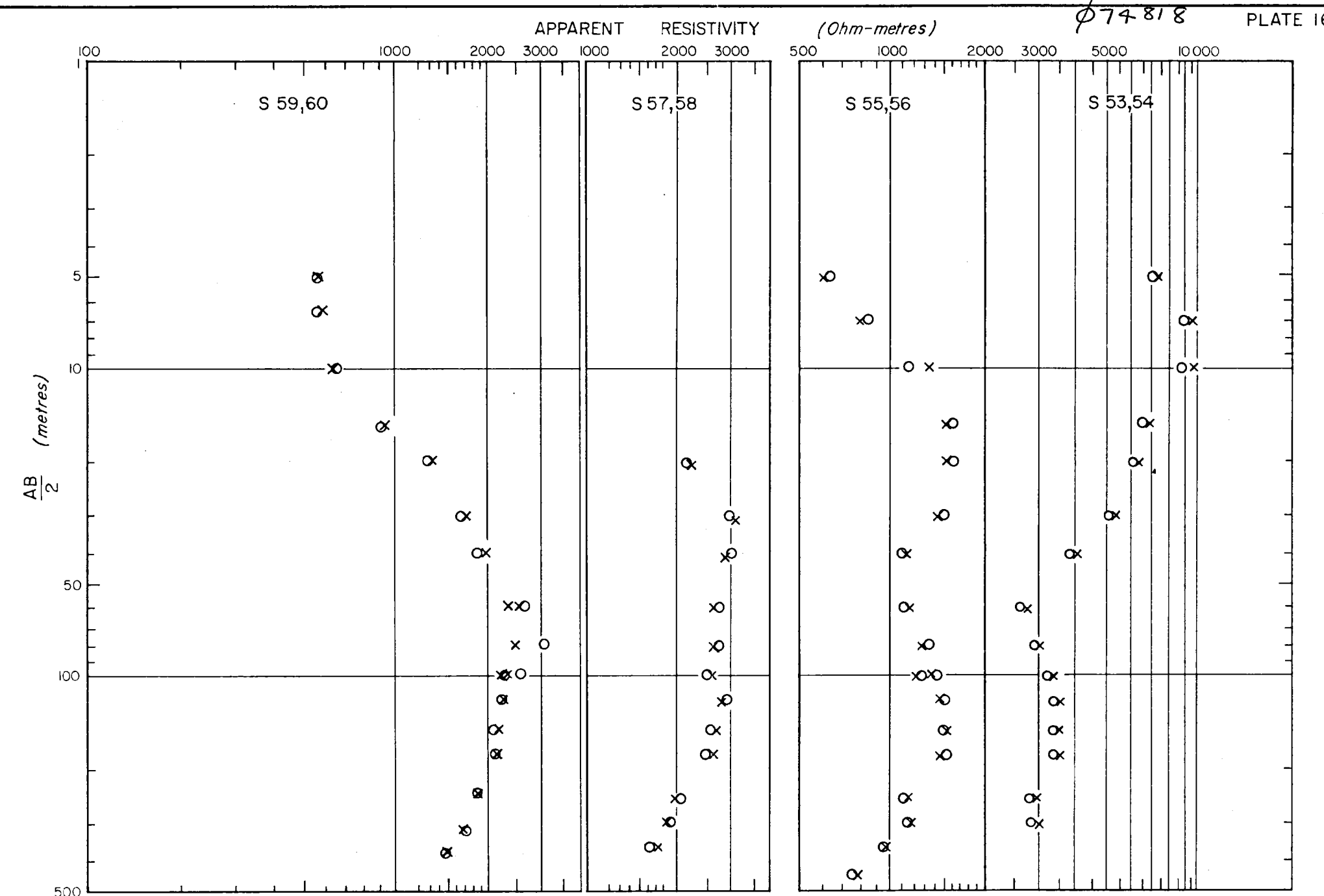
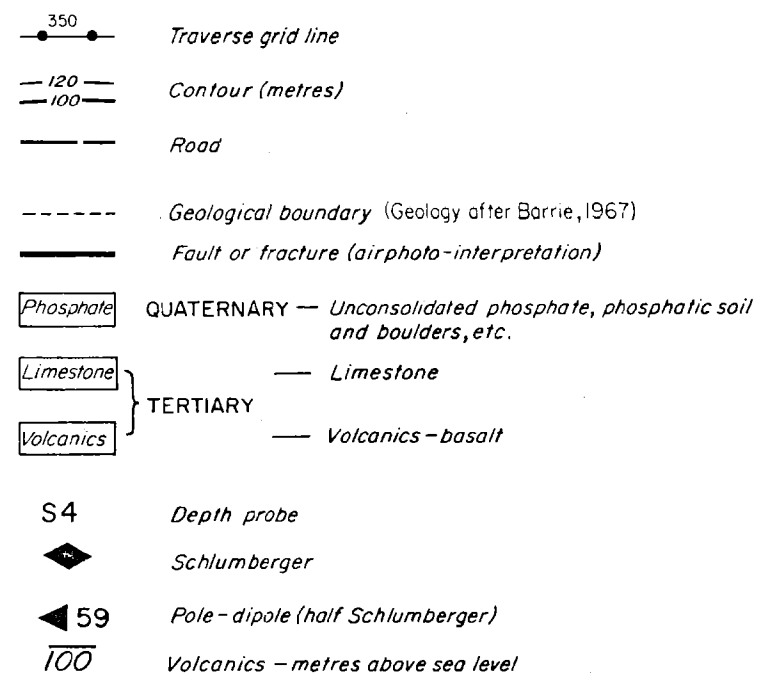
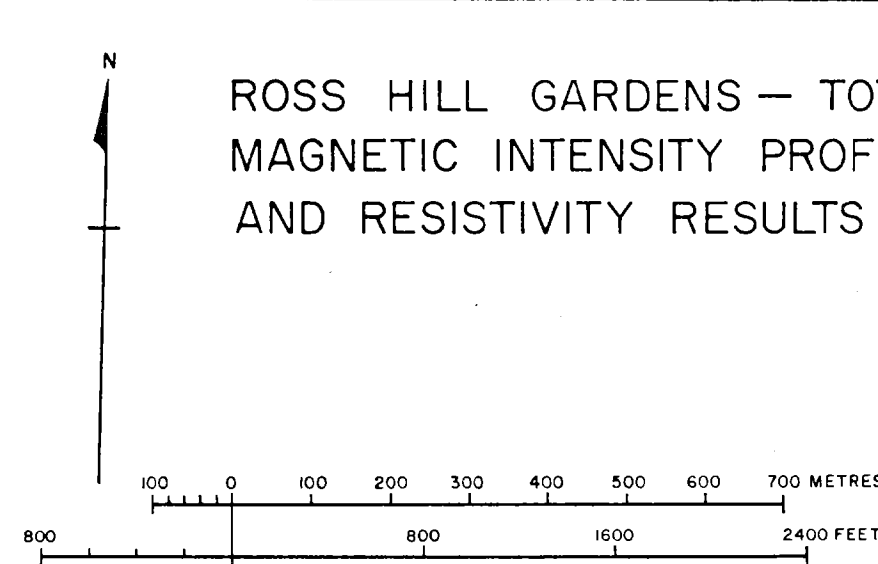
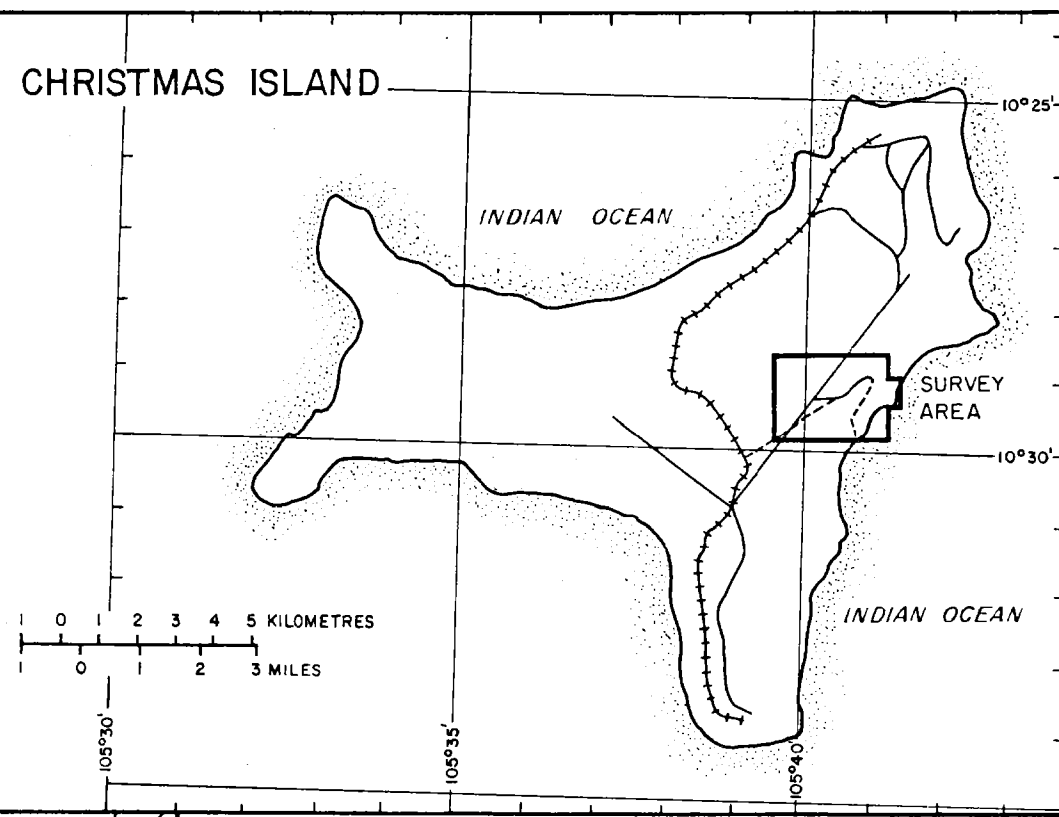
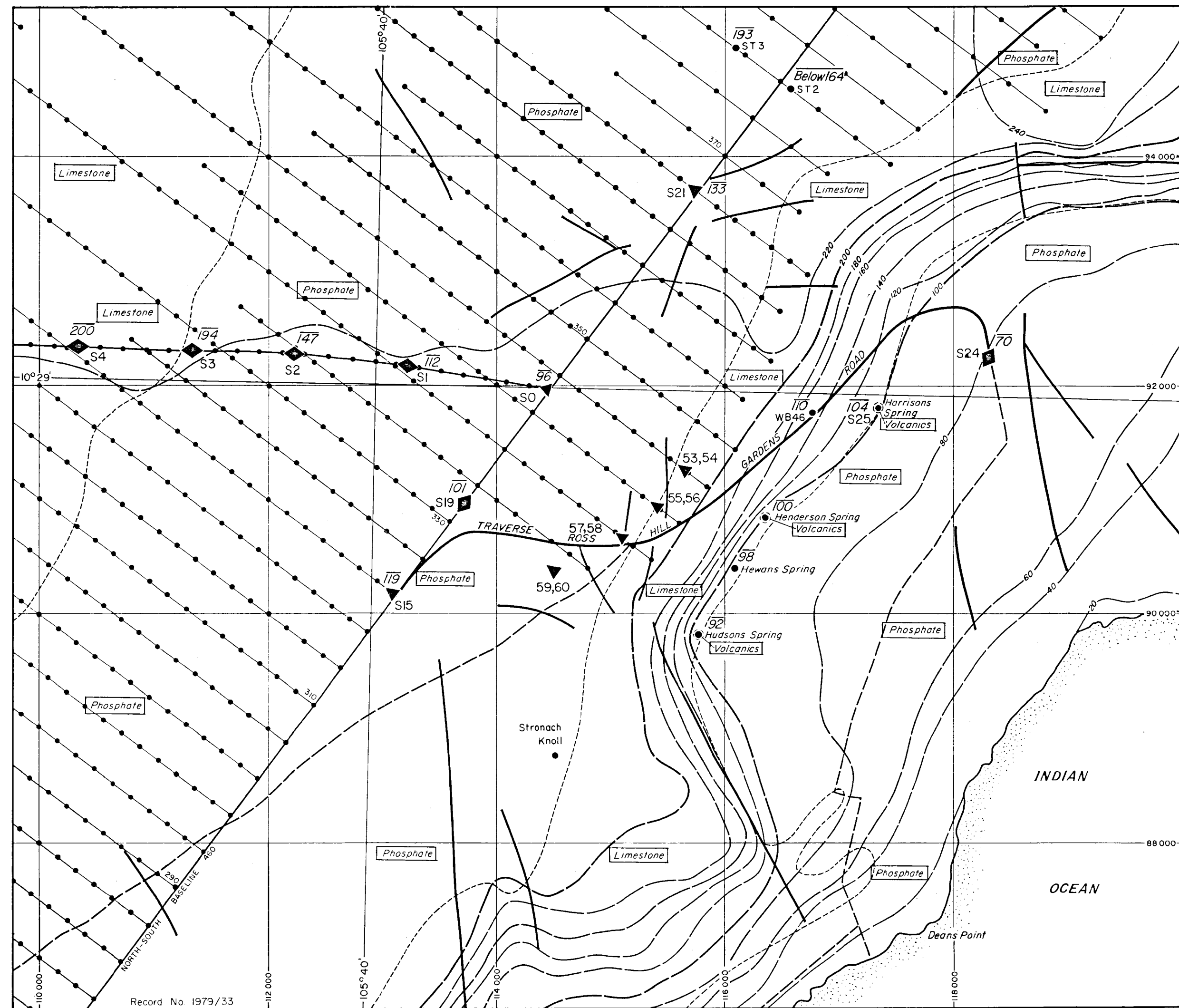


074818

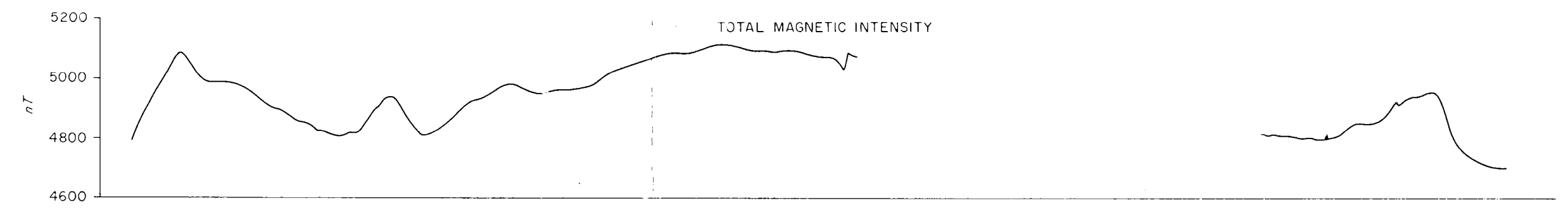


GRADIENT ARRAY RESULTS

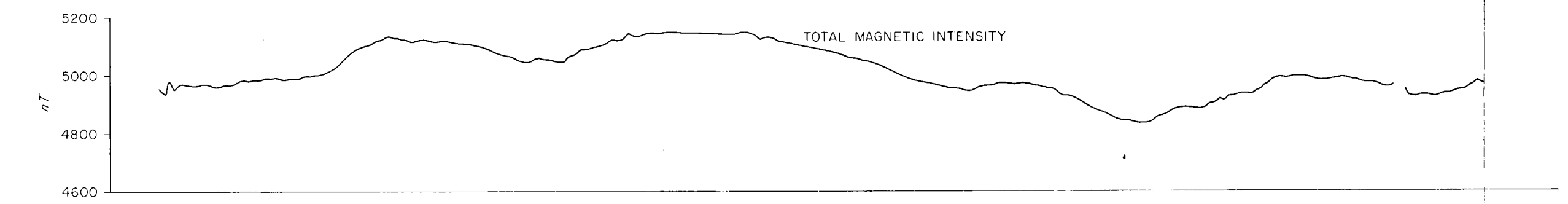
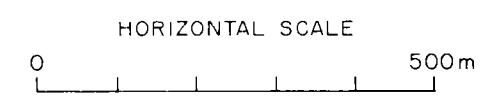
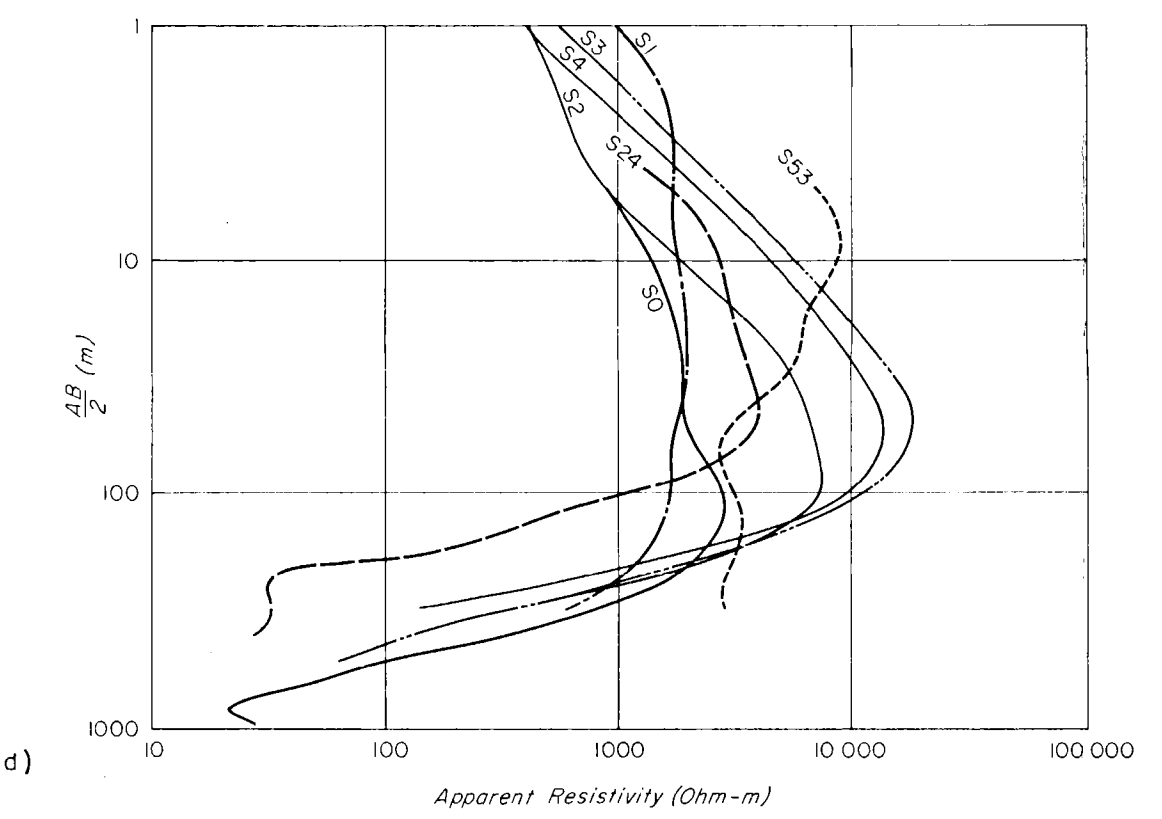
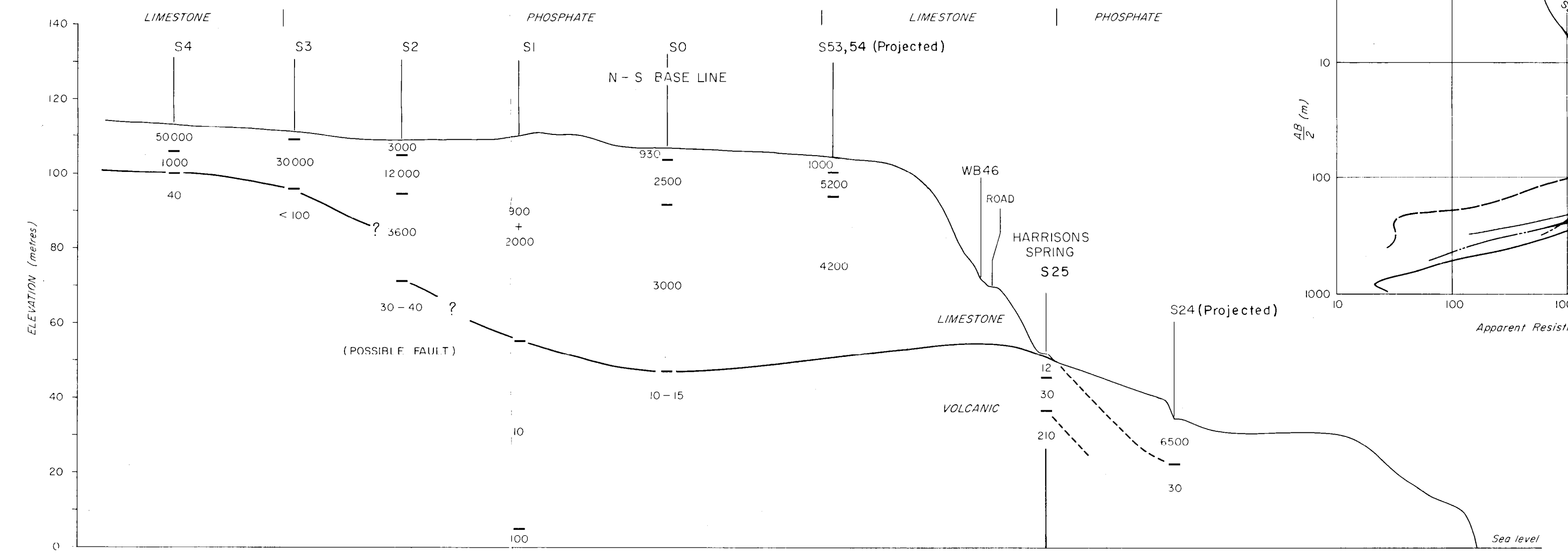




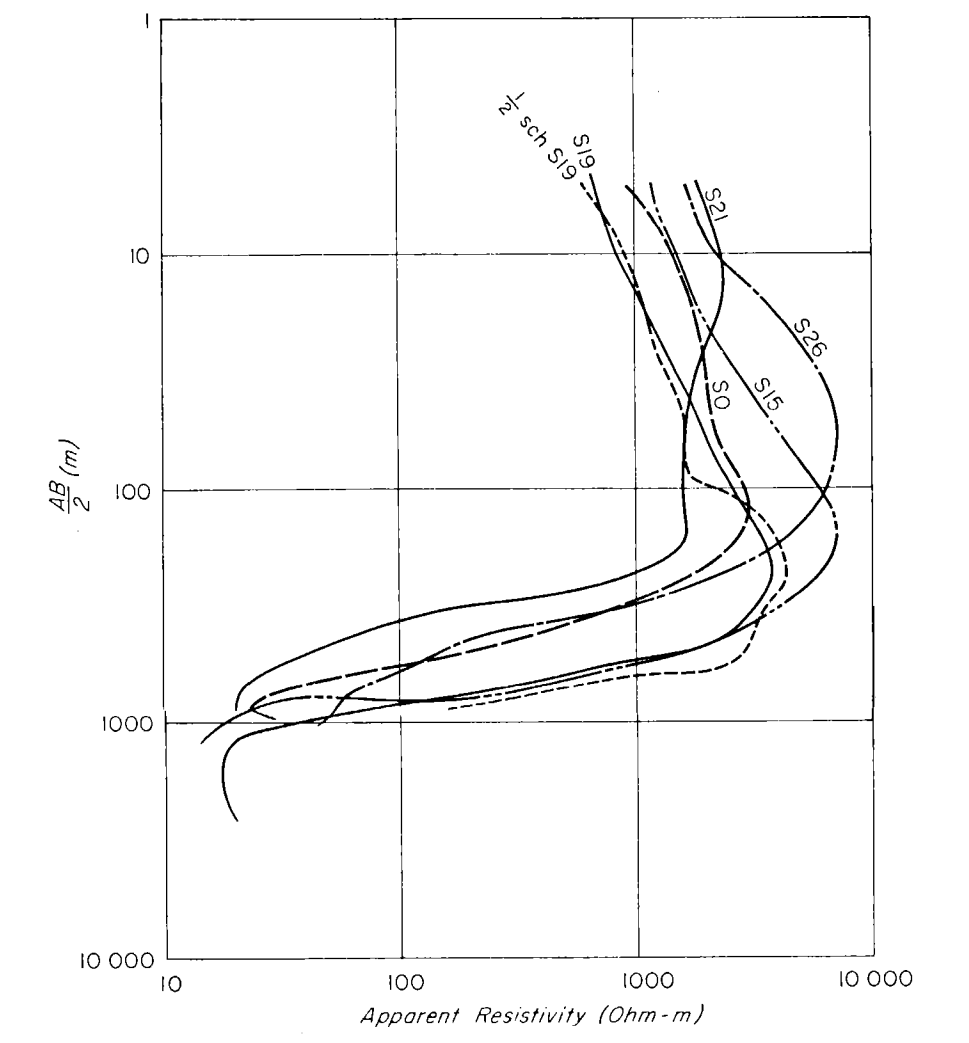
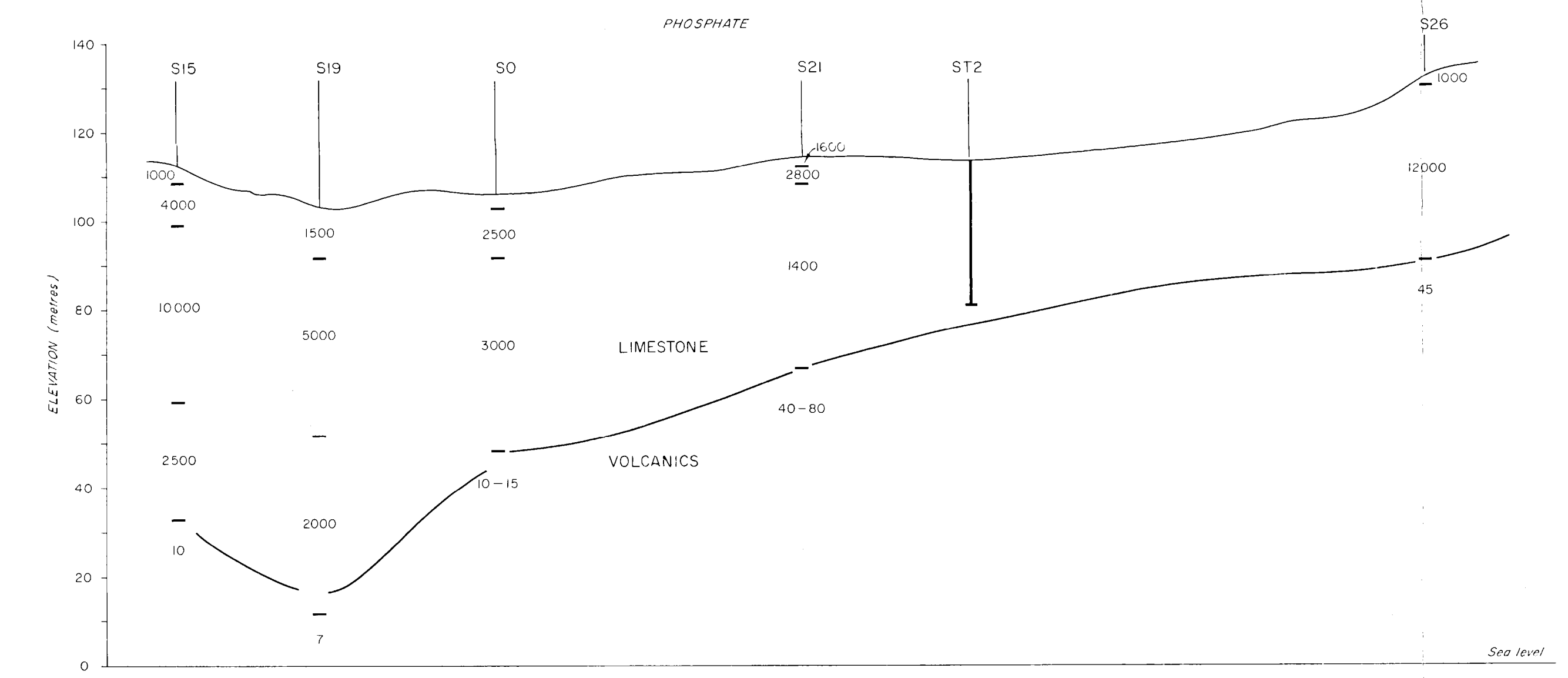
074818



SECTION FROM CENTRAL AREA ACROSS ROSS HILL GARDENS



SECTION ALONG N-S BASELINE



ROSS HILL GARDENS SECTIONS

